

JTRP

Joint
Transportation
Research
Program



PB99-140923

FHWA/IN/JTRP-98/13

Final Report

**DYNAMIC CONE PENETRATION TEST TO
ASSESS THE MECHANICAL PROPERTIES
OF THE SUBGRADE SOIL**

**X. Luo
R. Salgado
A. Altschaeffl**

September 1998

Indiana
Department
of Transportation

Purdue
University

REPRODUCED BY
U.S. DEPARTMENT OF COMMERCE
NATIONAL TECHNICAL
INFORMATION SERVICE
SPRINGFIELD, VA 22161

Final Report

FHWA/IN/JTRP-98/13

**DYNAMIC CONE PENETRATION TEST TO ASSESS THE MECHANICAL PROPERTIES
OF THE SUBGRADE SOIL**

Xiaodong Luo
Graduate Research Assistant

and

Rodrigo Salgado, P.E.
Assistant Professor
and

A. G. Altschaeffl, P.E.
Professor

Geotechnical Engineering
School of Civil Engineering
Purdue University

Joint Transportation Research Program
Project No: C-36-45N
File No: 6-18-13

Prepared in Cooperation with the
Indiana Department of Transportation and
the U.S. Department of Transportation
Federal Highway Administration

The contents of this report reflect the views of the authors who are responsible for the facts and the accuracy of the data presented herein. The contents do not necessarily reflect the official views or policies of the Federal Highway Administration and the Indiana Department of Transportation. This report does not constitute a standard, specification or regulation.

Purdue University
West Lafayette, Indiana
September 30, 1998

PROTECTED UNDER INTERNATIONAL COPYRIGHT
ALL RIGHTS RESERVED.
NATIONAL TECHNICAL INFORMATION SERVICE
U.S. DEPARTMENT OF COMMERCE

ACKNOWLEDGEMENTS

The authors are indebted to Athar Khan and Nayyar Zia of INDOT Materials and Tests Division and Tommy Nantung of INDOT Research Division for their assistance with the selection of sites for testing, for facilitating the testing in a number of ways, and for invaluable discussions about the potential applications of the dynamic cone penetration test in the daily practice of their work.

IMPLEMENTATION REPORT

The scope of this research project was to develop an interpretational tool, which could make the dynamic cone penetrometer test (DCPT) a practical and simple technique for assessing the in-situ soil characteristics under the pavement in the approximate zone of influence of traffic. Also, DCPT could be employed to determine the densities of the compacted subgrade instead of other methods. This method could also be employed to verify the INDOT proof-rolling operation. These tasks became the objective of this study.

A correlation between DCPT penetration index (inch/blow or mm/blow), water content, density and other commonly used parameters was proposed. The goals were to explore the ways in which the DCPT could effectively be used by INDOT geotechnical and construction personnel and to perform testing and analysis that will lead to knowledge of necessary relationships between Indiana Soils and DCPT measurements.

The DCPT can be applied to characterize the subgrade soils in many different scenarios, such as in confined areas, during preliminary geotechnical investigation, and in small earth works. It is an ideal tool for construction monitoring. For low volume roads, a relationship between CBR and penetration index could be established. DCPT is to be utilized in lieu of proof-rolling on projects that are too short (to justify expense of proof-rolling) or have shallow utilities (which would prevent proof-rolling).

There is a need to further verify/enhance the correlations and methods proposed in this report. This can be done by allowing INDOT crews to use the DCPT equipment, initially together with other techniques. The data should be aggregated to existing data and analyzed for further validation and extension of correlations. This could also be done, perhaps in a more effective way, by funding an implementation project with the specific goal of turning the correlations into a useful method for INDOT's use. The specific goals should be to (1) enlarge the database of soil types, (2) to refine the correlations by considering more data, (3) to carry out resilient modulus testing to refine the correlations with resilient modulus, (4) to develop a relationship between DCPT and other soils parameters, and (5) to establish the appropriate frequency of DCPT testing on a particular project.

TECHNICAL REPORT STANDARD TITLE PAGE


1. Report No. FHWA/IN/JTRP-98/13		 PB99-140923		3. Recipient's Catalog No.	
4. Title and Subtitle Dynamic Cone Penetration Test to Assess the Mechanical Properties of the Subgrade Soil		5. Report Date September 30, 1998		6. Performing Organization Code	
7. Author(s) Xiadong Luo, Rodrigo Salgado and A. G. Altschaeffl		8. Performing Organization Report No.		10. Work Univ No.	
9. Performing Organization Name and Address Joint Transportation Research Program 1284 Civil Engineering Building Purdue University West Lafayette, Indiana 47907-1284		11. Contract or Grant No.		13. Type of Report and Period Covered Final Report	
12. Sponsoring Agency Name and Address Indiana Department of Transportation State Office Building 100 North Senate Avenue Indianapolis, IN 46204		14. Sponsoring Agency Code		15. Supplementary Notes Prepared in cooperation with the Indiana Department of Transportation and Federal Highway Administration.	
16. Abstract <p>The purpose of the present study was to investigate the relationships between penetration resistance, dry density, moisture content, and resilient modulus of subgrade soils. The DCPT tests were conducted at eight sites. The nuclear gage and sand cone methods were used to estimate the dry density and moisture content of the subgrade soils. Disturbed soil samples were collected in the field. Atterberg limits and sieve analysis tests were conducted in the laboratory. For selected sites, laboratory DCPT tests were performed in a 12-inch mold along the compaction curves, and unconfined compression tests were conducted on 2.8-inch samples. The contours of laboratory penetration index with respect to dry density and moisture content were developed. Based on this information, the relationships between laboratory penetration index, unconfined compression test results and resilient modulus were found. Based on the field test results and unconfined compression test results, the relationship between field penetration index, dry density, moisture content, and resilient modulus for sandy lean clay was also found for select soil types. A framework for further development of such correlations for different soil types is now in place, which should facilitate future research.</p>					
17. Key Words dynamic cone penetration, DCPT, subgrade soil, resilient modulus, soil compaction			18. Distribution Statement No restrictions. This document is available to the public through the National Technical Information Service, Springfield, VA 22161		
19. Security Classif. (of this report)	20. Security Classif. (of this page)	21. No. of Pages 144	22. Price		

TABLE OF CONTENTS

	Page
List of Figures	v
List of Tables	xiii
Chapter 1 The Dynamic Cone Penetrometer	1
1.1 Introduction.....	1
1.2 Development of the DCP	2
1.3 Research Objectives.....	5
1.4 Description of the DCP used in this Study	5
1.5 Existing DCP Correlations.....	7
1.5.1 DCP/CBR Correlations.....	7
1.5.2 DCP/Unconfined Compressive Strength Correlation	8
1.5.3 DCP/SPT Correlation.....	8
1.5.4 DCP/Shear Strength Correlation for Granular Materials.....	8
1.6 Advantages and Limitations of the DCP	10
1.6.1 Advantages.....	10
1.6.2 Disadvantages	10
1.7 Summary	10
Chapter 2 Testing Program	12
2.1 Preliminary Test Results	12
2.2 Review of Soil Compaction Concepts	12
2.3 Testing Philosophy	14
2.4 Testing Procedure	15
2.5 Summary	16
Chapter 3 Test Results and Analysis	17
3.1 Introduction.....	17
3.2 Test Results and Analysis	17
3.2.1 The Railroad Relocation Project at West Lafayette.....	17
3.2.2 The New Interchange of I65 at Johnson Co.....	32
3.2.3 The SR67 at Delaware Co (1).....	53
3.2.4 The SR67 at Delaware Co. (2).....	61
3.2.5 The SR62 in Evansville	69

	Page
3.2.6 The US24 by-pass in Logansport.....	78
3.2.7 The SR24 in Logansport.....	89
3.2.8 The US41 in Parke Co.....	101
3.3 The Results for Sandy Lean Clay and Sandy Silty Clay.....	108
3.4 The Relationship between DCPT and SPT.....	114
3.5 Summary.....	119
Chapter 4 Conclusions and Future Work.....	121
4.1 Conclusions.....	121
4.2 Application to Compaction Control.....	122
4.3 Future work.....	123
List of References.....	124

LIST OF FIGURES

Figure	Page
1.1 The Dynamic Cone Penetrometer	6
1.2 The Relationship between Penetration Index and Unconfined Compression Test (after Kleyn, 1983)	9
2.1 The Relationship between Penetration Index and Dry Density from the Testing Results of Summer, 1997	13
3.1 The Log of the DCPT (Station: 138+75, Offset: 4.9m RT)	22
3.2 The Log of the DCPT (Station: 138+50, Offset: 3.0m RT)	22
3.3 The Log of the DCPT (Station: 138+25, Offset: 3.0m RT)	23
3.4 The Log of the DCPT (Station: 136+00, Offset: 3.0m RT)	23
3.5 The Log of the DCPT (Station: 135+75, Offset: 7.6m RT)	24
3.6 The Log of the DCPT (Station: 141+50, Offset: 6.1m RT)	24
3.7 The Log of the DCPT (Station: 141+75, Offset: 5.5m RT)	25
3.8 The Relationship between Dry Density and Moisture Content from Field DCPT for West Lafayette Railroad Relocation Project	26
3.9 The Relationship between Penetration Index and Moisture Content From Field DCPT for West Lafayette Railroad Relocation Project	26
3.10 The Relationship between Penetration Index and Dry Density from Field DCPT for West Lafayette Railroad Relocation Project	27
3.11 The Results of Sieve Analysis for West Lafayette Railroad Relocation Project	27

Figure	Page
3.12 The Relationship between Dry Density and Moisture Content from the Laboratory DCPT for West Lafayette Railroad Relocation Project . . .	29
3.13 The Relationship between Penetration Index and Moisture Content from the Laboratory DCPT for West Lafayette Railroad Relocation Project . . .	29
3.14 The Relationship between Penetration Index and Dry Density from the Laboratory DCPT for West Lafayette Railroad Relocation Project . . .	30
3.15 Contour of Penetration Index for West Lafayette Railroad Relocation Project (Unit of I_p : $\times 25.4\text{mm/blow}$)	31
3.16 The log of the DCPT (Station: 32+25 Ramp SWR, Offset: 3.0m RT) . . .	37
3.17 The log of the DCPT (Station: 27+50 Ramp SWR, Offset: 3.0m RT) . . .	38
3.18 The log of the DCPT (Station: 36+50 Ramp SWR, Offset: 3.0m RT) . . .	39
3.19 The log of the DCPT (Station: 36+50 Ramp SWR, Offset: 4.6m RT) . . .	39
3.20 The log of the DCPT (Station: 36+45 Ramp SWR, Offset: 3.0m RT) . . .	40
3.21 The log of the DCPT (Station: 36+45 Ramp SWR, Offset: 4.6m RT) . . .	40
3.22 The log of the DCPT (Station: 36+48 Ramp SWR, Offset: 3.0m RT) . . .	41
3.23 The Relationship between Dry Density and Moisture Content from Field DCPT for the New Interchange of I65 in Johnson CO., IN	42
3.24 The Relationship between Penetration Index and Moisture Content from Field DCPT for the New Interchange of I65 in Johnson CO., IN	42
3.25 The Relationship between Penetration Index and Dry Density from Field DCPT for the New Interchange of I65 in Johnson CO., IN	43
3.26 The Results of Sieve Analysis for the New Interchange of I65 in Johnson CO., IN	43
3.27 The Relationship between Dry Density and Moisture Content from the Laboratory DCPT for the New Interchange of I65 in Johnson CO., IN	44

Figure	Page
3.28 The Relationship between Penetration Index and Moisture Content from the Laboratory DCPT for the New Interchange of I65 in Johnson CO., IN	44
3.29 The Relationship between Penetration Index and Dry Density from the Laboratory DCPT for the New Interchange of I65 in Johnson CO., IN	45
3.30 Contour of Penetration Index for the New Interchange of I65 in Johnson CO., IN (Unit of I_p : $\times 25.4$ mm/blow)	46
3.31 The Relationship between Moisture Content and Dry Density from Unconfined Compression Tests for the New Interchange of I65 in Johnson CO. IN	48
3.32 The Relationship between Moisture Content and $S_{u1.0\%}$ for the New Interchange of I65 in Johnson CO., IN	48
3.33 The Relationship of Dry Density and $S_{u1.0\%}$ for the New Interchange of I65 in Johnson CO., IN	49
3.34 Contour of $S_{u1.0\%}$ for the New Interchange of I65 in Johnson CO., IN	51
3.35 The Relationship between $S_{u1.0\%}$ and Penetration Index for the New Interchange of I65 in Johnson CO., IN	52
3.36 The Relationship between Penetration Index and Resilient Modulus for the New Interchange of I65 in Johnson CO., IN	52
3.37 The Log of the DCPT (Station: 43+485, Offset: 2m RT)	55
3.38 The Log of the DCPT (Station: 43+480, Offset: 3m RT)	56
3.39 The Log of the DCPT (Station: 43+480, Offset: 5m RT)	56
3.40 The Log of the DCPT (Station: 43+482, Offset: 9m RT)	57
3.41 The Log of the DCPT (Station: 43+485, Offset: 7m LT)	57
3.42 The Log of the DCPT (Station: 43+490, Offset: 10m LT)	58
3.43 The Log of the DCPT (Station: 43+492, Offset: 7m LT)	58

Figure	Page
3.44 The Relationship between Moisture Content and Dry Density from Field DCPT for SR67 in Delaware CO., IN (1)	59
3.45 The Relationship between Moisture Content and Penetration Index from Field DCPT for SR67 in Delaware CO., IN (1)	59
3.46 The Relationship between Dry Density and Penetration Index for SR67 from Field DCPT in Delaware CO., IN (1)	60
3.47 The Results of Sieve Analysis for SR67 in Delaware CO., IN (1)	60
3.48 The Log of the DCPT (Station: 39+790, Offset: 1.9m EB RT)	63
3.49 The Log of the DCPT (Station: 39+790, Offset: 2.6m EB RT)	63
3.50 The Log of the DCPT (Station: 39+790, Offset: 3.3m EB RT)	64
3.51 The Log of the DCPT (Station: 39+790, Offset: 4.2m EB RT)	64
3.52 The Log of the DCPT (Station: 39+790, Offset: 5.3m EB RT)	65
3.53 The Log of the DCPT (Station: 39+790, Offset: 6.4m EB RT)	65
3.54 The Log of the DCPT (Station: 39+790, Offset: 7.5m EB RT)	66
3.55 The Relationship between Dry Density and Moisture Content from Filed DCPT for SR67 in Delaware CO., IN (2)	66
3.56 The Relationship between Moisture Content and Penetration Index from Field DCPT for SR67 in Delaware CO., IN (2)	67
3.57 The Relationship between Dry Density and Penetration Index from Field DCPT for SR67 in Delaware CO., IN (2)	67
3.58 The Results of Sieve Analysis for SR67 in Delaware CO., IN (2)	68
3.59 The Results of Sieve Analysis for The Intersection of SR62 and Garvin St. in Evansville, IN	70
3.60 The DCPT Log 1 for the Intersection of SR62 and Garvin St. in Evansville, IN	71

Figure	Page
3.61 The DCPT Log 2 for the Intersection of SR62 and Garvin St. in Evansville, IN	72
3.62 The DCPT Log 3 for the Intersection of SR62 and Garvin St. in Evansville, IN	73
3.63 The DCPT Log 4 for the Intersection of SR62 and Garvin St. in Evansville, IN	74
3.64 The DCPT Log 5 for the Intersection of SR62 and Garvin St. in Evansville, IN	75
3.65 The Relationship between DCPT and SPT for the Intersection of SR62 and Garvin St. in Evansville, IN	77
3.66 The Log of the DCPT (Station: 438+67, Offset: 5.18m LT)	80
3.67 The Log of the DCPT (Station: 438+67, Offset: 3.66m LT)	80
3.68 The Log of the DCPT (Station: 438+67, Offset: 2.44m RT)	81
3.69 The Log of the DCPT (Station: 405-26, Offset: 7.92m LT)	81
3.70 The Log of the DCPT (Station: 405-26, Offset: 4.88m LT)	82
3.71 The Log of the DCPT (Station: 405-26, Offset: 2.44m LT)	82
3.72 The Log of the DCPT (Station: 405+2, Offset: 1.52m RT)	83
3.73 The Relationship between Dry Density and Moisture Content with Nuclear Gage Method for US24 By-pass in Logansport, IN	84
3.74 The Relationship between Penetration Index and Moisture Content with Nuclear Gage Method for US24 By-pass in Logansport, IN	85
3.75 The Relationship between Penetration Index and Dry Density with Nuclear Gage for US24 By-pass in Logansport, IN	85
3.76 The Relationship between Dry Density and Moisture Content with Sand Cone Method for US24 Bypass in Logansport, IN	86

Figure	Page
3.77 The Relationship between Penetration Index and Moisture Content with Sand Cone Method for US24 By-pass in Logansport, IN	86
3.78 The Relationship between Penetration Index and Dry Density with Sand Cone Method for US24 By-pass in Logansport,IN	87
3.79 Comparison of the Testing Results of Moisture Content from Sand Cone Method and Nuclear Gage for US24 By-pass in Logansport, IN	87
3.80 Comparison of the Testing Results of Dry Density from Sand Cone Method and Nuclear Gage for US24 By-pass in Logansport, IN	88
3.81 The Test Results of Sieve Analysis for US24 By-pass in Logansport, IN	88
3.82 the Log 1 of the DCPT for SR24 in Logansport, IN	91
3.83 the Log 2 of the DCPT for SR24 in Logansport, IN	91
3.84 the Log 3 of the DCPT for SR24 in Logansport, IN	92
3.85 the Log 4 of the DCPT for SR24 in Logansport, IN	92
3.86 the Log 5 of the DCPT for SR24 in Logansport, IN	93
3.87 the Log 6 of the DCPT for SR24 in Logansport, IN	93
3.88 the Log 7 of the DCPT for SR24 in Logansport, IN	94
3.89 The Relationship between Dry Density and Moisture Content with Nuclear Gage Method for SR24 in Logansport, IN	95
3.90 The Relationship between Penetration Index and Moisture Content with Nuclear Gage Method for SR24 in Logansport, IN	95
3.91 The Relationship between Penetration Index and Dry Density with Nuclear Gage for SR24 in Logansport, IN	96
3.92 The Relationship between Dry Density and Moisture Content with Sand Cone Method for SR24 in Logansport, IN	96
3.93 The Relationship between Penetration Index and Moisture Content	

Figure	Page
with Sand Cone Method for SR24 in Logansport, IN	97
3.94 The Relationship between Penetration Index and Dry Density with Sand Cone Method for SR24 in Logansport,IN	97
3.95 Comparison of the Testing Results of Moisture Content from Sand Cone Method and Nuclear Gage for SR24 in Logansport, IN	98
3.96 Comparison of the Testing Results of Dry Density from Sand Cone Method and Nuclear Gage for SR24 in Logansport, IN	99
3.97 The Test Results of Sieve Analysis for SR24 By-pass in Logansport, IN	100
3.98 The Results of Sieve Analysis for US41 in Parke CO., IN	102
3.99 the Log 1 of the DCPT for US41 in Parke CO.	104
3.100 the Log 2 of the DCPT for US41 in Parke CO.	105
3.101 the Log 3 of the DCPT for US41 in Parke CO.	106
3.102 The Relationship between DCPT and SPT for US41 in Parke CO, IN	107
3.103 The Relationship between Moisture Content and Dry Density for Sandy Lean Clay with Nuclear Gage	109
3.104 The Relationship between Moisture Content and Penetration Index for Sandy Lean Clay with Nuclear Gage	109
3.105 The Relationship between Dry Density and Penetration Index for Sandy Lean Clay with Nuclear Gage	110
3.106 The Relationship between Moisture Content and Dry Density for Sandy Lean Clay with Sand Cone Method	110
3.107 The Relationship between Moisture Content and Penetration Index for Sandy Lean Clay with Sand Cone Method	111
3.108 The Relationship between Dry Density and Penetration Index for Sandy Lean Clay Sand Cone Method	111

Figure	Page
3.109 The Relationship between Field PI and $S_{u1.0\%}$	113
3.110 The Relationship between Field PI and M_r	113
3.111 The Relationship between the DCPT and SPT (0 to 6 inches)	115
3.112 The Relationship between the DCPT and SPT (6 to 12 inches)	115
3.113 The Relationship between the DCPT and SPT (12 to 18 inches)	116
3.114 The Relationship between the DCPT and SPT (18 to 24 inches)	117
3.115 The Relationship between the DCPT and SPT (24 to 30 inches)	117
3.116 The Relationship between the DCPT and SPT (30 to 36 inches)	118
3.117 The Relationship between the DCPT and SPT (36 to 42 inches)	119

LIST OF TABLES

Table	Page
3.1.1 The Information of The Testing Sites	18
3.2.1 Field DCPT Results for West Lafayette Railroad Relocation Project	21
3.2.2 The Results of the Laboratory DCPT for West Lafayette Railroad Relocation Project	28
3.2.3 The Field DCPT Results at the New Interchange of I65 in Johnson CO.	33
3.2.4 The Results of the Laboratory Penetration Testing for I65 Interchange Soil in Johnson CO.	34
3.2.5 The Information of the Blows for Each Soil Layer	35
3.2.6 The Test Results of Unconfined Compression Test	47
3.2.7 The Relationship between $S_{u1.0\%}$, Penetration Index and Resilient Modulus	50
3.2.8 Field Test Results for the SR67 in Delaware CO., IN (1)	54
3.2.9 Field Test Results for SR67 in Delaware CO., IN (2)	62
3.2.10 The Relationship between SPT and DCPT for the Interchange of SR62 and Garvin St. in Evansville, IN	76
3.2.11 Field Test Results for US24 By-pass in Logansport, IN (with nuclear gage)	79

Table	Page
3.2.12 Field Test Results for US24 By-pass in Logansport, IN (with Sand Cone Method)	79
3.2.13 Field Test Results for SR24 in Logansport, IN (with nuclear gage)	90
3.2.14 Field Test Results for SR24 in Logansport, IN (with Sand Cone Method)	90
3.2.15 The Relationship between SPT and DCPT for US41 in Parke CO., IN	103
3.3.1 The Relationships between Field PI, $S_{u1.0\%}$ and M_r for Sandy Silty Clay	108
3.3.2 The Relationships between Field PI, $S_{u1.0\%}$ and M_r for Sandy Lean Clay	112
3.3.3 The Relationship between M_r from Field and M_r from Laboratory	114
3.4.1 The Relationship between DCPT and SPT (0 to 6 inches)	114
3.4.2 The Relationship between DCPT and SPT (6 to 12 inches)	115
3.4.3 The Relationship between DCPT and SPT (12 to 18 inches)	116
3.4.4 The Relationship between DCPT and SPT (18 to 24 inches)	116
3.4.5 The Relationship between DCPT and SPT (24 to 30 inches)	117
3.4.6 The Relationship between DCPT and SPT (30 to 36 inches)	118
3.4.7 The Relationship between DCPT and SPT (36 to 42 inches)	118

Chapter 1

The Dynamic Cone Penetrometer

1.1 Introduction

Dynamic or static penetration tests are widely used in geotechnical engineering. Various penetrometers and testing methods are utilized in soil exploration in response to different purposes and requirements. During the preliminary exploratory phase, penetration tests are employed to determine the soil conditions, such as soil type, the depth, thickness and lateral extent of the soil strata. During the detailed exploration phase, penetration tests are also important. The shear strength and stiffness of the soil can be estimated from penetration testing data, so that the ultimate bearing capacity and the compressibility of the soil can be assessed.

Penetration tests have a very long history (Broms and Flodin, 1988). In the 15th century, test piles were used to determine the required length of pile foundations. Thus, pile driving can be regarded as an early type of penetration testing. The earliest dynamic penetrometer may have been a "ram penetrometer" developed in Germany at the end of the 17th century by Nicholaus Goldmann. The standard penetration test (SPT) can be traced back to Colonel Charles R. Gow in 1902, who developed a 25mm diameter sampler which was driven by a 50kg hammer into the bottom of a borehole. Earlier, Sir Stanford Fleming (Broms and Flodin, 1988) had proposed a soil investigation method in 1872, in which a steel rod was pushed into the soil and the resistant force was measured. This was probably the first modern static penetrometer. Today, the cone penetration test (CPT) is commonly used as static sounding method in engineering practice, and different cones are available for different purposes.

Each kind of penetration test has advantages and limitations so that they can't be used in all circumstances. This study focuses on the dynamic cone penetrometer (DCP), which is used to assess the mechanical properties of subgrade soils in highway and airport engineering.

1.2 Development of the DCP

The invention of the dynamic cone penetrometer (DCP) was attributed to Scala (1956). The DCP was developed in Australia in response to the need for a simple and rapid device for the characterization of the subgrade soil. The DCP used by Scala included a 9kg (20 pound) hammer with a dropping distance of 508mm (20 inches). A 15.875mm (5/8 inch) diameter rod with a 30 degree angle cone was used to penetrate 762mm (30 inches) into the soil. In his study, Scala tried to find the correlations between DCPT results and CBR, and also between DCPT results and the bearing capacity of soils estimated by a static cone.

In the late 1960's, D.J. Van Vuuren continued to develop the DCP in Pretoria. He used a similar device, except for some differences in dimensions: a 10kg (22-pound) hammer was dropped from a height of 460mm (18.1 inches), forcing a 30 degree cone connected to a (16mm) 0.63 inch diameter rod into the soil up to 1000mm (39.4 inches). DCP tests were preferred to CBR tests in Pretoria, and the DCP was believed to be applicable in soils with CBR values of 1 to 50.

In 1973, the Transvaal Roads Department in South Africa decided to use the DCP as a rapid evaluation device for the extensive evaluation of existing roads. The drop weight of the DCP was 8kg (17.6 pounds) and the falling height was 574 mm (22.6 inches); two kinds of cones with 30 and 60 degree angles were utilized. E.G. Kleyn (1975) evaluated the effects of soil type, plasticity, moisture content, and density on the test results of DCPT. He indicated that these factors affect the DCPT and CBR in similar

ways, and generalized DCP/CBR correlations applicable to the full range of materials tested were proposed. Other researchers developed the relations between DCP and unconfined compressive strength (Bester et al 1977 and Villiers 1980). Kleyn et al. (1982) discussed the application of the DCP to characterization of stabilized materials, evaluation of potentially collapsible soils, use as a construction control method, and use as a structural evaluation technique. They also introduced the concepts of "DCP Structure Number (DSN)" and "Pavement Strength-Balance (PSB)", and developed a pavement design model based on correlations with the Heavy Vehicle Simulator (HVS). Later, Kleyn (1983) used the DCP as a means to optimize pavement rehabilitation.

Livneh and Ishai (1985) refined DCP/CBR correlations in Israel, adapting a device that was used in the South Africa, except for the cone angle, which was 30 degrees. Livneh (1987) presented a comparison of 21 DCP/CBR correlations from Australia, England, South Africa and Israel. He also indicated that the variability associated with DCP testing is less than that associated with "field" CBR testing.

The advancement of the DCP may be attributed primarily to the research done in Australia, New Zealand, South Africa and Israel. The DCP was not accepted in the United States until the early 1980's. Yoder et al (1982) first mentioned the DCP as a technique for the determination of in-situ CBR. His study focused on the use of the Clegg Hammer and presented the DCP/CBR correlations by van Vuuren. Based on the work of Yankelevski and Adin (1980), Chua (1988) developed a model to connect the initial elastic modulus of soils to the penetration resistance of the DCP. Chua and Lytton (1988) mounted an accelerator on the top of the DCP, and used this modified DCP to estimate the hysteretic and the viscous damping ratios in situ. In their study, the DCP is modeled as a series of springs and masses, and the soil as a dashpot. Ayers et al (1989) conducted a series of DCP tests on granular materials in the laboratory, relating the shear strength of granular materials to DCP test data. When comparing compaction methods in narrow subsurface drainage trenches, Ford et al. (1993) utilized the DCP as a control method, indicating that the DCPT results generally correlated well with Proctor compaction data, thus showing promise for evaluating compaction in narrow, granular-backfilled trenches.

Burnham and Johnson (1993) reported the application of the DCP in the projects of the Minnesota Department of Transportation. Little (1996) used the DCP to determine the in-situ strength and to verify the effective stiffness of lime-stabilized soils for backcalculation purposes.

From the above historical review of the development of the DCP, we see that the DCP testing can be applied to the characterization of subgrade and base material properties. The greatest strength of the DCP device lies in its ability to provide quickly and simply a continuous profile of relative soil strength with depth. The small and relatively lightweight design of the DCP enables it to be used in confined areas such as inside buildings, or used at congested sites that would prevent larger testing equipment from being used. The DCP is also ideal for testing through core holes drilled through existing pavement. The applications of the DCP may be summarized as follows: (1) preliminary soil exploration, (2) construction control, (3) structural evaluation of existing pavements, (4) pavement design.

Many factors affect the results of the field and laboratory DCPT testing and were studied by many researchers. Usually those factors are attributed to variability induced by human factors, mechanical conditions, and material factors. For shallow depth (less than about 20cm, which is the meaningful range for subgrade soils), we can identify the following factors:

- (1) human factors (testing procedure and operation);
- (2) mechanical conditions (size of the mold, geometry of the penetrometer, cone apex angle);
- (3) material factors (gradation, density, moisture content).

1.3 Research Objectives

The primary objectives of this study were:

1. establish the correlation of the penetration resistance of the DCP with the dry density and moisture content of subgrade soils, so that these relationships can be used in preliminary exploration, quality control and engineering design;
2. establish the correlation of the DCP penetration resistance with resilient modulus of the subgrade soil, which is an important pavement design parameter.

1.4 Description of the DCP used in this Study

The DCP consists of two 16mm (0.63in) diameter rods. The lower rod, containing an anvil and a replaceable 60° cone tip, is marked at every 5.1mm (0.2 inches). The upper rod contains an 8kg (17.6 lb) drop hammer with a 575mm (22.6 inches) drop distance, an end plug for connection to the lower rod, and a top grab handle. All materials (except the drop hammer) are stainless steel for corrosion resistance.

Operation of the DCP requires two persons, one to drop the hammer and the other to record the depth of penetration. The test begins with the operator "seating" the cone tip by dropping the hammer until the widest part of the cone is just below the testing surface. At this point, the other person records this initial penetration as "Blow 0". The operator then lifts and drops the hammer either one or more times depending upon the strength of the soil at the test location. Following each sequence of hammer drops, a penetration reading is recorded. This process continues until the desired depth of testing is reached, or the full length of the lower rod is buried. The maximum penetration depth is about 1.02m (40 inches). After the testing is completed, a special adapted jack is used to extract the device. The DCP device is shown in Figure 1.1.

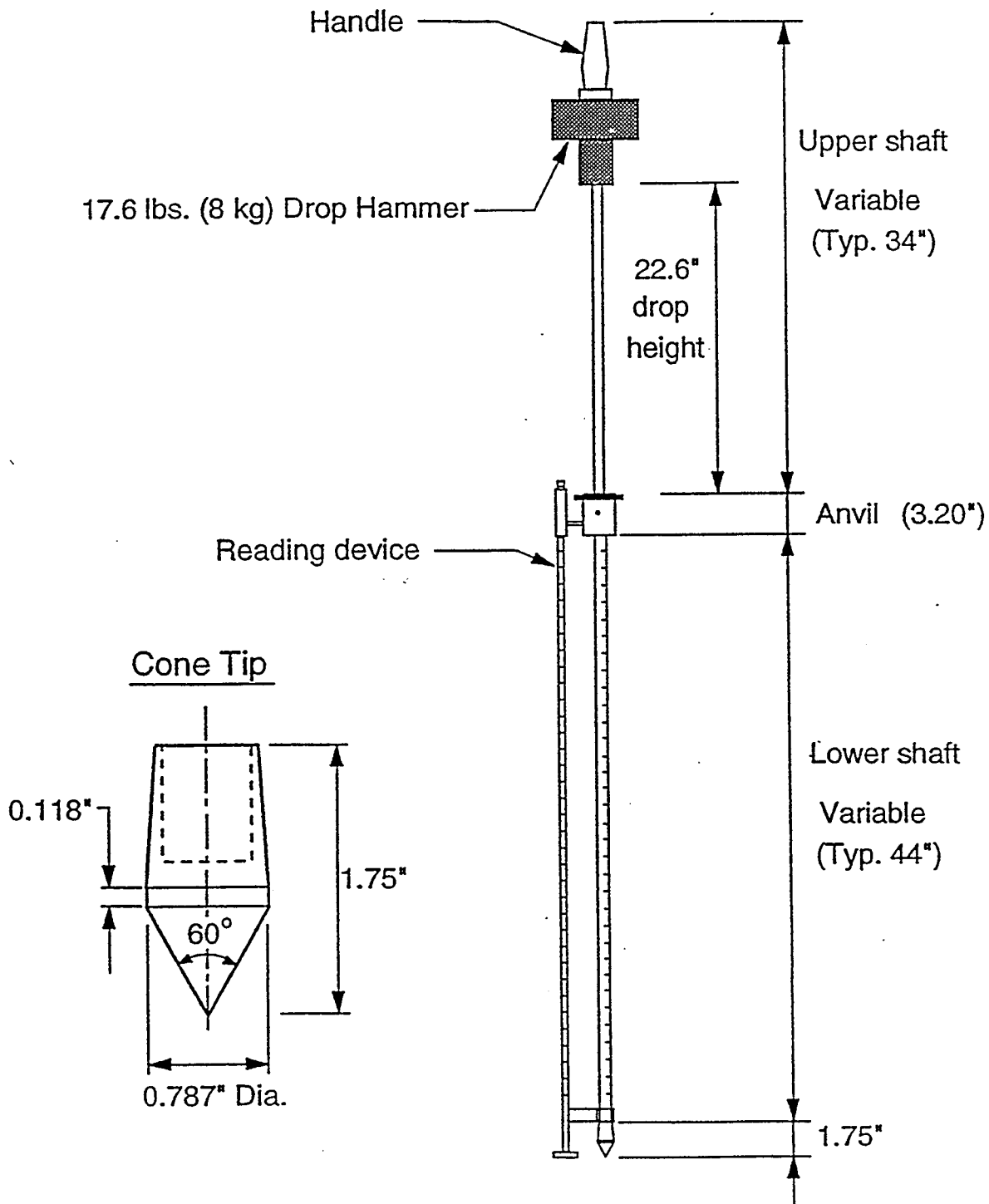


Figure 1.1 The Dynamic Cone Penetrometer
(after the Minnesota Department of Transportation)

Data from a DCP test is processed to produce the penetration index (PI), which is simply the distance that the cone penetrates with each drop of the hammer. The PI is expressed in terms of either inches per blow or millimeters per blow. The penetration index reflects the varying strength and stiffness of different soil layers, but may be directly correlated with a number of common pavement design parameters. Some of these correlations will be described in the next section.

1.5 Existing DCP Correlations

DCP test results have been correlated with other testing results for a broad range of material types.

1.5.1 DCP/CBR Correlations

Many studies have been done on DCP/CBR correlations and numerous relations have been developed. In 1987, Livneh presented 20 DCP/CBR correlations; several of the most accepted correlations are summarized below:

1. $\log\text{CBR}=3.38-0.71(\log\text{PI})^{1.5}$
2. $\log\text{CBR}=4.66-1.32(\log\text{PI})$
3. $\text{CBR}=405.3(\text{PI})^{-1.259}$
4. $\log\text{CBR}=2.0-1.3\log(\text{PI}-0.62)$

PI is the penetration index (mm/blow). Equation 1 was developed from a 30 degree cone tip; the other equations were developed for a 60-degree cone tip.

1.5.2 DCP/Unconfined Compressive Strength Correlation

A graphical relationship between DCP test results, in terms of DN (mm/blow), and q_u is shown in Figure 1.2. The relationship was developed for a broad range of materials.

1.5.3 DCP/SPT Correlation

Livneh and Ishai (1988) developed a relationship between DCP and SPT. The correlation equation took the form:

$$\text{Log}(\text{PI}) = -A + B \log(N_{\text{SPT}})$$

where PI = penetration index (mm/blow), N_{SPT} = SPT blow count.

It should be noted that the above equation is suitable for values of SPT blow count less than 30.

1.5.4 DCP/Shear Strength Correlation for Granular Materials

Ayers et al (1989) conducted the DCP test in the laboratory to determine a relationship between the DCP and the shear strength of granular materials. The equations took the form,

$$\text{DS} = A - B(\text{PI})$$

where DS = deviator stress at failure and PI = penetration index.

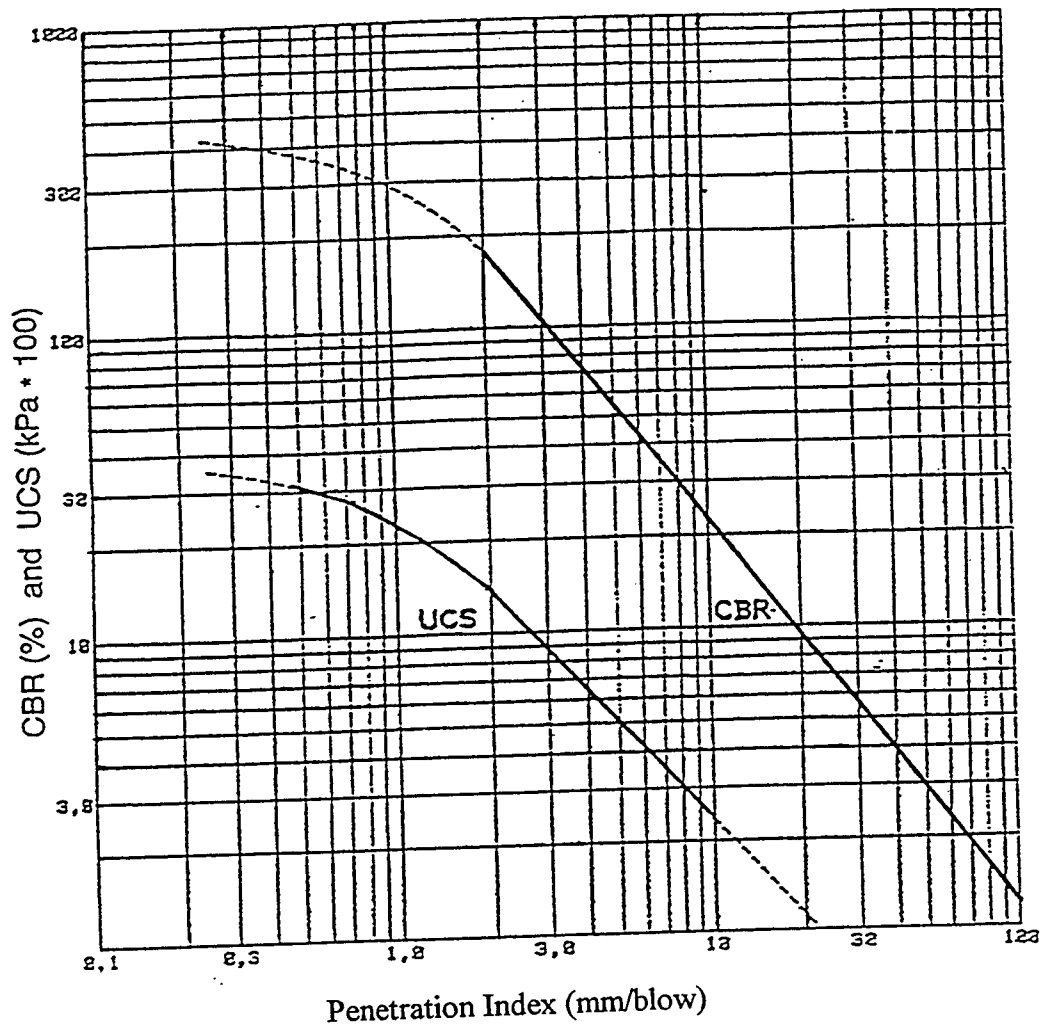


Figure 1.2 The Relationship between Penetration Index and Unconfined Compression Test (after Kleyn, 1983)

1.6 Advantages and Limitations of the DCP

1.6.1 Advantages:

1. The DCP is a simple device, requiring 2 people for its operation, whereas the automated DCP requires only one operator.
2. The DCP is portable and easy to operate; it is not expensive.
3. The testing results are easy to process.
4. The DCP can be used to quickly characterize the subgrade soil; it is suitable for congested areas.
5. The DCPT measurements can be correlated with the shear strength of the subgrade soil or other common design parameters (for example, CBR).

1.6.2 Disadvantages:

1. The DCPT is not yet a standard testing method, although a proposed ASTM standard is being considered.
2. The DCP is not suitable for gravel soils: the DCP rod may be bent during testing. Variability of the results can be expected to be significant in such soils.
3. The DCP is a dynamic test, which means it is somewhat difficult to analyze and interpret.

1.7 Summary

In this chapter, we reviewed the historical development of the DCPT. Like the SPT and other dynamic penetration tests, the DCPT is a destructive testing method. The factors affecting the DCPT test results were discussed. The dynamic cone penetrometer used in this study was described.

The measurement of penetration resistance provides an almost continuous profile of relative shear strength of subgrade soils. The penetration index may be correlated to other regular pavement design parameters, including CBR, SPT and unconfined compression strength. However, the test is dynamic, which introduces difficulties in its analysis and interpretation.

Chapter 2

Testing Program

2.1 Preliminary Test Results

Figure 2.1 shows the results of preliminary testing done at different sites in the summer of 1997 to develop familiarity with the test equipment and better understand the research problem. The test data in this figure are put together independently of soil classification. The data points are rather scattered, and apparently no relationship can be found between penetration index (PI) and dry density or moisture content of soils. So the question arises as to how to reduce this scatter.

2.2 Review of Soil Compaction Concepts

In this study, the DCP is used to determine the mechanical properties of the subgrade soil; however, compaction is often conducted to improve the properties of the subgrade soil, and we focus our study mainly on this compacted soil. So it is necessary to review the properties of compacted soil before we continue.

The compaction tests can be conducted in the laboratory according to ASTM standard. When the dry densities of samples are determined and plotted versus the water contents for each sample, a curve called the compaction curve is obtained. The peak point of the curve corresponds to the maximum dry density and so-called optimum moisture

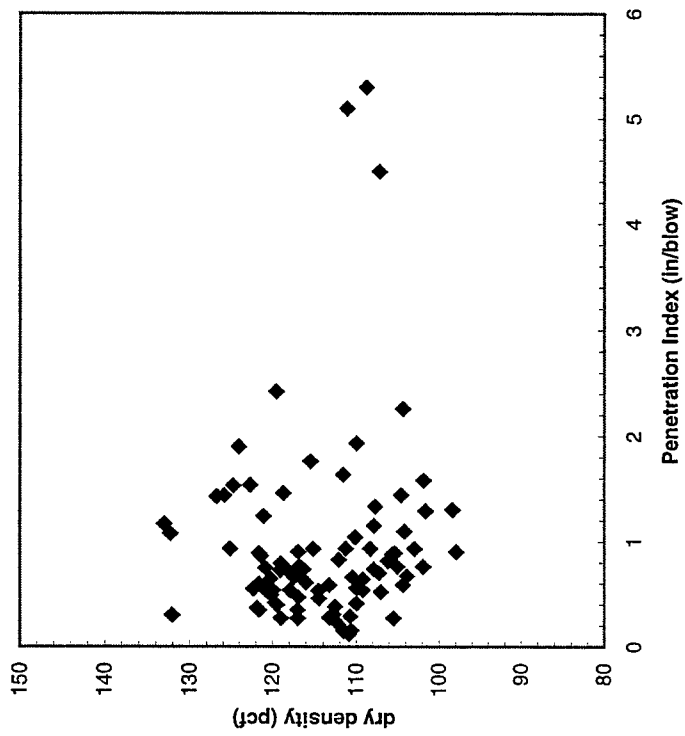


Figure 2.1 The Relationship between Penetration Index and Dry Density from the Testing Results of Summer, 1997

content (OMC). Many scholars did significant study on compacted soil. Lambe (1958) investigated the influence of compaction on clay structure and particle orientation. His study showed that many factors affect compaction: (1) dry density, (2) water content, (3) compactive effort, and (4) soil type (gradation, amount of clay minerals, etc.). The research by these scholars addressed the following: (1) the effect of dry density and moisture content of the compacted soil on shrinkage, swelling, swell-pressures, stress-deformation characteristics, undrained strength, pore-water pressures and effective strength characteristics (Seed et al. 1959); (2) settlement analysis of foundations on saturated clay (Skempton and Bjerrum 1957); (3) hydraulic conductivity of compacted clay (Boynton and Daniel 1985; Day and Daniel 1985); (4) permeability of sandy soils (Juang and Holtz 1986); (5) influence of clods on hydraulic conductivity of compacted clay (Benson and Daniel 1990); (6) water-content-density criteria for compacted soil liners (Daniel Benson 1990); (7) CBR values along compaction curves (Turnbull and Foster, 1957; Faure and Mata, 1994). The fabric of the compacted soil is very complicated, as indicated by Holtz (1981): "at the same compactive effort, with increasing water content, the soil fabric becomes increasingly oriented. Dry of optimum the soils are always flocculated, whereas wet of optimum the fabric becomes more oriented or dispersed". The fabric of the soil affects its properties, such as permeability, compressibility, swelling, and shear strength. So when we use compaction to stabilize soils and improve their engineering behavior, we must note what the desired engineering properties of the fill are: they are not just its dry density and water content, because the desired properties do not necessarily correspond to the maximum dry density or optimum moisture content.

2.3 Testing Philosophy

Let's return to the question posed earlier: how to reduce the scatter in the penetration test data? In order to address that, it is desirable that the dynamic cone

penetration testing be conducted along the compaction curve, and that the penetration resistance along the compaction curve be studied with different compaction efforts. In this way, the contour of the Penetration Index (PI) with respect to dry density and moisture content can be developed, as will be explained in detail later. It is desired to perform the penetration testing along the field compaction curve; however, field compaction testing requires equipment that was not available for this project. As the best alternative, DCPT should be conducted along the compaction curves obtained in the laboratory.

In order to determine the correlation of penetration resistance and resilient modulus, the DCPT is performed in the laboratory and unconfined compression tests on disturbed soil samples are conducted in the laboratory. The relationship between results of unconfined compression testing and resilient modulus proposed by Lee (1993, 1997) is then used to correlate penetration resistance and resilient modulus. A similar approach is followed to correlate field penetration resistance and resilient modulus.

2.4 Testing Procedure

The dynamic cone penetration testing was conducted in the as-compacted subgrade soil. However, there is usually a time gap between the compaction work and the DCPT. The dry density and moisture content were measured with the nuclear gage, and in some sites, the sand cone method was used. The DCPT was performed at the same time and location as the density tests. Because the nuclear gage usually measures the density of the top 152mm (6 inches) of soils (the top lift), the penetration depth of the DCP is also 152mm (6 inches) when the nuclear gage is used.

Disturbed soil samples were collected in the field. Sieve analysis and Atterberg limits testing were conducted on these soils. The laboratory DCPT was conducted on these soils within a 304.8mm (12 inch) diameter metal mold. The soil sample is 304.8mm (12 inch) in diameter, 165.1mm (6.5 inch) in height. Four different compaction energies are applied: 213970 J/m³ , 320940 J/m³ , 427950 J/m³ , 591980 J/m³ (4469 ft.lb/ft³ , 6703

ft.lb/ft³, 8938 ft.lb/ft³ and 12364 ft.lb/ft³). The last energy level corresponds to the standard Proctor compaction test. For the same energy level, samples were made at four different moisture contents in order to obtain a complete compaction curve. The confinement of the wall and the base of the mold has an effect on the penetration testing results. Ayers (1990) studied the confining effect of the mold on the DCPT, and concluded that a diameter of 304.8mm (12 inches) is large enough to eliminate the effect of the confinement. We remain cautious about possible mold boundary effects and believe that field compaction testing is recommended for developing relationships for use in engineering practice. After the laboratory penetration testing, the contour of penetration index PI with respect to dry density and moisture content can be developed.

After the penetration testing, unconfined compression test were performed in the laboratory for clay soils. The disturbed soil samples are 71.12mm (2.8 inch) in diameter and 152.4mm (6 inch) in height. The samples are made in the 71.12mm (2.8 inch) mold with the same compaction energies as those used in the 304.8mm (12 inch) mold. The correlation between the stress associated with 1.0% strain ($S_{u1\%}$) in the unconfined compression test and resilient modulus (M_r) suggested by Lee (1993, 1997) is used to relate the Penetration Index (PI) to resilient modulus (M_r).

2.5 Summary

This chapter reviewed basic soil compaction concepts, and described how the testing program was designed for this study.

In order to develop the relationship between penetration resistance, dry density and moisture content of subgrade soils, DCPT tests were performed in the field and conducted along the compaction curves obtained in the laboratory. Unconfined compression tests were also performed in the laboratory to relate the penetration index to resilient modulus. However, field compaction tests are highly recommended for further development of correlations for use in practice.

Chapter 3

Test Results and Analysis

3.1 Introduction

Field DCPT testing was conducted at 8 different sites. The soils range from clayey sand to sandy lean clay. The information for the testing sites is shown in Table 3.1.1.

3.2 Test Results and Analysis

3.2.1 The Railroad Relocation Project at West Lafayette

The compaction work was finished at 6:00 p.m., 4/18/1998. The DCPT was conducted at 11 am, 4/20/1998, 41 hours later than the compaction work. The compaction was done with a Caterpillar CAT CS563 smooth drum vibratory roller. The dry density and moisture content were measured with the nuclear gage at the same time as the DCPT. During compaction the numbers of passes of the compaction equipment were not controlled. The dry density and moisture content were used for quality control. The field test results are shown in Table 3.2.1. The logs of the DCPT are shown in Figures 3.1 through 3.7. After the field tests, disturbed soil samples were collected for laboratory testing.

The relationships between moisture content, dry density and penetration index from the field tests are shown in Figures 3.8, 3.9, and 3.10, respectively.

Table 3.1.1 Test Sites

No.	Date	Location	Road	Station	Soil Classification
1	4/20/1998	West Lafayette	SR 25	135+75, 136+00, 138+25, 138+50, 138+75, 141+50, 141+75	Clayey Sand
2	5/13/1998	Johnson CO.	I65	32+25 Ramp SWR, 27+50 Ramp SWR, 36+50 Ramp SER	Sandy Silty Clay
3	5/19/1998	Delaware CO.	SR 67	43+485, 43+480, 43+482, 43+490, 43+492	Sandy Lean Clay
4	5/19/1998	Delaware CO.	SR 67	39+790	Sandy Lean Clay
5	6/8/1998	Evansville	SR 62	The Northeast Corner of the Intersection of SR62 and Garvin St.	Clayey Sand
6	7/2/1998	Logansport	US 24 by-pass	438+67, 405-26, 405+2	Sandy Lean Clay
7	7/15/1998	Logansport	SR 24	Northeastern Corner of US35 and SR 24	Sandy Lean Clay
8	7/29/1998	Parke CO.	US 41	9+997, 9+900, 10+003	Silty Sand

Sieve analysis and Atterberg Limits testing were conducted in the laboratory. The sieve analysis results are shown in Figure 3.11. The w_p is 12.4, the w_L is 21, the plasticity index (I_p) is 8.6. The soil is a clayey sand.

As mentioned in the previous chapter, the DCPT was conducted on samples of 30.48cm (12 inches) in diameter, 16.51cm (6.5 inches) in height. Each sample was compacted in three layers. A 44.5N hammer was used to compact the soil from a dropping height of 0.46m. The numbers of blows for each soil layer corresponding to the compaction energies of 213.97×10^3 , 320.94×10^3 , 427.95×10^3 , 591.98×10^3 J/m³ (4469, 6703, 8938, 12364 ft.lb/ft³) are 42, 63, 84, 116 respectively. Test results are shown in Table 3.2.2.

The relationships between moisture content, dry density and penetration index measured in the laboratory are shown in Figure 3.12, 3.13, 3.14 respectively. In order to get more convenient presentation of penetration index, the data in Figure 3.12 and 3.13 are transferred to a plot of dry density versus moisture content. By finding the points of intersection of curves with any horizontal lines in Figure 3.13, it is possible to read a series of corresponding values of moisture content and dry density which correspond to the same penetration index value. These points define a contour of penetration index in a plot of dry density versus moisture content. The contours for this clayey sand is shown in the Figure 3.15. The curves are from laboratory testing; the seven scattered points represent the field testing results.

Analysis:

(1) In the field, the compaction energy was not uniform, because the number of passes of the compaction equipment was not controlled. In Figure 3.8, the scattered data points may be on different compaction curves corresponding to different compaction energies. However, from Figure 3.9 and 3.10, we can still see the trend, i.e., when moisture content decreases or dry density increases, the penetration index decreases.

(2) About 28.8% of soil passes the 200# sieve; the soil is a clayey sand. From Figure 3.12, there are four laboratory compaction curves corresponding to 4 different compaction energies. Under low compaction effort, the dry density increases with increasing moisture content; under high compaction effort, the dry density first increases and then decreases with increasing moisture content. The change in between occurs approximately at a moisture content of 10%.

(3) In Figure 3.13 and 3.14, we can see that higher compaction effort corresponds to lower penetration index. With moisture content and dry density increasing, the penetration index first decreases a little and then increases quickly, which means the shear strength increases a little and then decreases quickly with increasing moisture content and dry density. This phenomenon results from the combined effect of different dry density, moisture content and soil fabric.

(4) In Figure 3.15, we see the contours of PI with respect to moisture content and dry density. This is the relationship between penetration resistance and moisture content and dry density which is required for this project, although this contour is developed from laboratory tests. This contour may be useful in preliminary investigation, quality control or engineering design. However, the field testing data points do not fit the laboratory testing curves. This is expected, because the compaction condition is different between the field and laboratory: the non-uniform compaction energy in the field, the confining effect of the wall of the 12 inch mold, the small impact hammer used in the laboratory, are all complicating factors.

Table 3.2.1 Field DCPT Results for West Lafayette Railroad Relocation Project

State Route: 25, Weather: Sunny, Date: 4/20/1998

Station	Offset	Dry Density (kN/m ³)	M/C (%)	PI (mm/blow)
135+75	7.6m RT	19.10	5.9	11.94
136+00	3.0m RT	22.13	5.6	4.06
138+25	3.0m RT	21.06	6.7	10.92
138+50	3.0m RT	20.45	6.6	5.84
138+75	4.9m RT	20.80	7.6	9.65
141+50	6.1m RT	21.99	6.6	7.11
141+75	5.5m RT	22.73	5.2	4.32

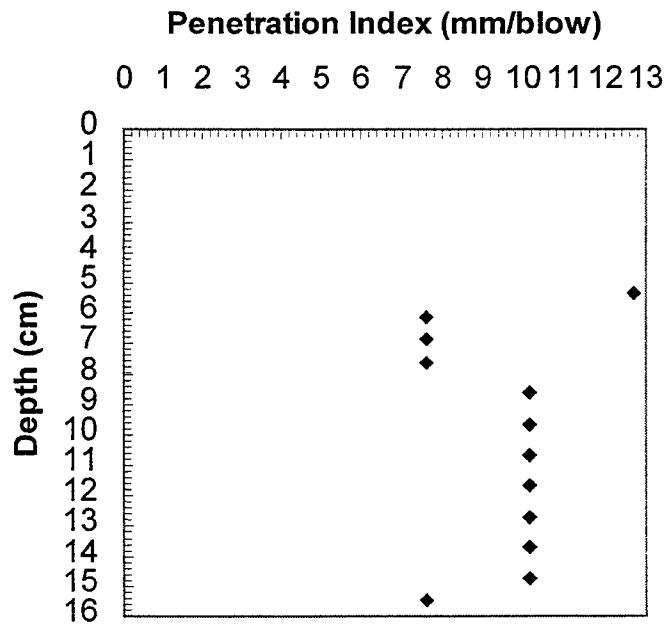


Figure 3.1 The Log of the DCPT (Station: 138+75, Offset: 4.9m RT)

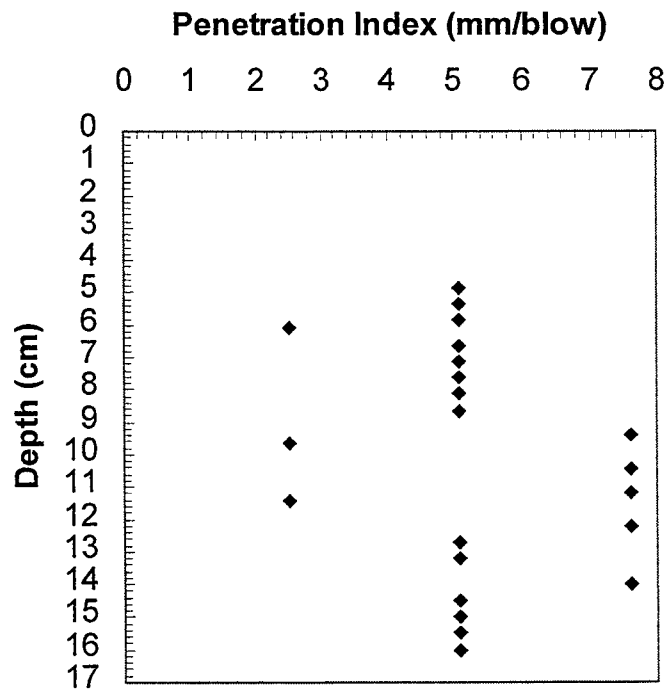


Figure 3.2 The Log of the DCPT (Station: 138+50, Offset: 3.0m RT)

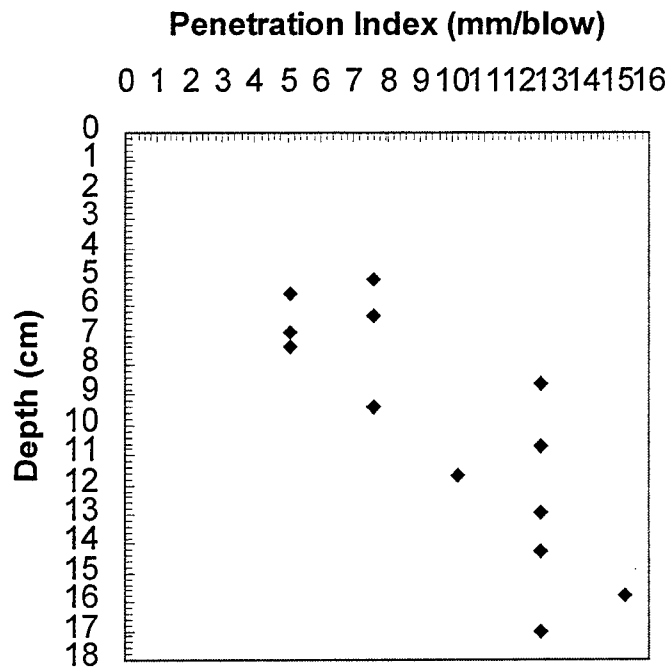


Figure 3.3 The Log of the DCPT (Station: 138+25, Offset: 3.0m RT)

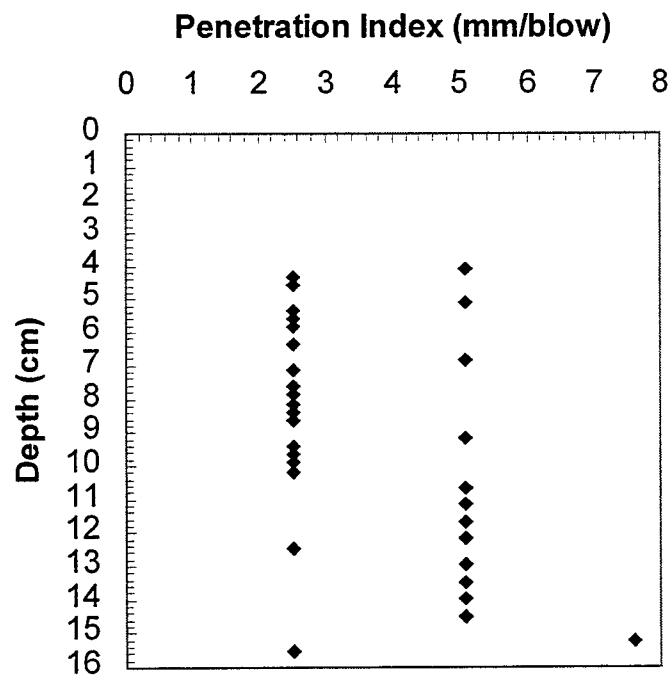


Figure 3.4 The Log of the DCPT (Station: 136+00, Offset: 3.0m RT)

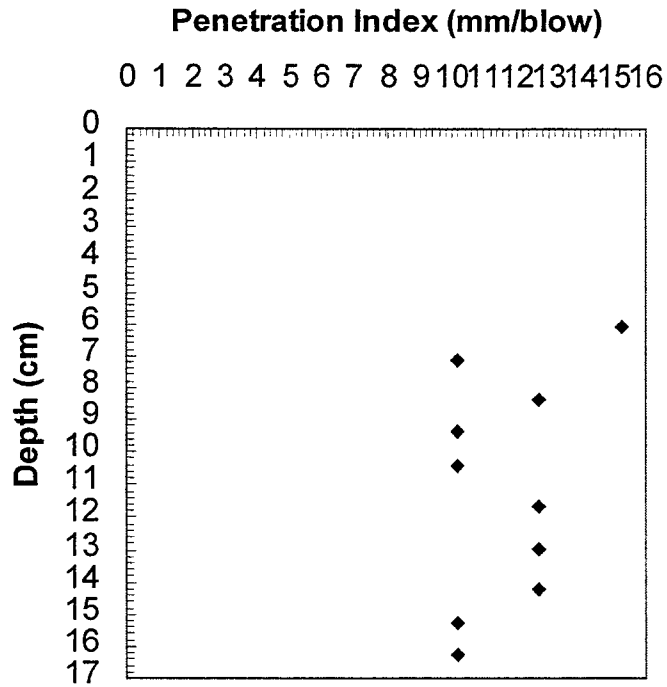


Figure 3.5 The Log of the DCPT (Station: 135+75, Offset: 7.6m RT)

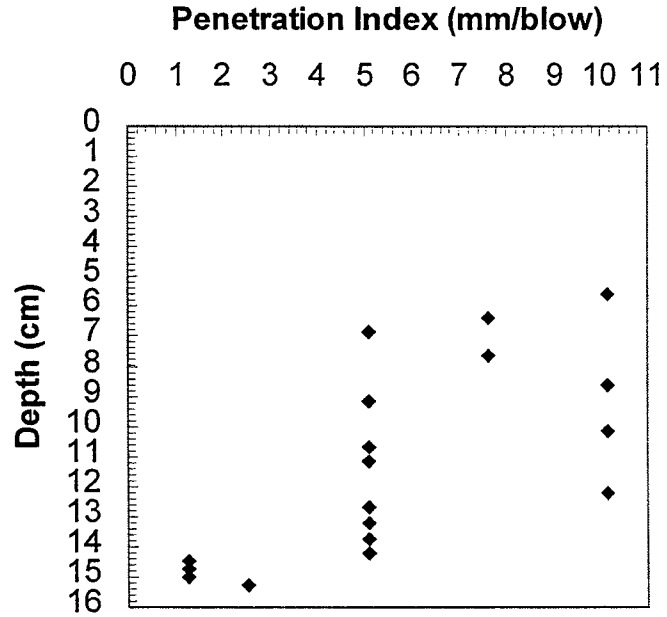


Figure 3.6 The Log of the DCPT (Station: 141+50, Offset: 6.1m RT)

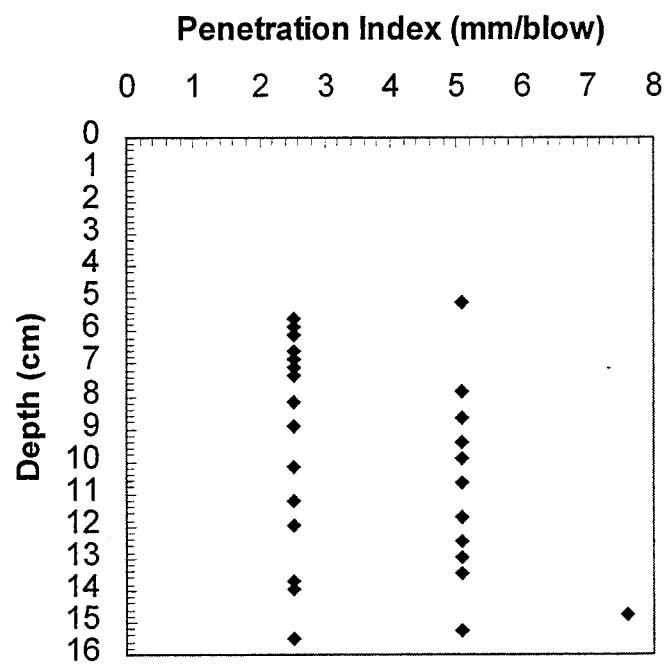


Figure 3.7 The Log of the DCPT (Station: 141+75, Offset: 5.5m RT)

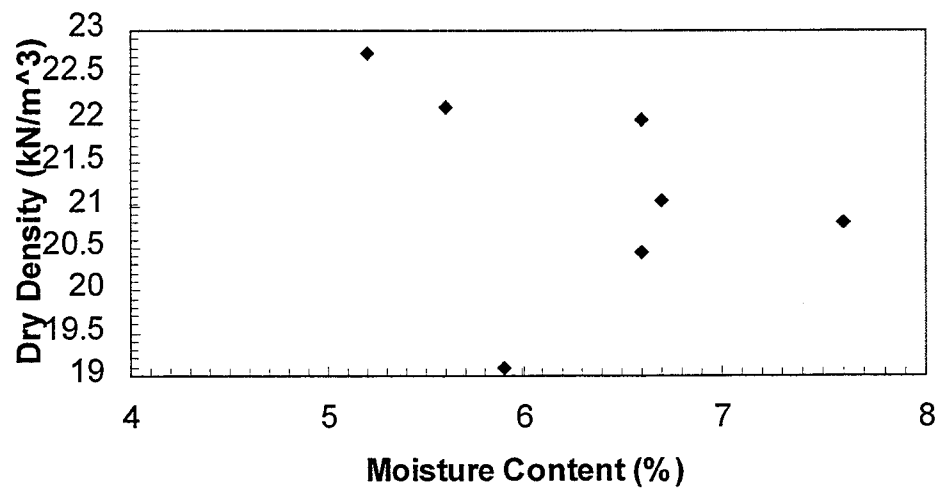


Figure 3.8 The Relationship between Dry Density and Moisture Content from Field DCPT for West Lafayette Railroad Relocation Project

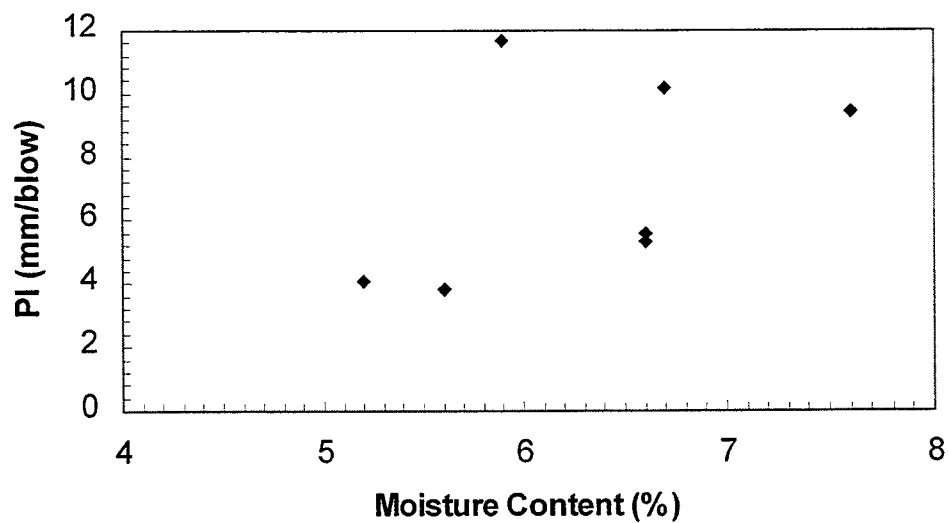


Figure 3.9 The Relationship between Penetration Index and Moisture Content From Field DCPT for West Lafayette Railroad Relocation Project

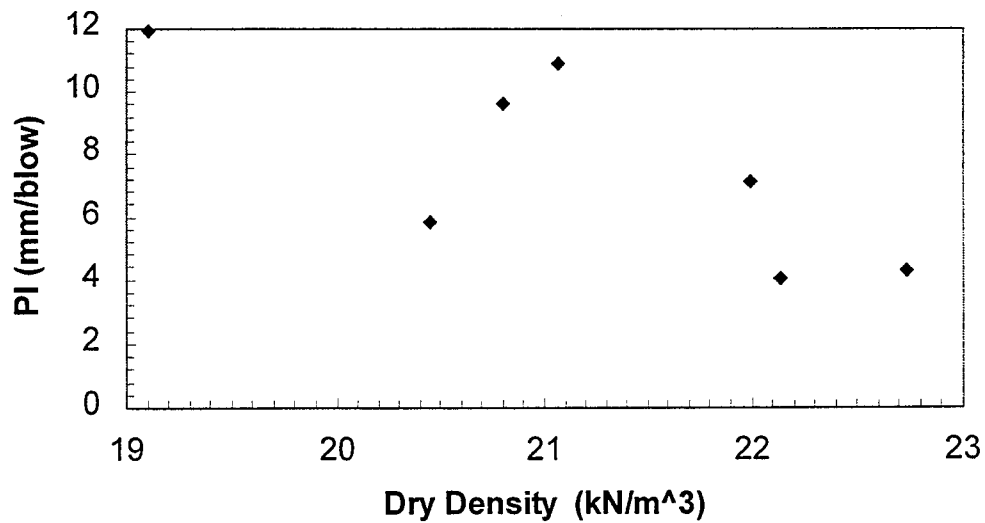


Figure 3.10 The Relationship between Penetration Index and Dry Density from Field DCPT for West Lafayette Railroad Relocation Project

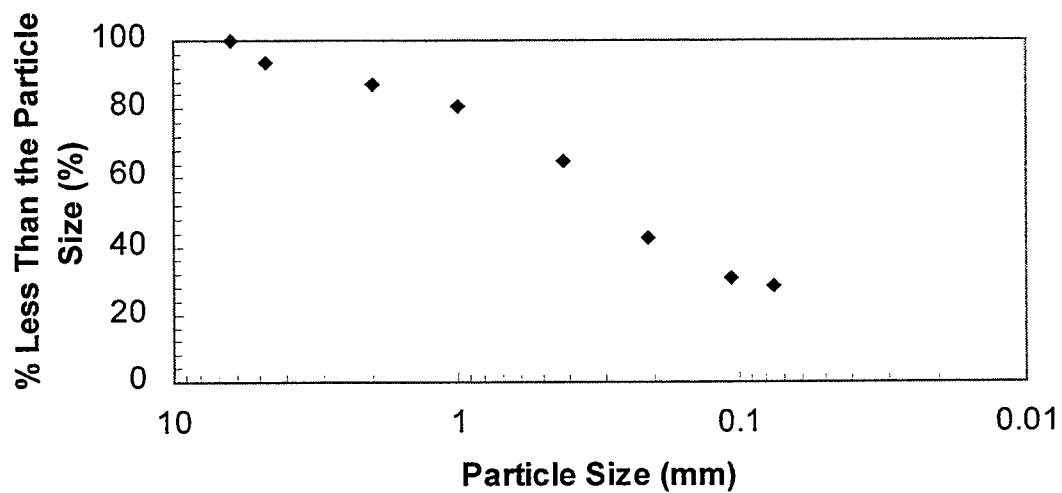


Figure 3.11 The Results of Sieve Analysis for West Lafayette Railroad Relocation Project

Table 3.2.2 The Results of the Laboratory DCPT for West Lafayette Railroad Relocation Project

Compaction Energy ($\times 10^3 \text{ J/m}^3$)	213.97		213.97		320.94		427.95		427.95		591.98		591.98	
	γ_d (kN/m^3)	PI (mm/blow)	γ_d (kN/m^3)	PI (mm/blow)	γ_d (kN/m^3)	PI (mm/blow)	γ_d (kN/m^3)	PI (mm/blow)	γ_d (kN/m^3)	PI (mm/blow)	γ_d (kN/m^3)	PI (mm/blow)	γ_d (kN/m^3)	PI (mm/blow)
5.4	15.70	30.48	16.41	21.08	17.16	16.51	18.15	16.51	17.16	16.51	18.15	16.51	17.16	9.65
8.04	17.26	19.05	18.58	13.46	19.43	10.92	19.79	10.92	19.43	10.92	19.79	10.92	19.43	7.62
9.71	18.08	25.15	19.79	22.86	20.36	21.34	20.52	21.34	20.36	21.34	20.52	21.34	20.36	21.08
11.45	18.83	124.46	19.57	81.28	20.22	86.36	20.60	86.36	20.22	86.36	20.60	86.36	20.22	81.28

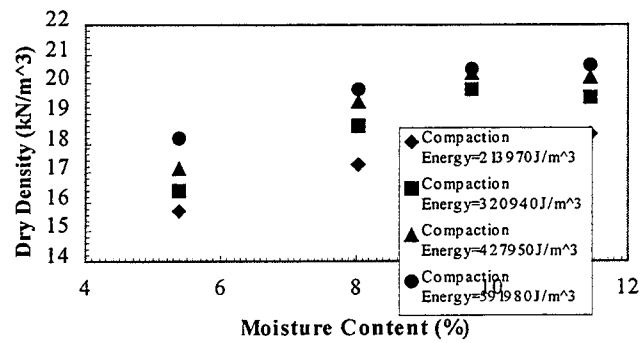


Figure 3.12 The Relationship between Dry Density and Moisture Content from the Laboratory DCPT for West Lafayette Railroad Relocation Project

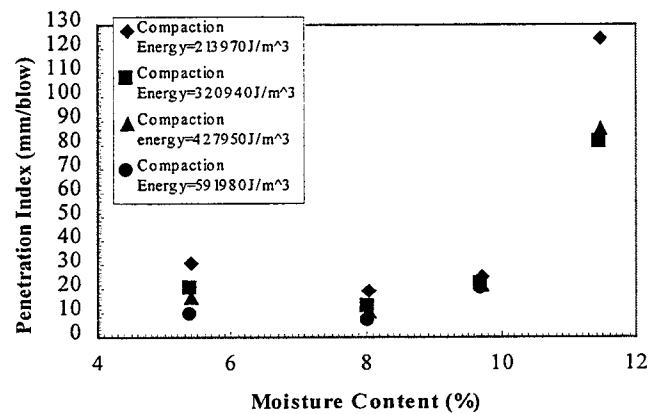


Figure 3.13 The Relationship between Penetration Index and Moisture Content from the Laboratory DCPT for West Lafayette Railroad Relocation Project

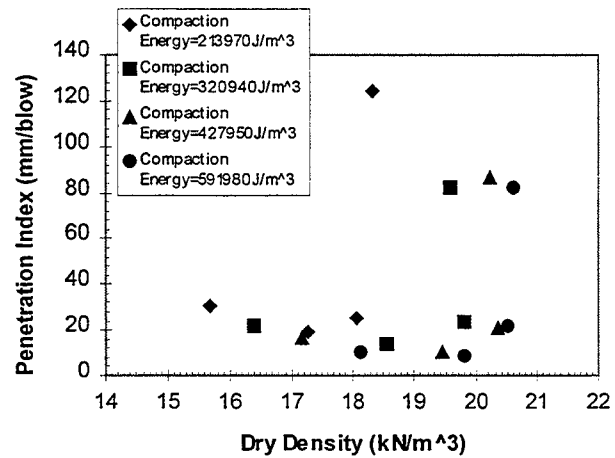


Figure 3.14 The Relationship between Penetration Index and Dry Density from the Laboratory DCPT for West Lafayette Railroad Relocation Project

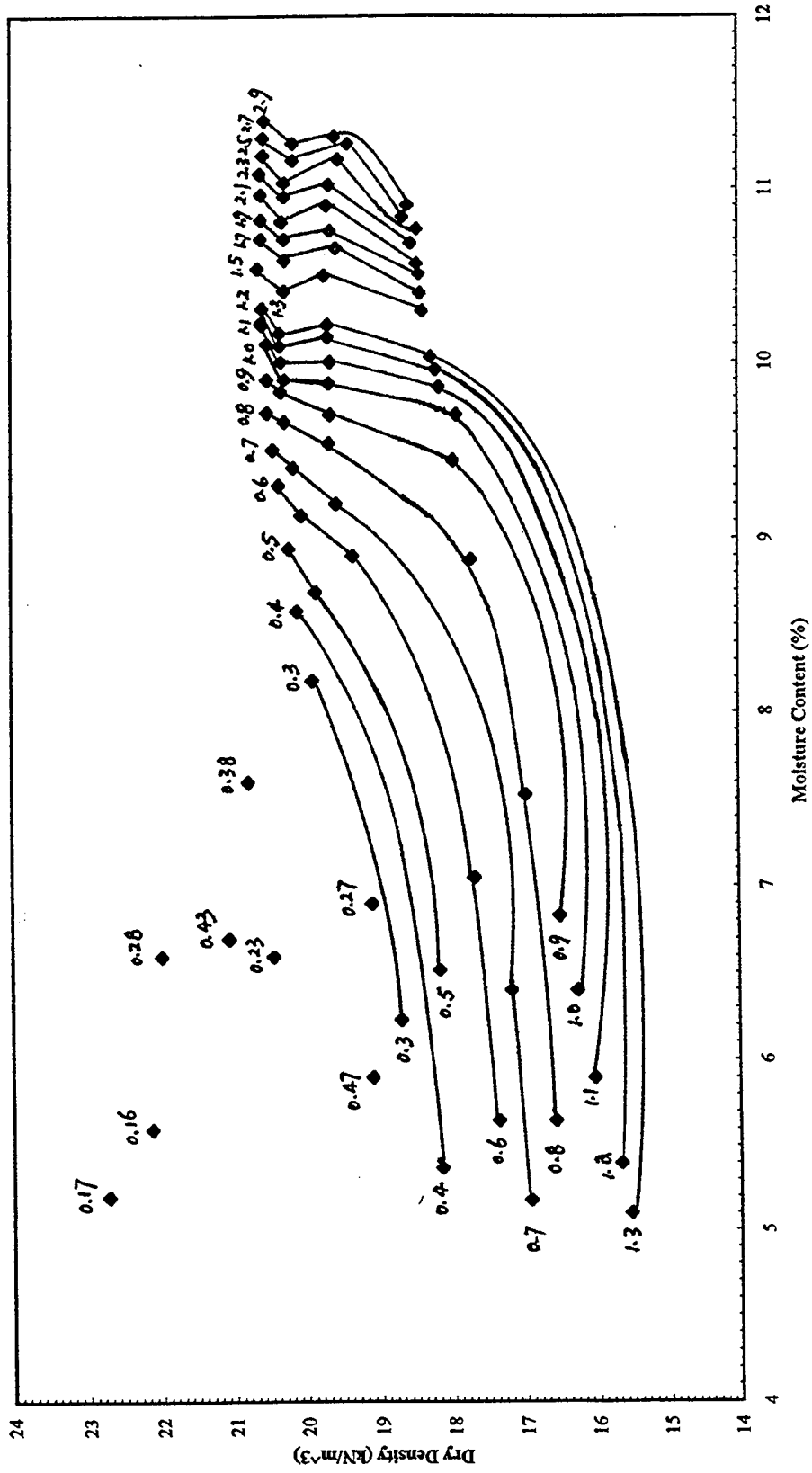


Figure 3.15 Contour of Penetration Index for West Lafayette Railroad Relocation Project (Unit of PI: x25.4mm/blow)

3.2.2 The New Interchange of I65 at Johnson CO.

The DCPT was performed just after compaction. In the compaction work, there were 4 passes of a Caterpillar CAT 815F sheepsfoot roller. The nuclear gage was utilized to measure the dry density and moisture content. The field test results are shown in Table 3.2.3. And the DCPT logs are shown in Figures 3.16 through 3.22.

The relationships between moisture content, dry density and field penetration index are shown in Figures 3.23, 3.24 and 3.25, respectively.

Sieve analysis and Atterberg Limits test were conducted in the laboratory. The sieve analysis results are shown in Figure 3.26. the w_p is 13.58, The w_L is 20.25, the plasticity index (I_p) is 6.67. The soil is a sandy silty clay (CL-ML).

The laboratory DCPT was conducted in the same way as mentioned previously. The test results are shown in Table 3.2.4.

The relationships between moisture content, dry density and penetration index from the laboratory DCPT are shown in Figures 3.27, 3.28 and 3.29, respectively. The contours of PI with respect to dry density and moisture content from the laboratory testing was developed in the same way as mentioned in the previous section, as shown in Figure 3.30.

Unconfined compression tests were also conducted in the laboratory; the samples were 7.112cm (2.8 inch) in diameter and 15.24 cm (6 inch) in height. The compaction energies were the same as the soil sample in the 30.48 cm (12 inch) mold. Each sample consisted of 3 layers. The hammer weight was 24.5N and the drop distance was 0.305m. The number of blows for each soil layer is shown in the Table 3.2.5.

The test results of unconfined compression test are shown in Table 3.2.6.

Table 3.2.3 The Field DCPT Results at the New Interchange of I65 in Johnson CO.

Road: I65, Weather: Sunny, Date: 5/13/1998

Station	Offset	Dry Density (kN/m ³)	M/C (%)	PI (mm/blow)
32+25 Ramp SWR	3.0m RT	18.57	9.5	74.42
27+50 Ramp SWR	3.0m RT	18.86	11.8	93.98
36+50 Ramp SER	3.0m RT	17.53	8.8	72.90
36+50 Ramp SER	4.6m RT	17.79	8.3	105.66
36+45 Ramp SER	3.0m RT	18.00	9.3	100.08
36+45 Ramp SER	4.6m RT	19.12	8.5	42.67
36+48 Ramp SER	3.0m RT	18.52	7.2	45.21

Table 3.2.4 The Results of the Laboratory Penetration Testing for I65 Interchange Soil in Johnson CO.

Compaction Energy ($\times 10^3 \text{ J/m}^3$) M/C (%)	213.97	213.97	320.94	320.94	427.95	427.95	591.98	591.98
	γ_d (kN/m^3)	PI (mm/blow)	γ_d (kN/m^3)	PI (mm/blow)	γ_d (kN/m^3)	PI (mm/blow)	γ_d (kN/m^3)	PI (mm/blow)
8.46	15.11	25.4	15.82	16.00	16.57	11.94	17.32	8.64
7.96	15.98	18.29	16.65	11.18	17.43	8.64	18.24	6.86
11.33	16.39	18.29	17.30	13.46	18.26	11.94	19.29	9.65
13.48	17.39	29.97	18.25	24.89	19.26	24.38	19.76	23.37

Table 3.2.5 Number of Blows for Each Soil Layer

Compaction Energy ($\times 10^3$ J/m ³)	Layer 1	Layer 2	Layer 3
213.97	6	6	7
320.94	9	10	10
427.95	12	13	13
591.98	17	18	18

The relationships between moisture content, dry density and the shear stress $S_{u1.0\%}$ at 1% strain measured in the unconfined compression test are shown in Figures 3.31, 3.32 and 3.33, respectively. Based on these results, the contours of $S_{u1.0\%}$ with respect to moisture content and dry density are developed, as shown in Figure 3.34. The corresponding PI values can be found in Figure 3.30. The results for $S_{u1.0\%}$, penetration index and resilient modulus are shown in Table 3.2.7.

According to the results of Lee (1993), the correlation between $S_{u1.0\%}$ and Resilient Modulus (M_r) is

$$M_r = 695.3604S_{u1.0\%} - 5.92966S_{u1.0\%}^2$$

This relationship is used to correlate PI to M_r .

The relationships between PI and $S_{u1.0\%}$, and between PI and M_r are shown in Figure 3.35 and Figure 3.36.

Analysis:

(1) In Figure 3.23, a clear relationship between moisture content and dry density from field testing is not evident; in Figures 3.24 and 3.25 the same tendency exists, as mentioned before, i.e., the penetration index increases with increasing moisture content or decreasing dry density.

(2) The soil is a sandy silty clay; however, an OMC is not evident from the laboratory compaction tests for the range of water contents found in the field compaction. From the available data (Fig. 3.23, 3.24) it is not possible to know what the target values were for field compaction.

(3) In Figures 3.28 and 3.29 for the laboratory DCPT, higher compaction effort corresponds to lower penetration index. With increasing moisture content and dry density, the penetration index decreases first and then increases at the moisture content of about 10%.

(4) In Figure 3.30, the field DCPT data points do not fit the contours from the laboratory DCPT; the reasons are the same as previously discussed. The contours for this sandy silty clay is different from that of clayey sand, but the shape is quite similar.

(5) As shown in Figure 3.31, the compaction curves from 2.8 inch samples used in unconfined compression tests are different from those obtained for the size samples used in laboratory DCPT testing. The reason is obvious: the 2.8 inch mold provides stronger confining effect than the 12 inch mold. The dry densities for the 2.8 inch mold are higher than those for the 12 inch mold.

(6) In Figure 3.32, $S_{u1.0\%}$ first increases and then decreases when the moisture content increases. The contours of $S_{u1.0\%}$ were also developed; as shown in Figure 3.34, the shapes of the $S_{u1.0\%}$ contours are similar to those of the PI contours lines.

(7) From Figure 3.35, the relationship between $S_{u1.0\%}$ and the penetration index contains significant scatter. When $S_{u1.0\%}$ increases, the penetration index decreases. Using the correlation suggested by Lee(1993), we can establish the relationship between PI and M_r , as shown in Figure 3.36.

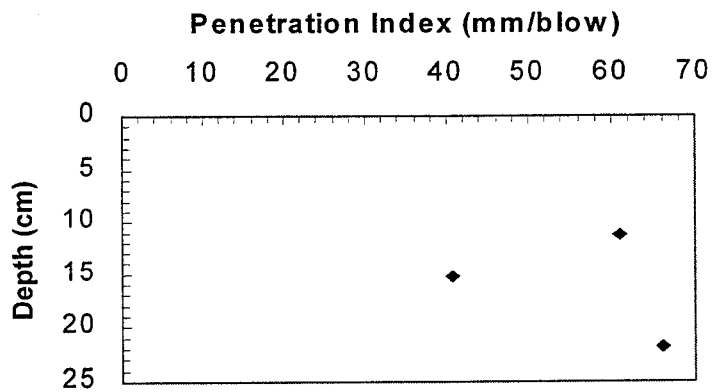
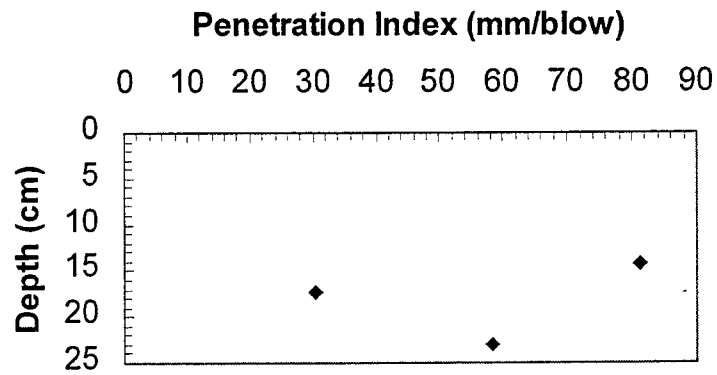
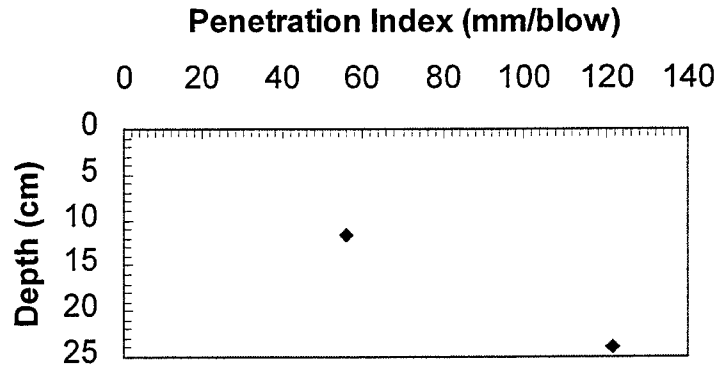


Figure 3.16 The log of the DCPT (Station: 32+25 Ramp SWR, Offset: 3.0m RT)

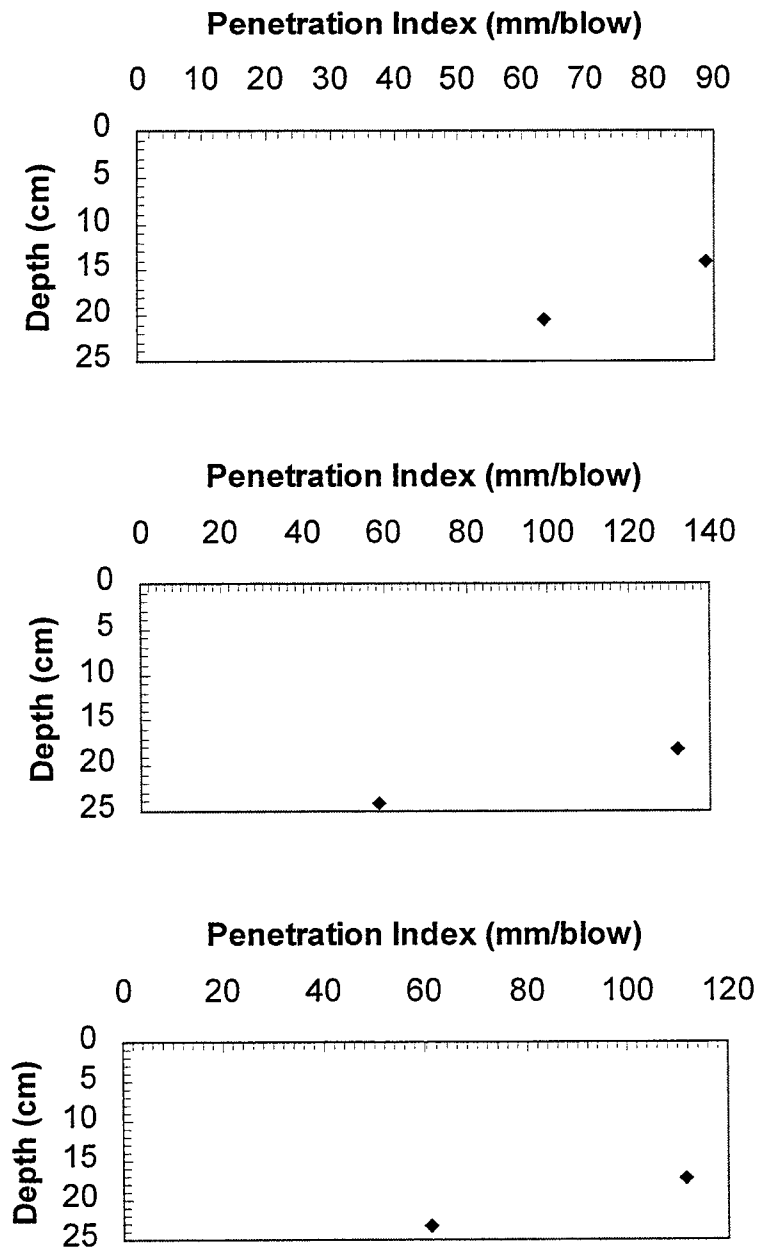


Figure 3.17 The log of the DCPT (Station: 27+50 Ramp SWR, Offset: 3.0m RT)

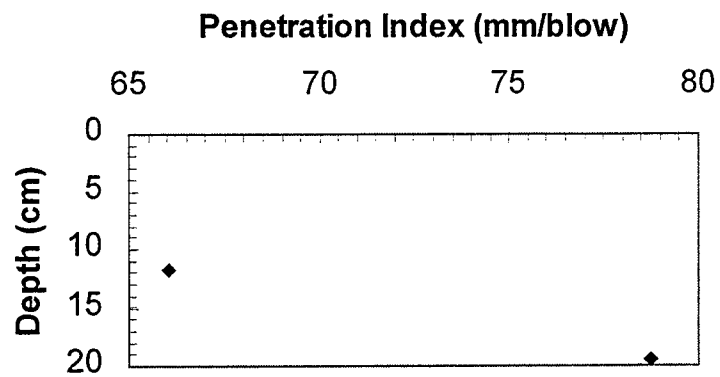


Figure 3.18 The log of the DCPT (Station: 36+50 Ramp SWR, Offset: 3.0m RT)

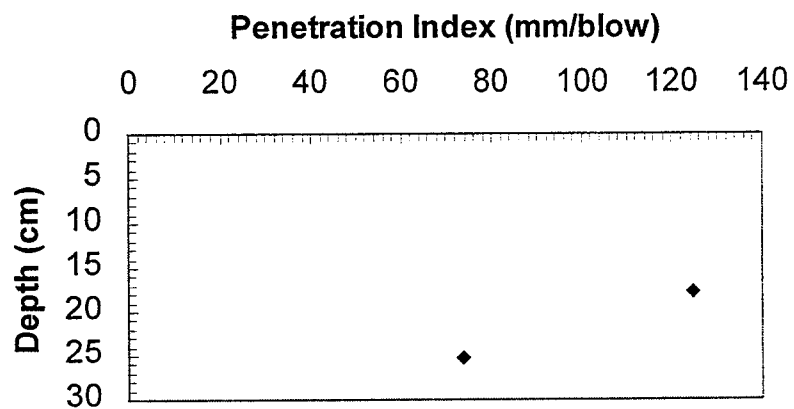


Figure 3.19 The log of the DCPT (Station: 36+50 Ramp SWR, Offset: 4.6m RT)

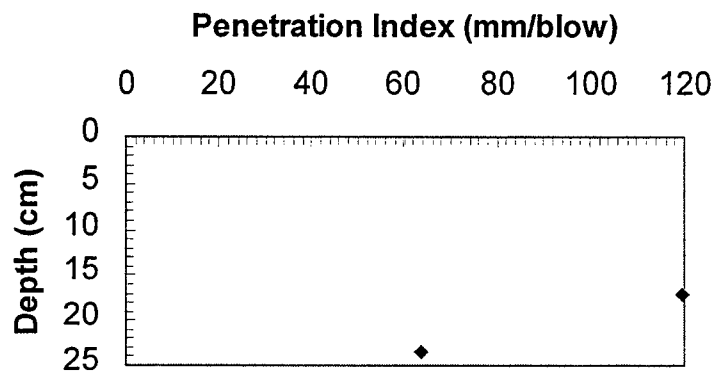


Figure 3.20 The log of the DCPT (Station: 36+45 Ramp SWR, Offset: 3.0m RT)

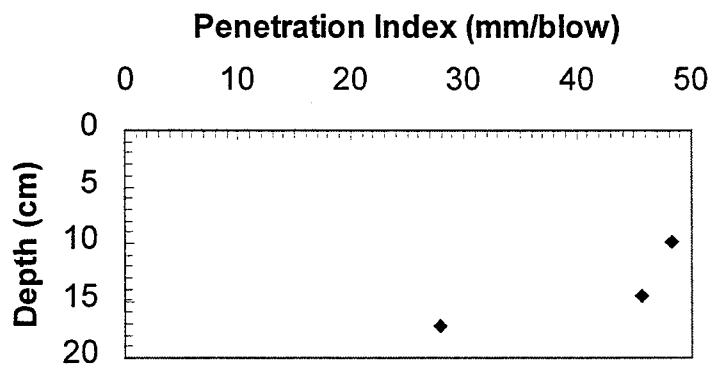


Figure 3.21 The log of the DCPT (Station: 36+45 Ramp SWR, Offset: 4.6m RT)

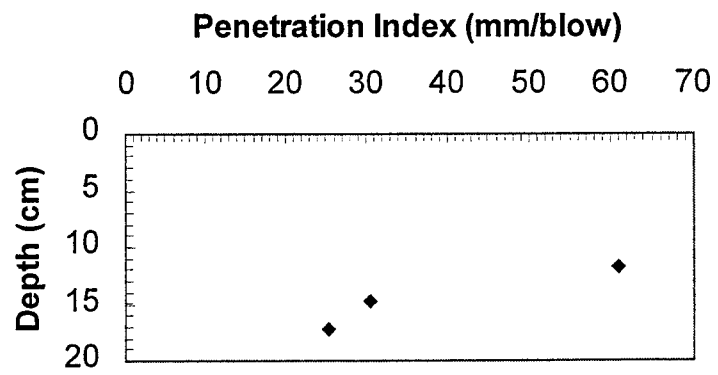


Figure 3.22 The log of the DCPT (Station: 36+48 Ramp SWR, Offset: 3.0m RT)

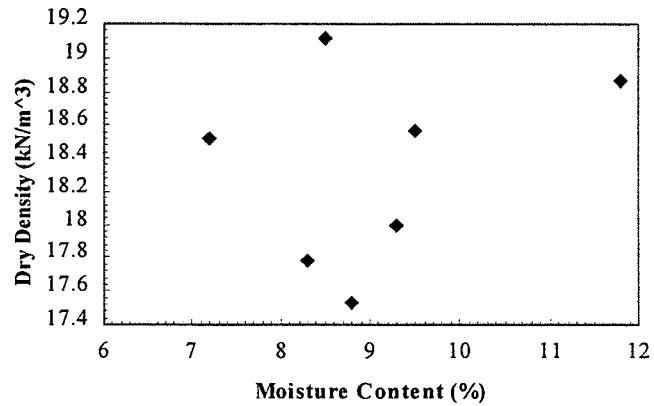


Figure 3.23 The Relationship between Dry Density and Moisture Content from Field DCPT for the New Interchange of I65 in Johnson CO., IN

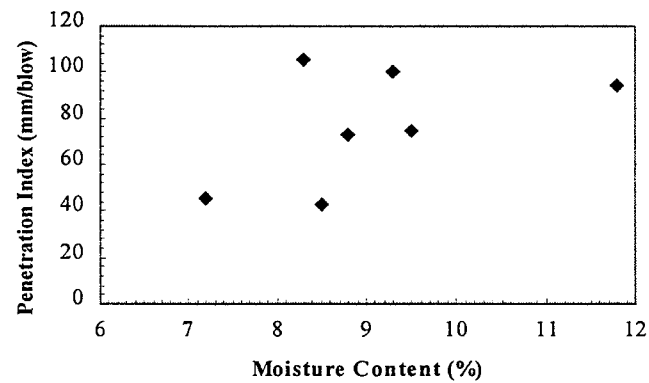


Figure 3.24 The Relationship between Penetration Index and Moisture Content from Field DCPT for the New Interchange of I65 in Johnson CO., IN

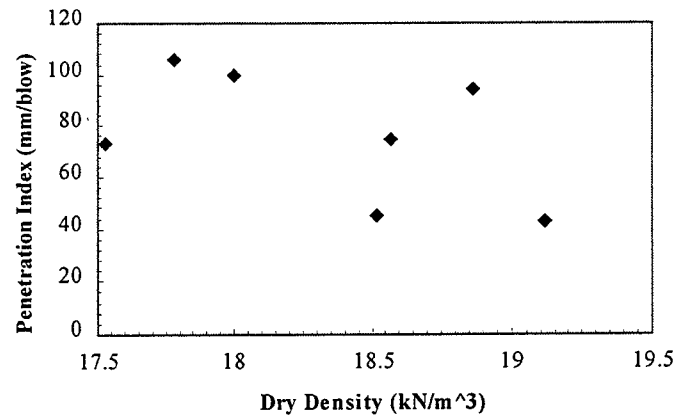


Figure 3.25 The Relationship between Penetration Index and Dry Density from Field DCPT for the New Interchange of I65 in Johnson CO., IN

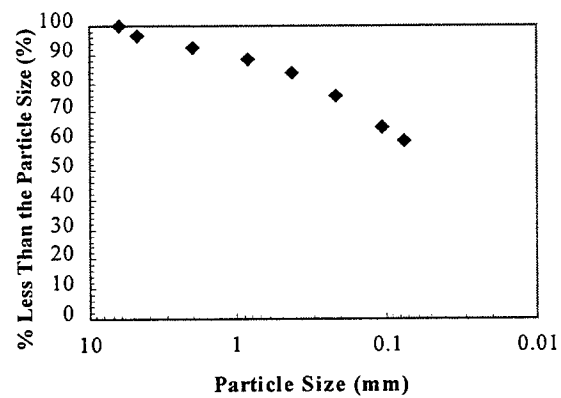


Figure 3.26 The Results of Sieve Analysis for the New Interchange of I65 in Johnson CO., IN

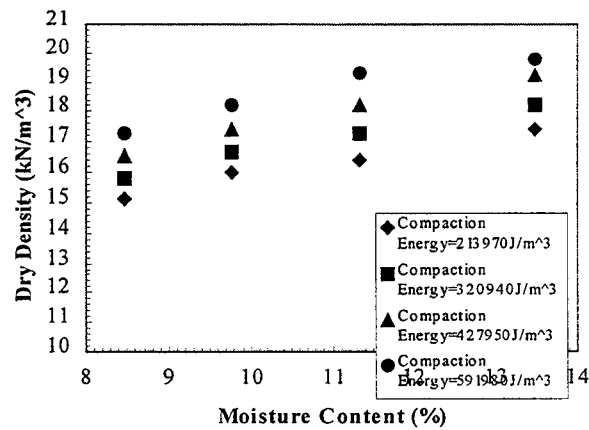


Figure 3.27 The Relationship between Dry Density and Moisture Content from the Laboratory DCPT for the New Interchange of I65 in Johnson CO., IN

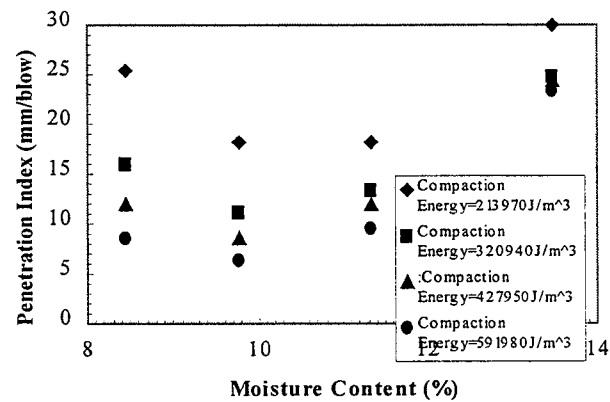


Figure 3.28 The Relationship between Penetration Index and Moisture Content from the Laboratory DCPT for the New Interchange of I65 in Johnson CO., IN

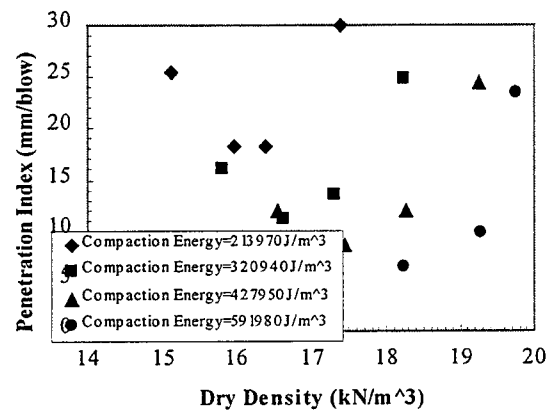


Figure 3.29 The Relationship between Penetration Index and Dry Density from the Laboratory DCPT for the New Interchange of I65 in Johnson CO., IN

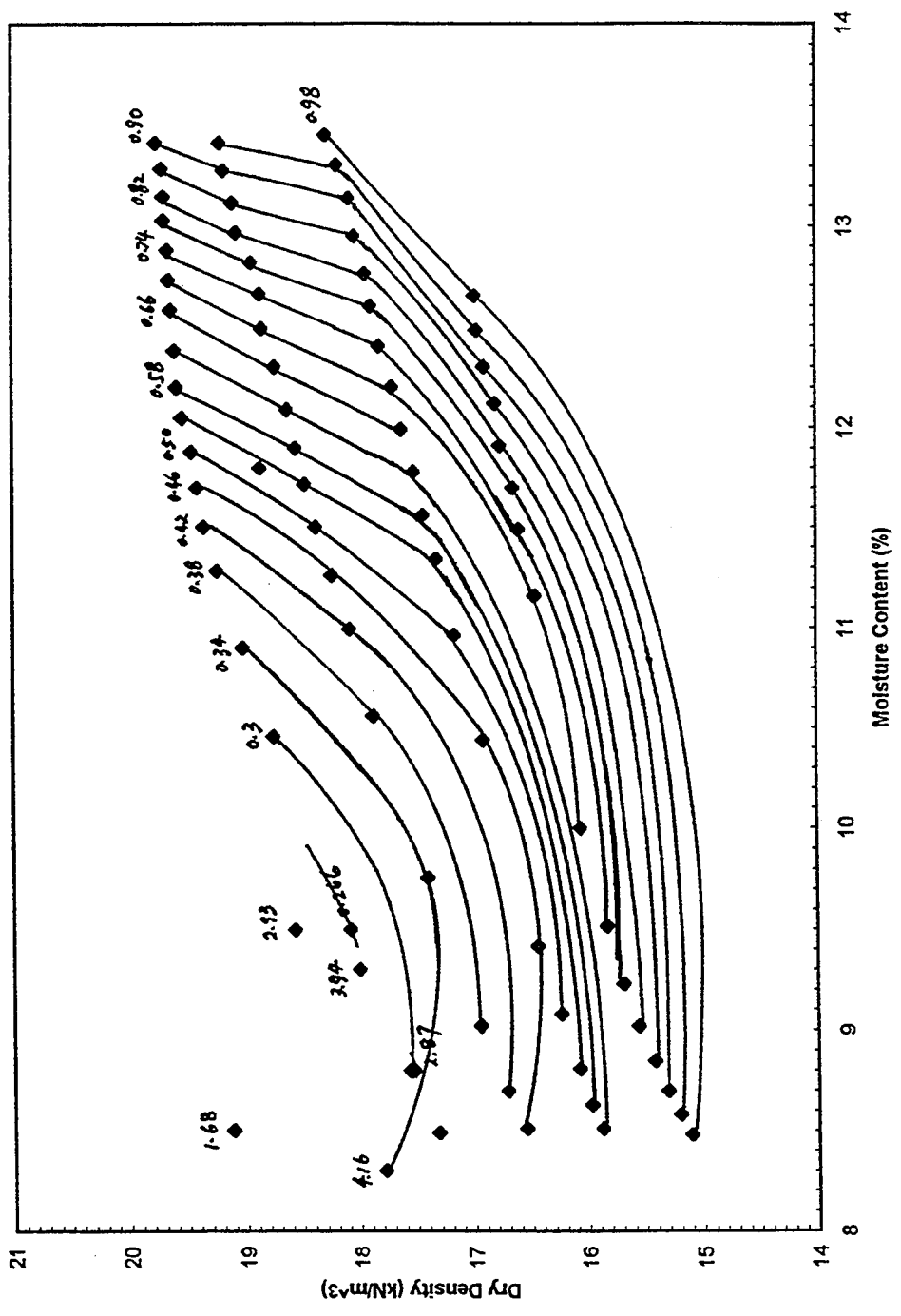


Figure 3.30 Contour of Penetration Index for the New Interchange of I65 in Johnson CO., IN (Unit of PI: $\times 25.4\text{mm/blow}$)

Table 3.2.6 The Test Results of Unconfined Compression Test

Compaction Energy ($\times 10^3 \text{J/m}^3$)	213.37	213.37	320.94	320.94	427.95	427.95	591.98	591.98
M/C (%)	γ_d (kN/m^3)	$Su_{1.0\%}$ (kN/m^2)	γ_d (kN/m^3)	$Su_{1.0\%}$ (kN/m^2)	γ_d (kN/m^3)	$Su_{1.0\%}$ (kN/m^2)	γ_d (kN/m^3)	$Su_{1.0\%}$ (kN/m^2)
8.46	17.12	11.40	17.40	11.84	18.10	13.60	18.75	13.79
7.96	17.43	13.31	18.01	19.03	18.27	22.41	18.56	26.55
11.33	18.00	9.31	18.56	17.24	18.78	18.00	19.31	18.48
13.48	18.42	6.62	18.94	6.14	19.08	5.03	19.26	1.82

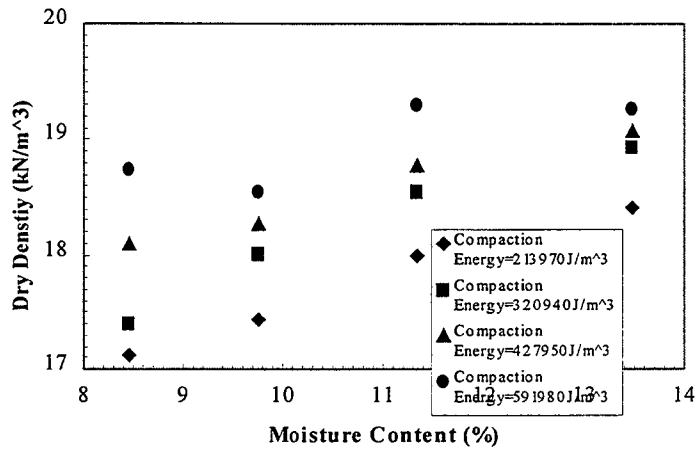


Figure 3.31 The Relationship between Moisture Content and Dry Density from Unconfined Compression Tests for the New Interchange of I65 in Johnson CO. IN

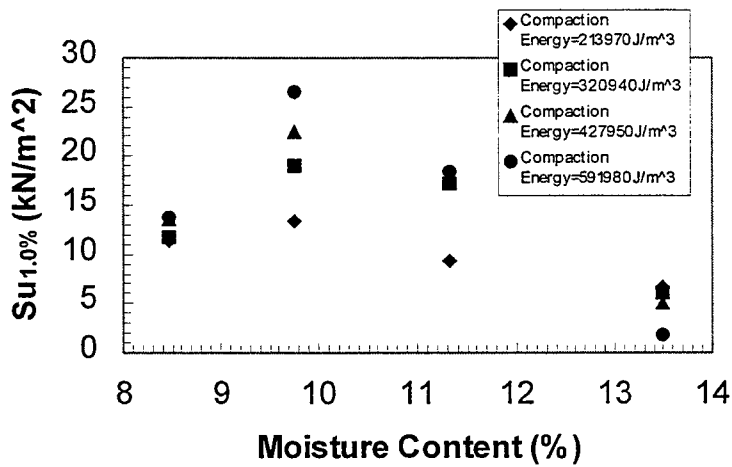


Figure 3.32 The Relationship between Moisture Content and S_{u1.0%} for the New Interchange of I65 in Johnson CO., IN

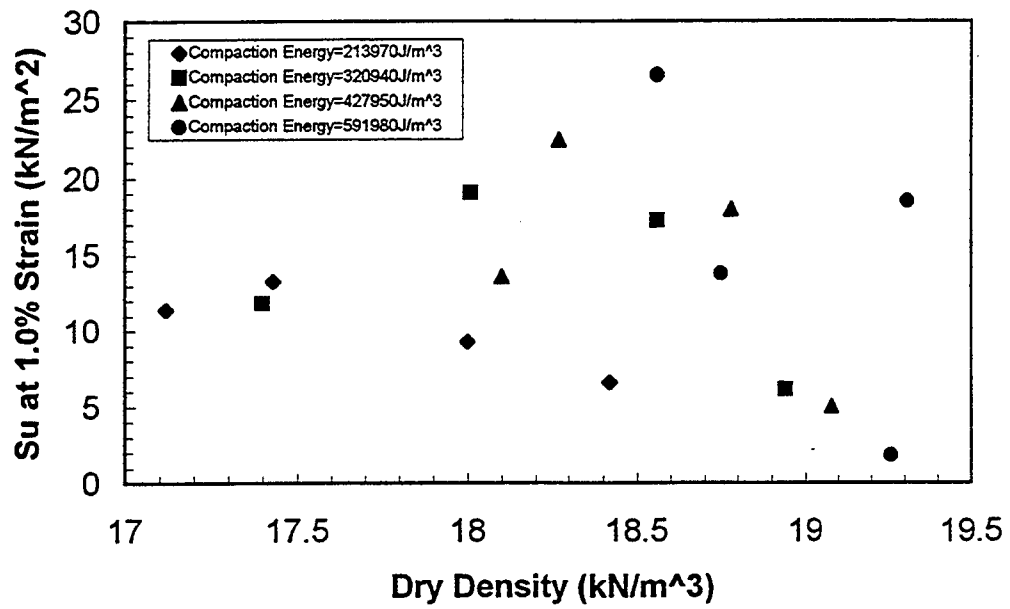


Figure 3.33 The Relationship of Dry Density and $S_{u1.0\%}$ for the New Interchange of I65 in Johnson CO., IN

Table 3.2.7 The Relationship between $S_{u1,0\%}$, Penetration Index and Resilient Modulus

Compaction Energy ($\times 10^3$ J/m ³)	213.97	213.97	213.97	213.97	320.94	320.94	320.94	320.94
M/C (%)								
	γ_d (kN/m ³)	$S_{u1,0\%}$ (kN/m ²)	PI (mm/blow)	M_r (kN/m ²)	γ_d (kN/m ³)	$S_{u1,0\%}$ (kN/m ²)	PI (mm/blow)	M_r (kN/m ²)
8.46	17.12	11.40	9.14	7818.72	17.40	11.84	8.38	8112.11
7.96	17.43	13.31	18.03	9101.61	18.01	19.03	70.10	12922.13
11.33	18.00	9.31	12.19	6398.42	18.56	17.24	11.68	11731.43
13.48	18.42	6.62	25.15	4565.32	18.94	6.14	24.64	4234.98
Compaction Energy (J/m ³)	427.95	427.95	427.95	427.95	591.98	591.98	591.98	591.98
M/C (%)								
	γ_d (kN/m ³)	$S_{u1,0\%}$ (kN/m ²)	PI (mm/blow)	M_r (kN/m ²)	γ_d (kN/m ³)	$S_{u1,0\%}$ (kN/m ²)	PI (mm/blow)	M_r (kN/m ²)
8.46	18.10	13.60	6.10	9296.32	18.75	13.79	---	---
7.96	18.27	22.41	6.86	15151.14	18.56	26.55	---	---
11.33	18.78	18.00	10.92	12235.87	19.31	18.48	9.91	12556.35
13.48	19.08	5.03	24.38	3478.39	19.26	1.82	24.38	1262.96

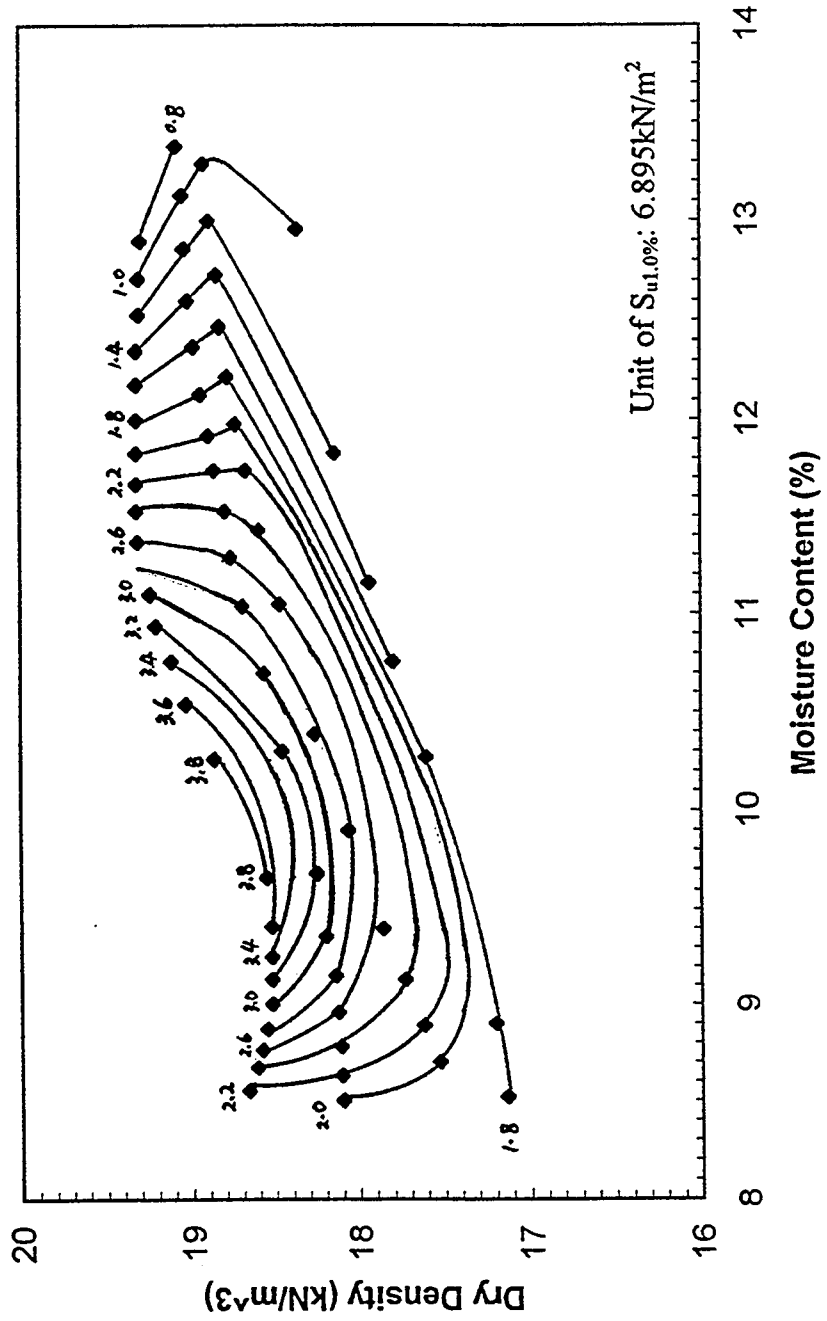


Figure 3.34 Contour of $S_{u1.0\%}$ for the New Interchange of I65 in Johnson CO., IN

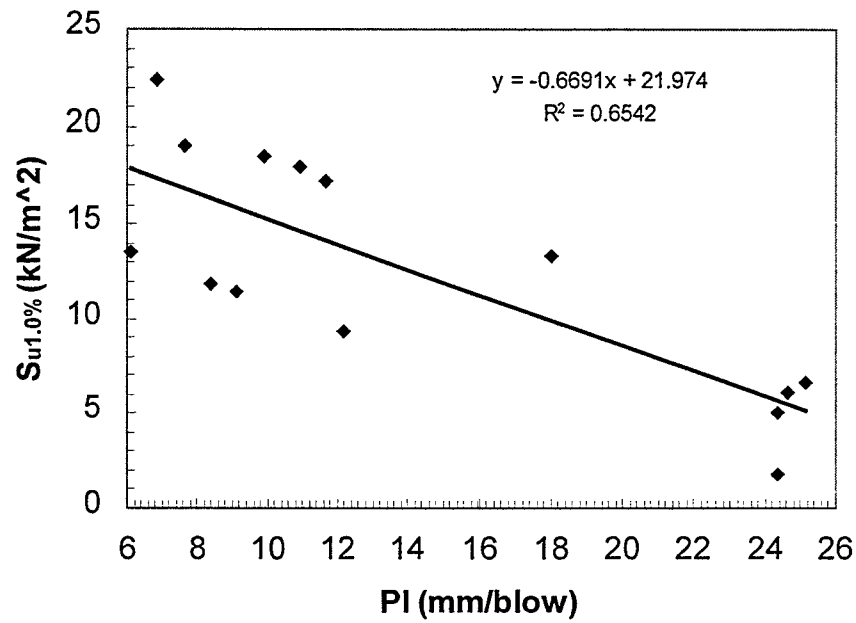


Figure 3.35 The Relationship between $S_{u1.0\%}$ and Penetration Index for the New Interchange of I65 in Johnson CO., IN

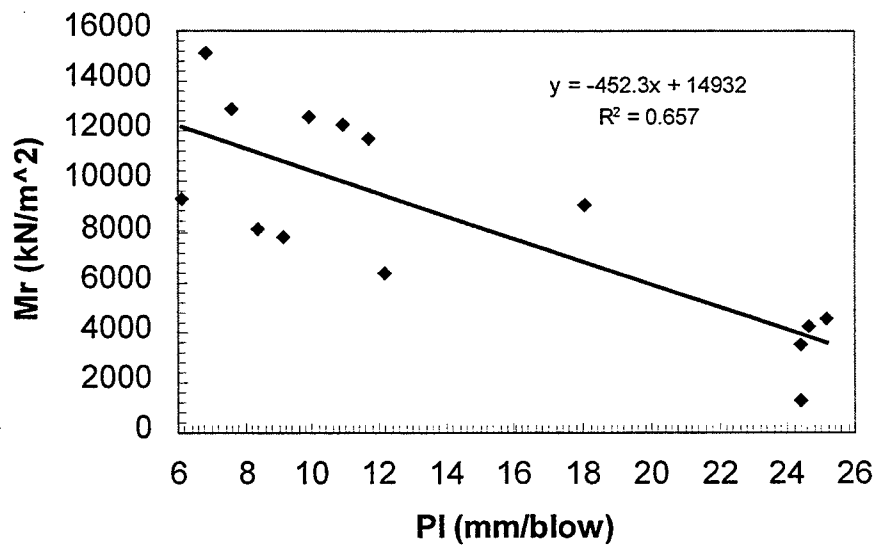


Figure 3.36 The Relationship between Penetration Index and Resilient Modulus for the New Interchange of I65 in Johnson CO., IN

3.2.3 The SR67 at Delaware CO. (1)

The compaction work ended about one week before the DCPT was performed. A sheepsfoot roller was used for compaction. The dry density and moisture content were measured with a nuclear gage at the same location as the DCPT. The field test results are shown in Table 3.2.8. The logs of the DCPT are shown in Figures 3.37 through 3.43.

The relationships between moisture content, dry density and penetration index from the field tests are shown in Figures 3.44, 3.45 and 3.46 respectively.

Sieve Analysis and Atterberg Limits tests were conducted in the laboratory. The sieve analysis results are shown in Figure 3.47. The w_p is 13.87, the w_L is 25.66 and the plasticity index (I_p) is 11.79. The soil is a sandy lean clay (CL).

Analysis:

The laboratory DCPT was not conducted on this soil. From Figures 3.44, 3.45, and 3.46, the trend can be observed that the field penetration index increases with increasing moisture content and decreasing dry density. We should note that, because there is a one week gap between compaction work and DCPT, and dry density and moisture content were measured only in the top lift soil, the measured moisture content may not reflect the as-compacted condition, but the dry density should be very close to the as-compacted dry density. The data for PI shown on Figures 3.42, 3.43, and 3.46 are, indeed, useful measures of how PI varies with those compaction variables.

Table 3.2.8 Field Test Results for the SR67 in Delaware CO., IN (1)

State Route: 67, Weather: Sunny, Date:5/19/1998

Station	Offset	Dry Density (kN/m ³)	M/C (%)	PI (mm/blow)
43+485	2m RT	21.98	7.17	7.62
43+480	3m RT	20.02	5.1	14.73
43+480	5m RT	21.70	6.0	8.38
43+482	9m RT	20.10	7.1	12.45
43+485	7m LT	20.30	7.2	12.95
43+490	10m LT	20.08	6.6	15.49
43+492	7m LT	19.19	6.2	16.26

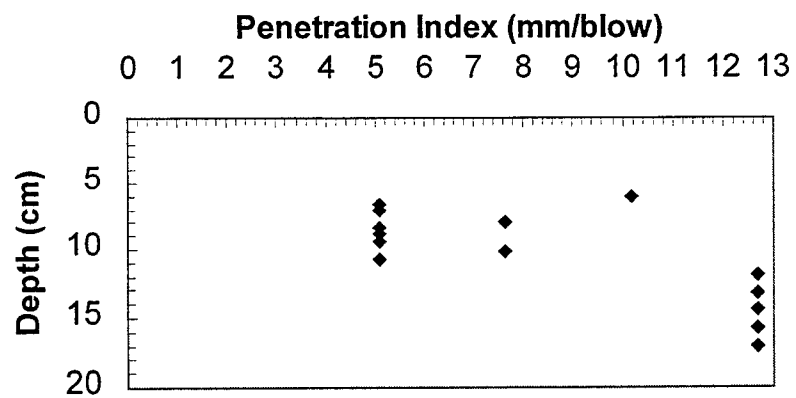
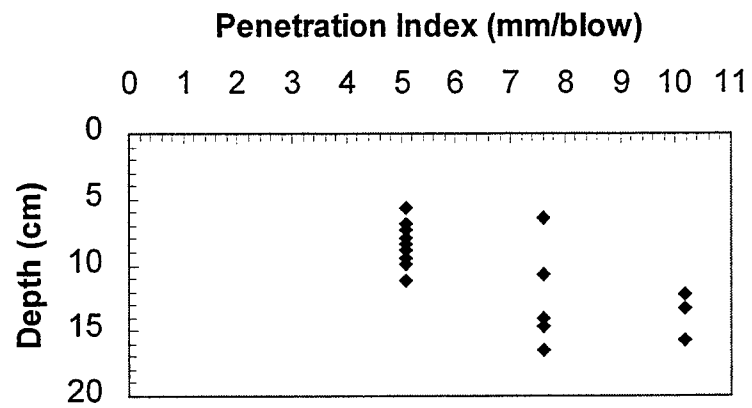
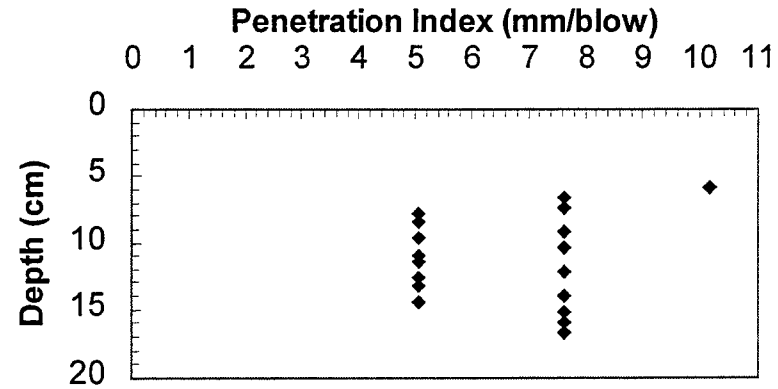


Figure 3.37 The log of the DCPT (Station: 43+485, Offset: 2m RT)

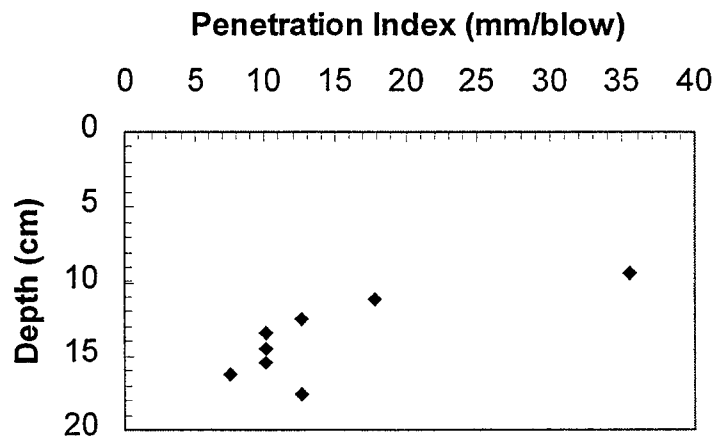


Figure 3.38 The log of the DCPT (Station: 43+480, Offset: 3m RT)

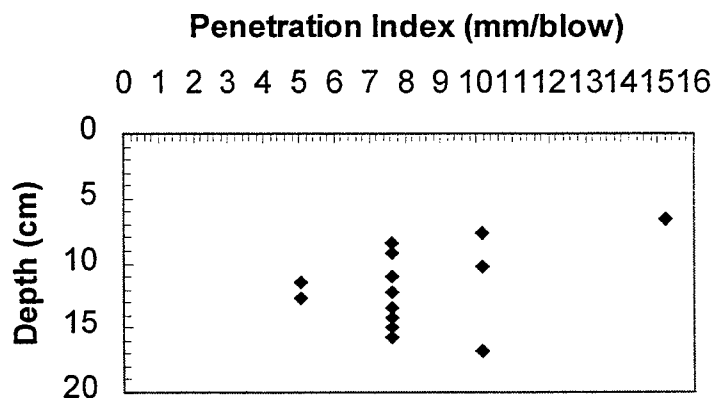


Figure 3.39 The log of the DCPT (Station: 43+480, Offset: 5m RT)

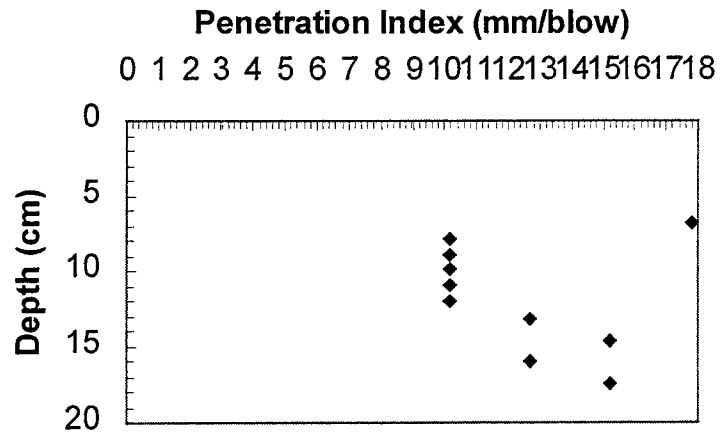


Figure 3.40 The log of the DCPT (Station: 43+482, Offset: 9m RT)

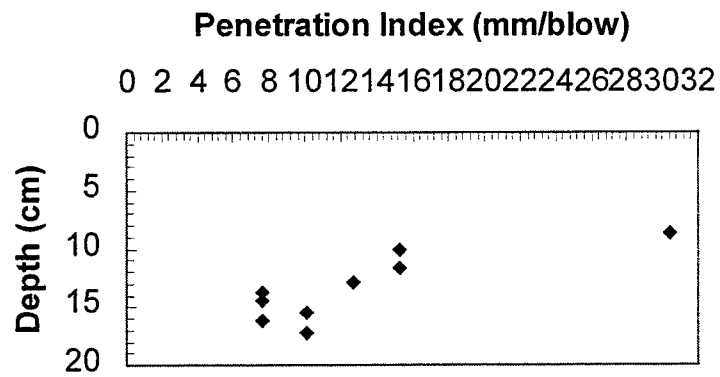


Figure 3.41 The log of the DCPT (Station: 43+485, Offset: 7m LT)

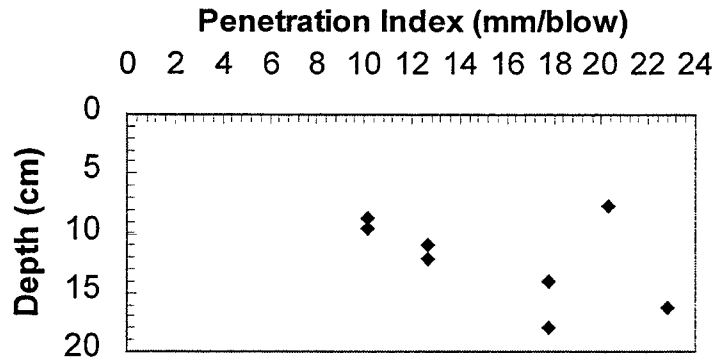


Figure 3.42 The log of the DCPT (Station: 43+490, Offset: 10m LT)

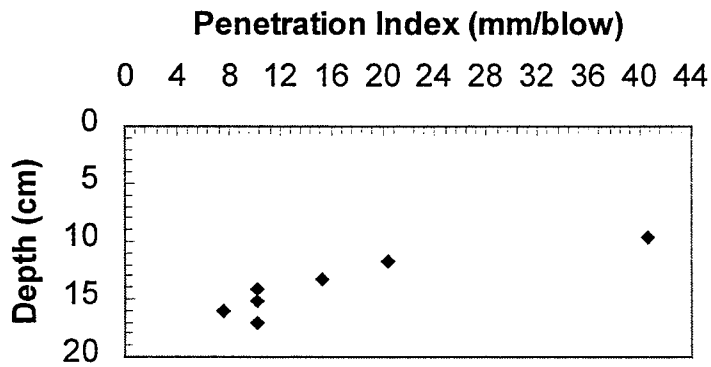


Figure 3.43 The log of the DCPT (Station: 43+492, Offset: 7m LT)

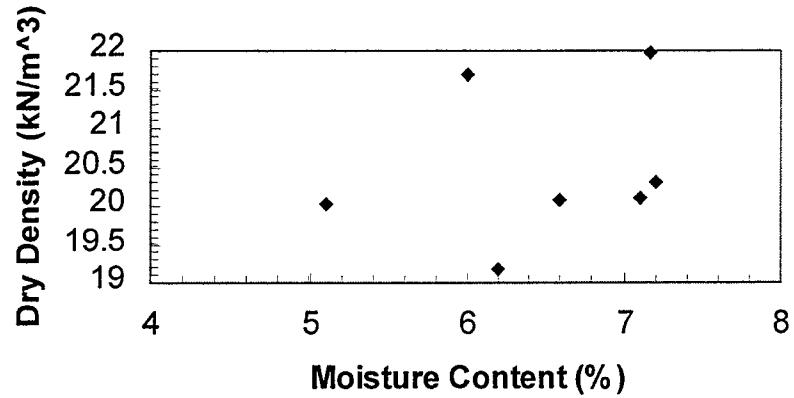


Figure 3.44 The Relationship between Moisture Content and Dry Density from Field DCPT for SR67 in Delaware CO., IN (1)

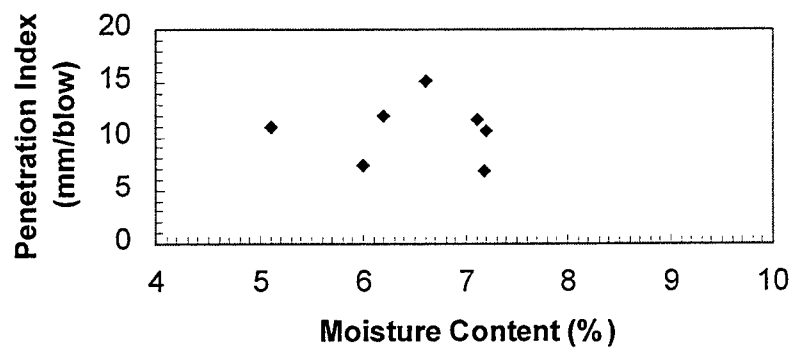


Figure 3.45 The Relationship between Moisture Content and Penetration Index from Field DCPT for SR67 in Delaware CO., IN (1)

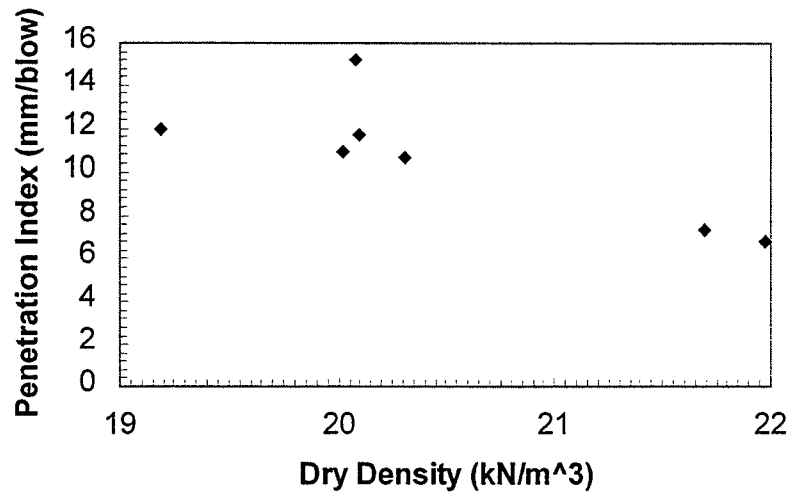


Figure 3.46 The Relationship between Dry Density and Penetration Index for SR67 from Field DCPT in Delaware CO., IN (1)

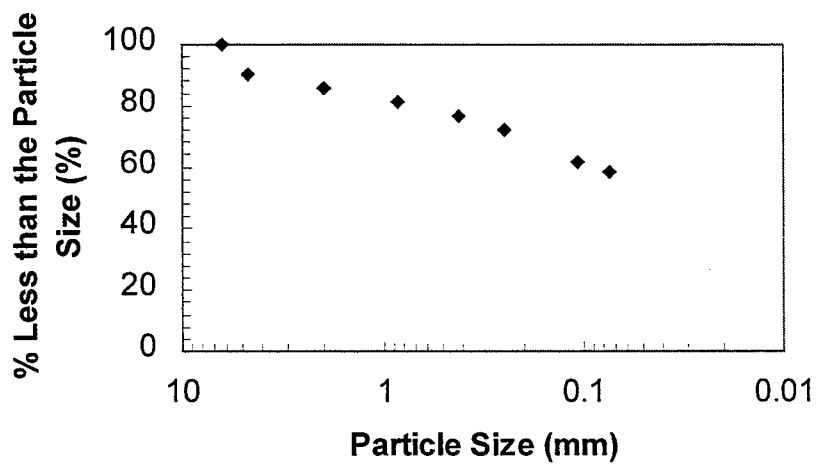


Figure 3.47 The Results of Sieve Analysis for SR67 in Delaware CO., IN (1)

3.2.4 The SR67 at Delaware CO. (2)

The DCPT was performed immediately after the compaction work was finished. A sheepsfoot roller was used for compaction. The dry density and moisture content were measured with a nuclear gage at the same locations where the DCPT was performed. The field test results are shown in the Table 3.2.9. The logs of the DCPT are shown in Figures 3.48 through 3.54.

The relationships between moisture content, dry density and penetration index are shown in Figures 3.55, 3.56 and 3.57, respectively.

Sieve Analysis and Atterberg Limits test were conducted in the laboratory. The sieve analysis results are shown in Figure 3.58. The w_p is 17.04, the w_L is 38.92 and the plasticity index (I_p) is 21.88. The soil is a sandy lean clay (CL).

Analysis:

The laboratory DCPT was not conducted on this soil. From Figures 3.55, 3.56 and 3.57, the trend can be observed that the penetration index increases with increasing moisture content and decreasing dry density.

Table 3.2.9 Field Test Results for SR67 in Delaware CO., IN (2)

State Route: 67, Weather: Sunny, Date: 5/19/1998

Station	Offset	Dry Density (kN/m ³)	M/C (%)	PI (mm/blow)
39+790	1.9m EB RT	17.97	12.8	14.73
39+790	2.6m EB RT	17.34	13.9	17.53
39+790	3.3m EB RT	17.72	13.7	25.4
39+790	4.2m EB RT	17.23	14.7	38.1
39+790	5.3m EB RT	16.80	15.0	22.10
39+790	6.4m EB RT	17.27	12.5	16.26
39+790	7.5m EB RT	17.39	16.3	28.45

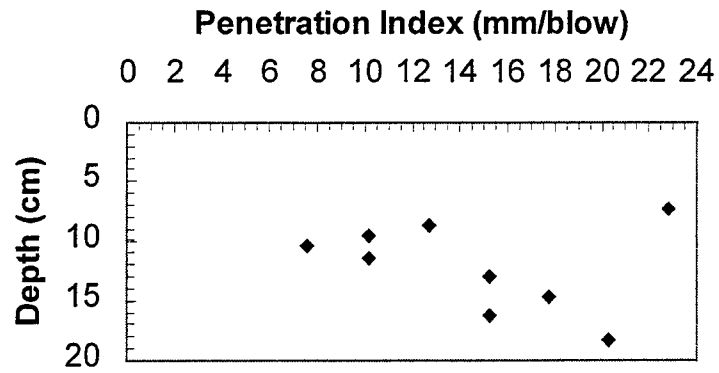


Figure 3.48 The log of the DCPT (Station: 39+790, Offset: 1.9m EB RT)

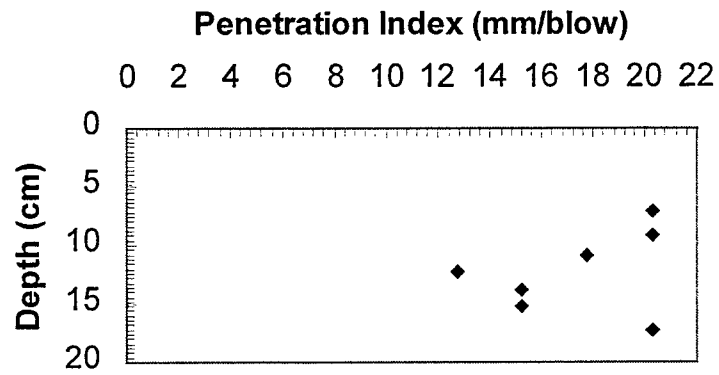


Figure 3.49 The log of the DCPT (Station: 39+790, Offset: 2.6m EB RT)

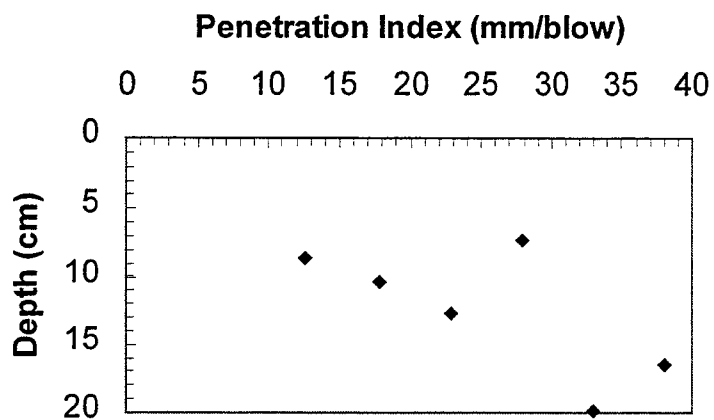


Figure 3.50 The log of the DCPT (Station: 39+790, Offset: 3.3m EB RT)

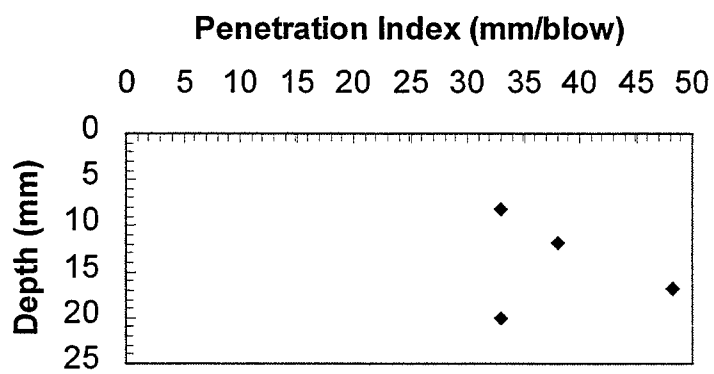


Figure 3.51 The log of the DCPT (Station: 39+790, Offset: 4.2m EB RT)

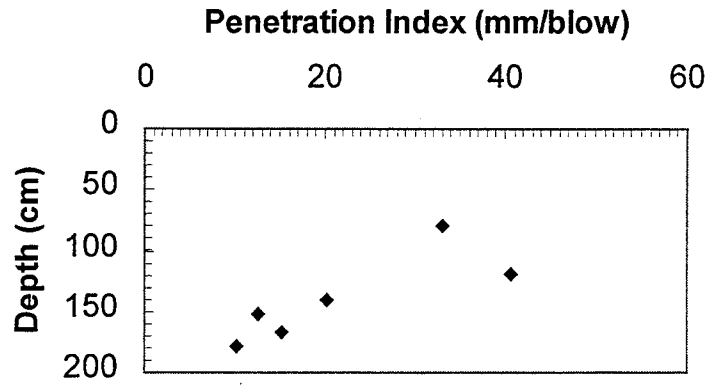


Figure 3.52 The log of the DCPT (Station: 39+790, Offset: 5.3m EB RT)

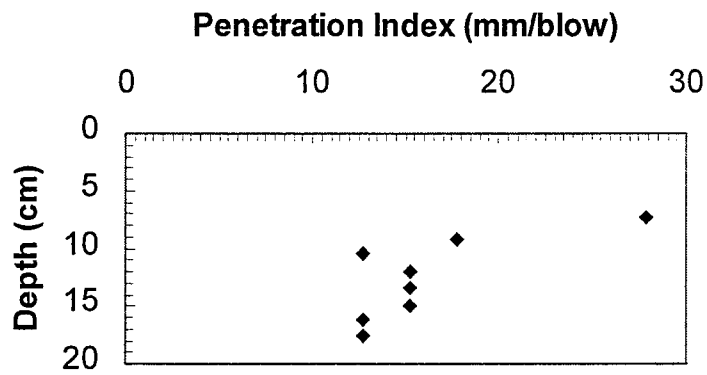


Figure 3.53 The log of the DCPT (Station: 39+790, Offset: 6.4m EB RT)

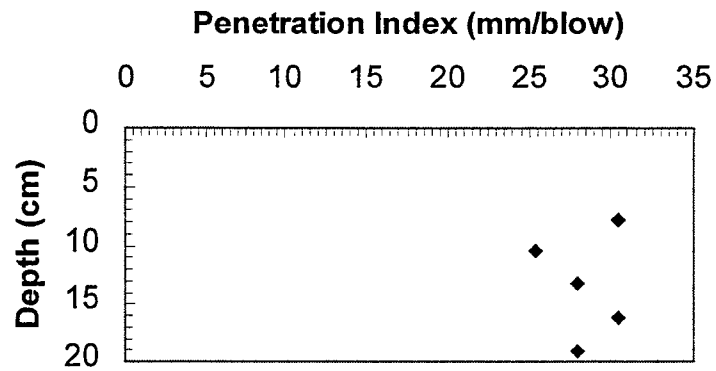


Figure 3.54 The log of the DCPT (Station: 39+790, Offset: 7.5m EB RT)

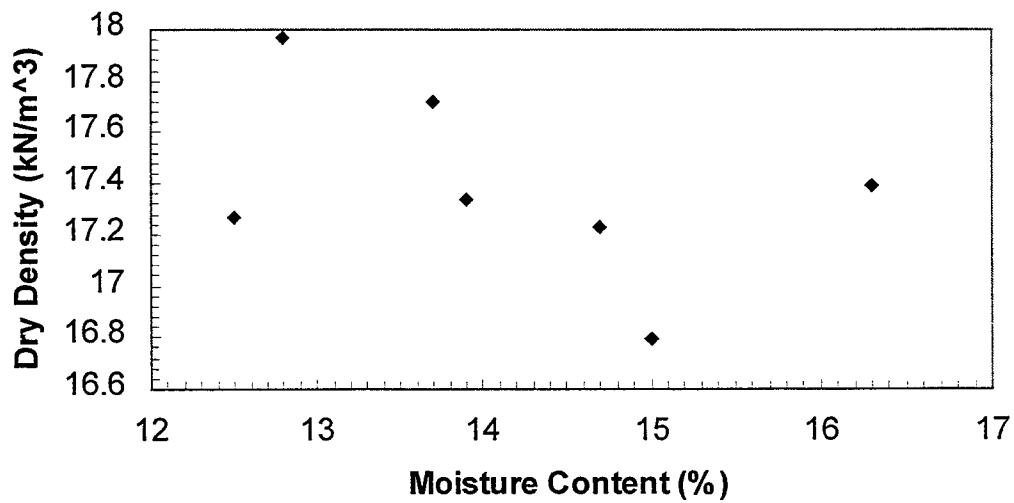


Figure 3.55 The Relationship between Dry Density and Moisture Content from Filed DCPT for SR67 in Delaware CO., IN (2)

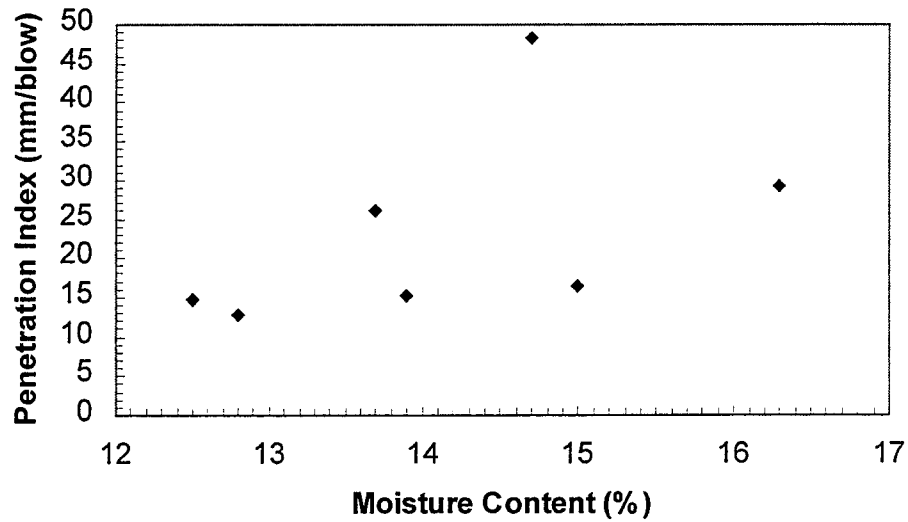


Figure 3.56 The Relationship between Moisture Content and Penetration Index from Field DCPT for SR67 in Delaware CO., IN (2)

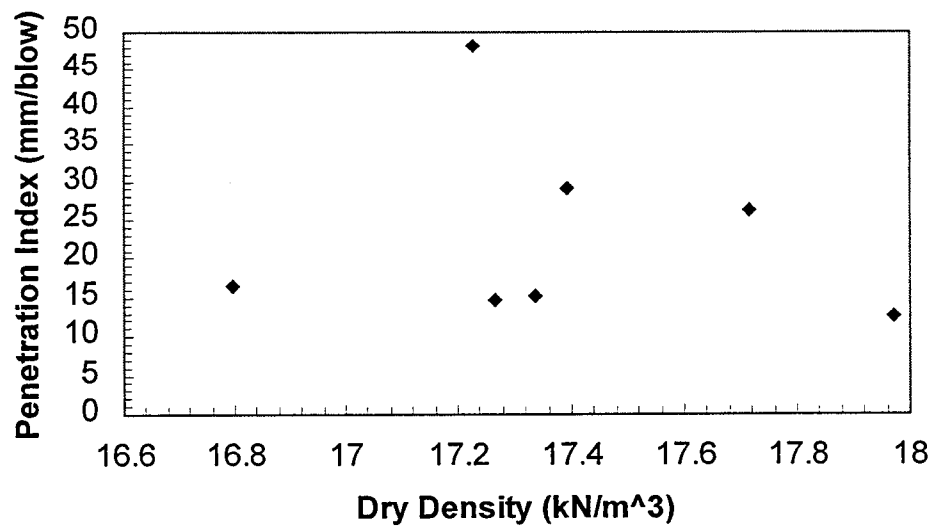


Figure 3.57 The Relationship between Dry Density and Penetration Index from Field DCPT for SR67 in Delaware CO., IN (2)

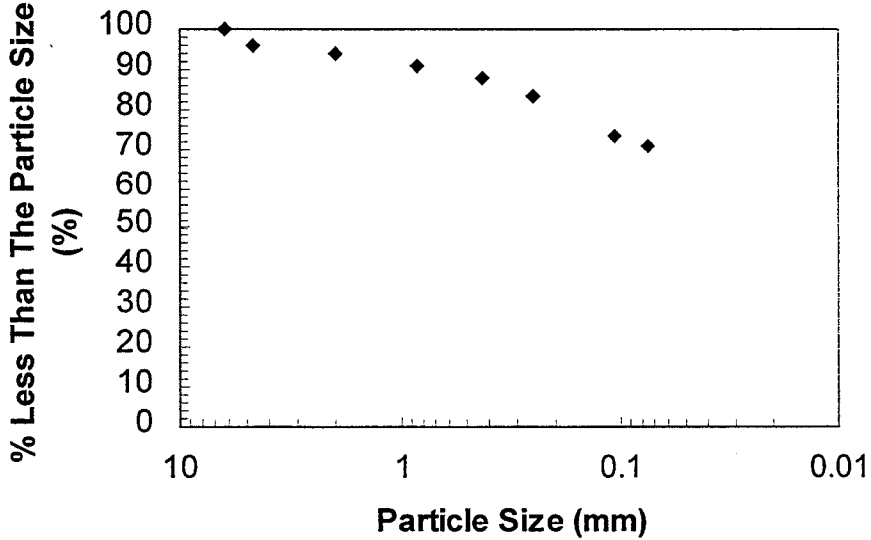


Figure 3.58 The Results of Sieve Analysis for SR67 in Delaware CO., IN (2)

3.2.5 The SR62 in Evansville

Five DCPTs and three SPT tests were conducted at the same time at the Northeast corner of the intersection of SR62 and Garvin Street in Evansville.

Sieve analysis results are shown in Figure 3.59. About 15.5% of the soil passes the 200# sieve. The PL is 16.4, the LL is 24.3, the I_p is 7.9. The soil is a clayey sand (SC).

The DCPT logs are shown in Figures 3.60 through 3.64. DCPT penetration index and SPT blow count are shown in Table 3.2.10 and plotted together in Figure 3.65.

Analysis:

The data in Figure 3.65 are scattered and not sufficient to establish the correlation between SPT blow count and penetration index.

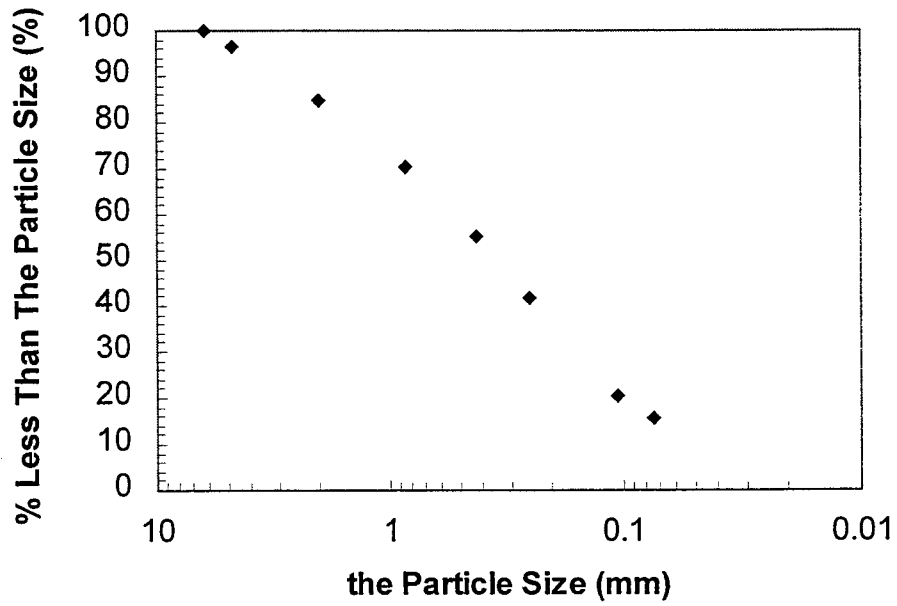


Figure 3.59 The Results of Sieve Analysis for The Intersection of SR62 and Garvin St. in Evansville, IN

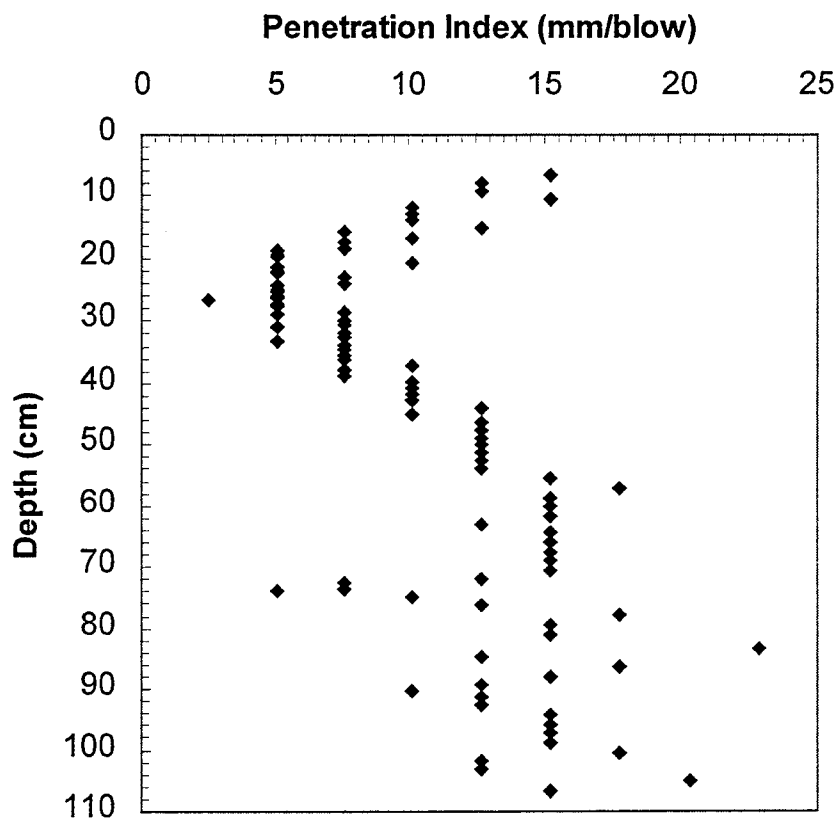
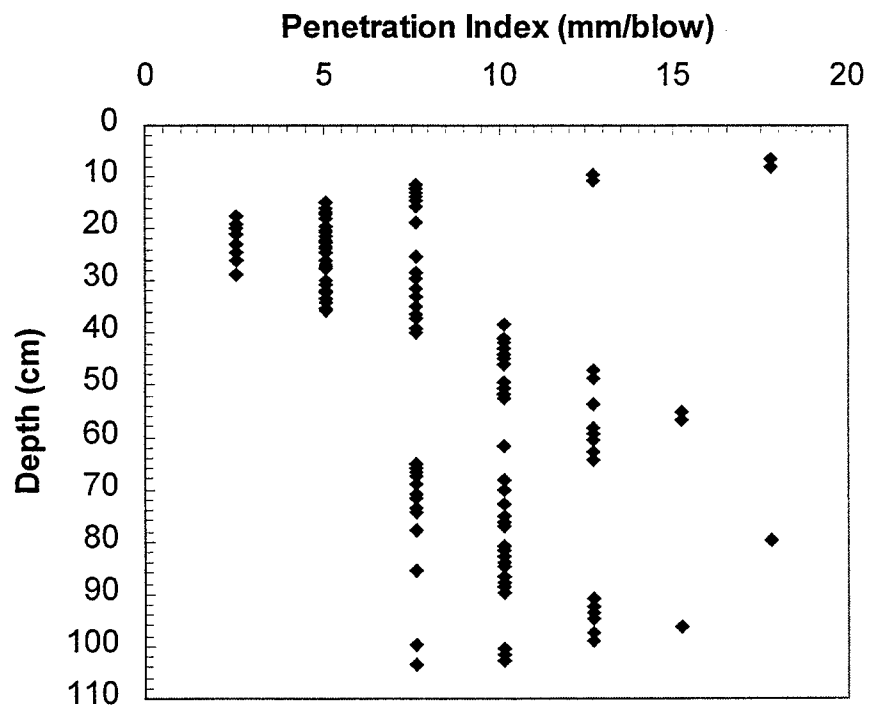


Figure 3.60 The DCPT Log 1 for the Intersection of SR62 and Garvin St. in Evansville, IN



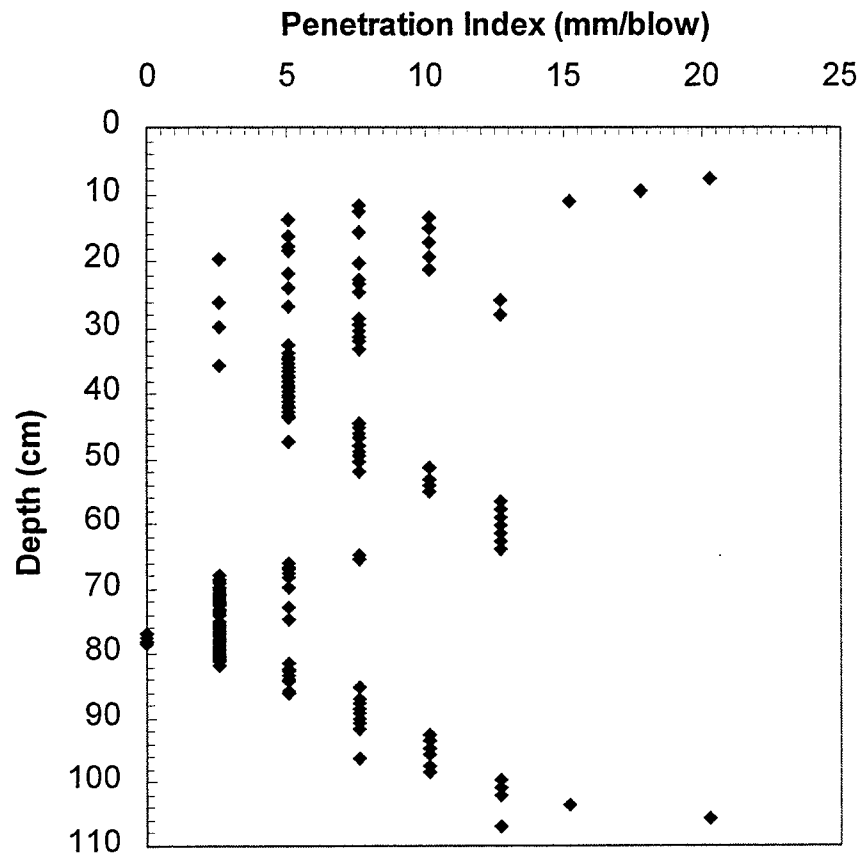


Figure 3.62 The DCPT Log 3 for the Intersection of SR62 and Garvin St. in Evansville, IN

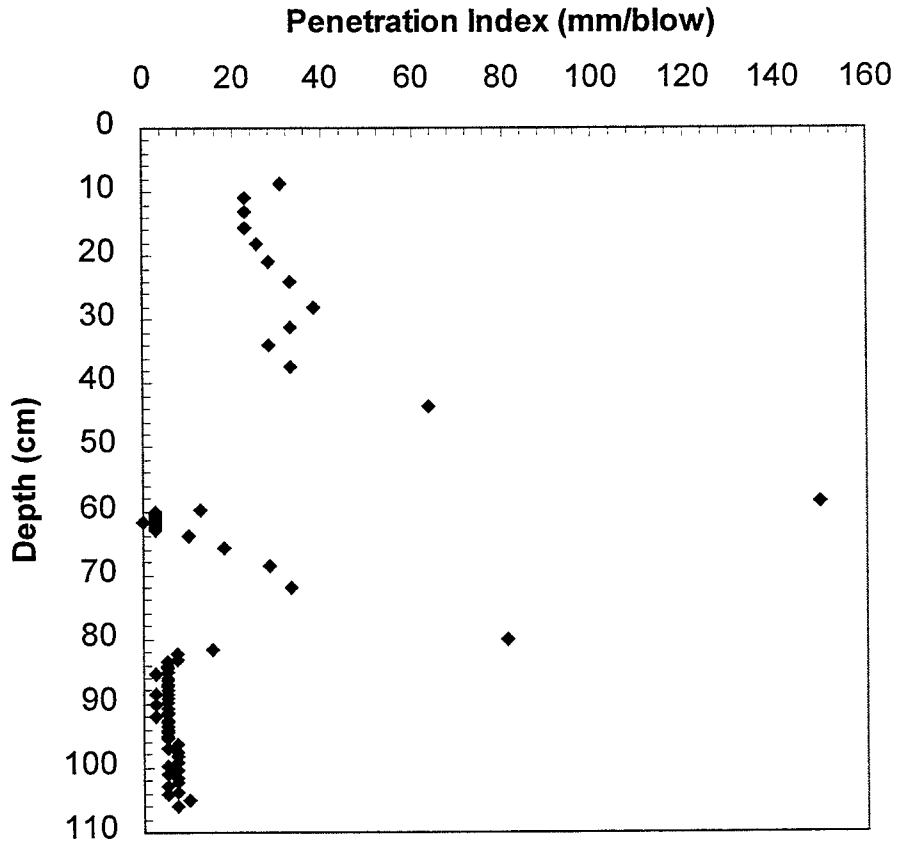


Figure 3.63 The DCPT Log 4 for the Intersection of SR62 and Garvin St. in Evansville, IN

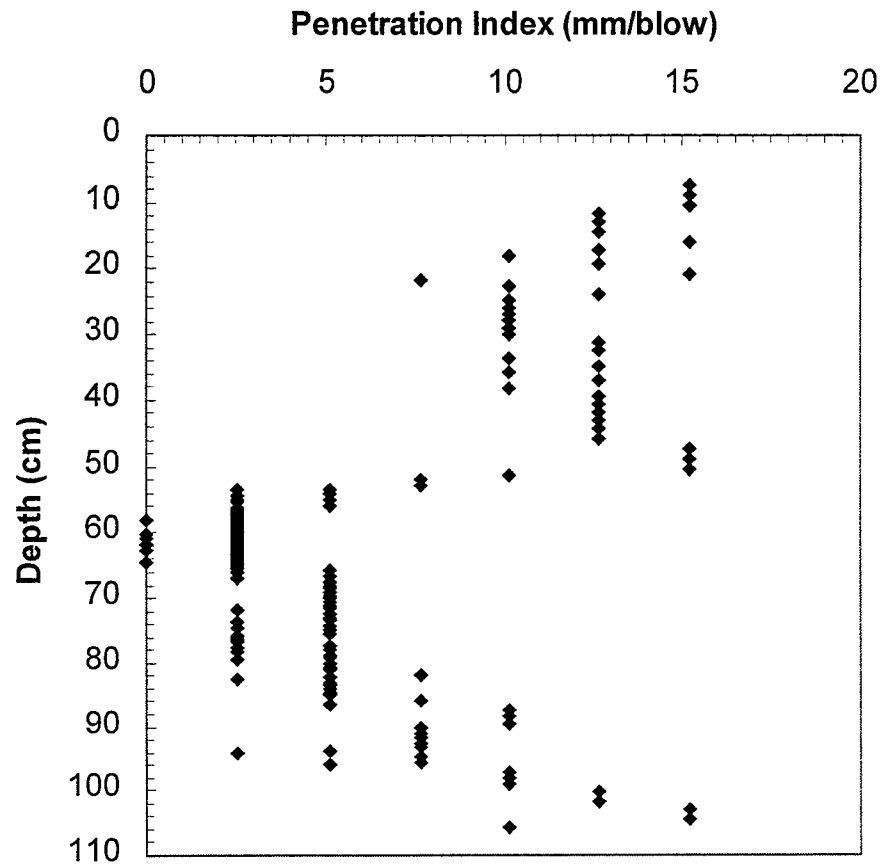


Figure 3.64 The DCPT Log 5 for the Intersection of SR62 and Garvin St. in Evansville, IN

Table 3.2.10 The Relationship between SPT and DCPT for the Interchange of SR62 and Garvin St. in Evansville, IN

PI	5.54	8.26	10.59	12.88	7.04	5.54	3.89	3.71	11.07	12.07	3.30	5.54
(mm/Blow)												
SPT	15	13	8	9	2	4	12	9	6	8	6	8

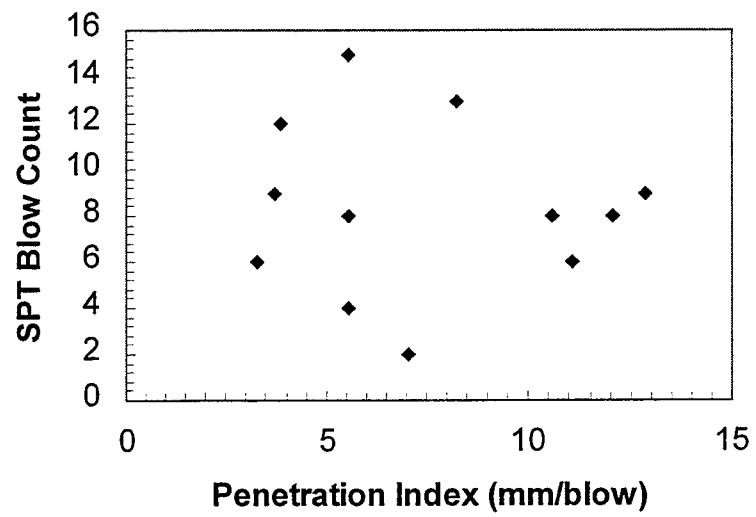


Figure 3.65 The Relationship between DCPT and SPT for the Intersection of SR62 and Garvin St. in Evansville, IN

3.2.6 The US.24 by-pass in Logansport

Seven DCPT tests were conducted at the site of the US24 by-pass in Logansport. The dry density and moisture content were measured, respectively, with the nuclear gage and sand cone methods. The compaction was done with a sheepsfoot roller. The field test results are shown in Tables 3.2.11 and 3.2.12. The DCPT logs are shown in Figure 3.66 to 3.72.

The relationship between penetration index, moisture content and dry density from the nuclear gage and sand cone methods are shown in Figure 3.73 and Figure 3.78. The measured dry density and moisture content are different for the two methods, as the comparisons of the two methods shown in Figures 3.79 and 3.80 illustrate.

Sieve analysis and Atterberg Limits tests were conducted in the laboratory. The sieve analysis results are shown in Figure 3.81. The w_p is 15.8, the w_L is 27.7 and the plasticity index (I_p) is 12.1. The soil is a sandy lean clay (CL).

Analysis:

(1) Similar results for penetration index versus moisture content and dry density can be obtained with the nuclear gage and sand cone method, as shown in Figures 3.73 through 3.78.

(2) The test results from nuclear gage method and sand cone method are different, as shown in Figures 3.79 and 3.80. There are two possible reasons for that: (1) the test location for the nuclear gage and sand cone methods are not exactly same; (2) there are inaccuracies in both methods. This suggests a need for a closer examination of how to measure compaction results when DCPT relationships are to be used in the future in practice.

Table 3.2.11 Field Test Results for US24 By-pass in Logansport, IN (with nuclear gage)

US24 by-pass, Weather: Sunny, Date: 7/2/1998

Station	Offset	Dry Density (kN/m ³)	M/C (%)	PI (mm/blow)
438+67	5.18m Left	18.44	8.8	7.80
438+67	3.66m Left	18.93	9.8	9.96
438+67	2.44m Right	18.91	10.7	17.15
405-26	7.92m Left	19.12	8.0	7.95
405-26	4.88m Left	18.93	7.3	8.59
405-26	2.44m Left	18.99	8.0	8.41
405+2	1.52m Right	17.88	7.7	18.62

Table 3.2.12 Field Test Results for US24 By-pass in Logansport, IN (with Sand Cone Method)

US24 by-pass, Weather: Sunny, Date: 7/2/1998

Station	Offset	Dry Density (kN/m ³)	M/C (%)	PI (mm/blow)
438+67	5.18m Left	18.88	8.86	7.80
438+67	3.66m Left	16.87	11.26	9.96
438+67	2.44m Right	17.58	12.02	17.15
405-26	7.92m Left	18.16	8.36	7.95
405-26	4.88m Left	18.07	7.41	8.59
405-26	2.44m Left	18.25	8.21	8.41
405+2	1.52m Right	16.16	9.5	18.62

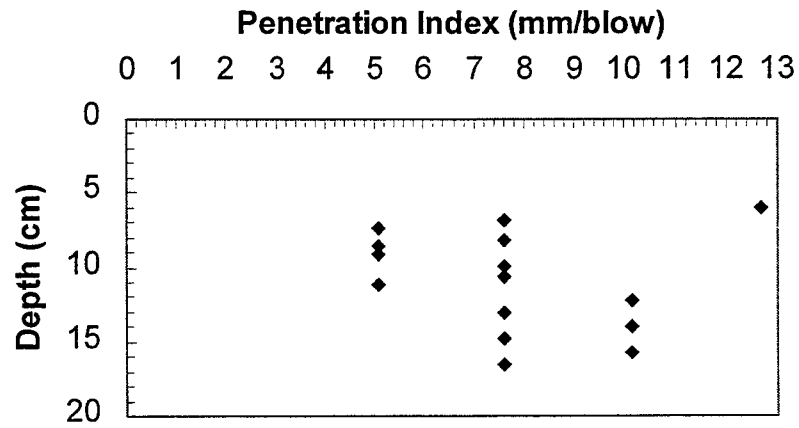


Figure 3.66 The Log of the DCPT (Station: 438+67, Offset: 5.18m LT)

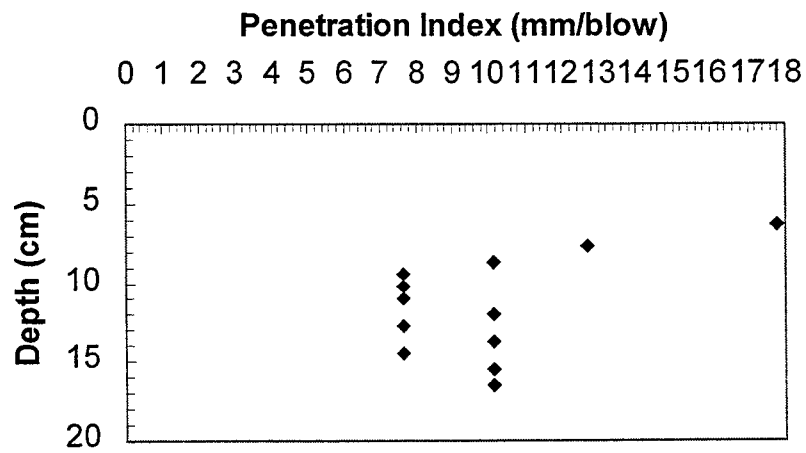


Figure 3.67 The Log of the DCPT (Station: 438+67, Offset: 3.66m LT)

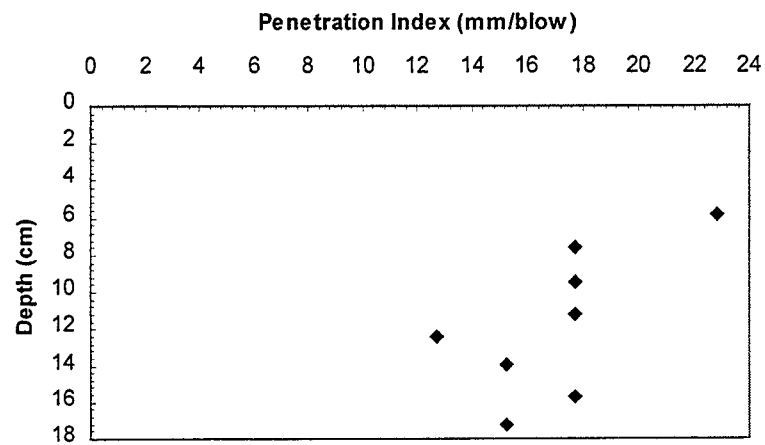


Figure 3.68 The Log of the DCPT (Station: 438+67, Offset: 2.44m RT)

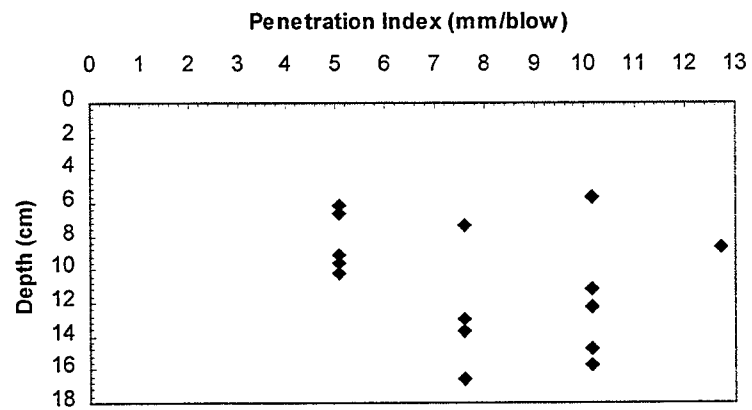


Figure 3.69 The Log of the DCPT (Station: 405-26, Offset: 7.92m LT)

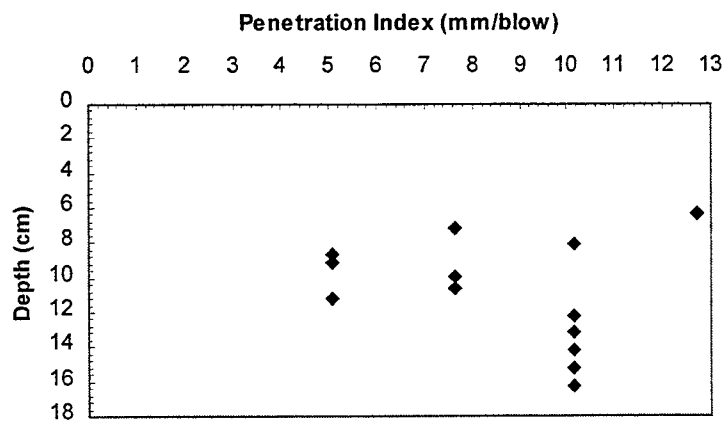


Figure 3.70 The Log of the DCPT (Station: 405-26, Offset: 4.88m LT)

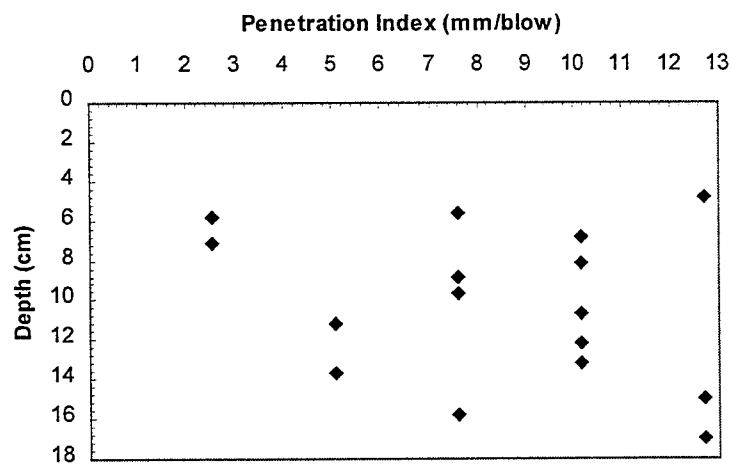


Figure 3.71 The Log of the DCPT (Station: 405-26, Offset: 2.44m LT)

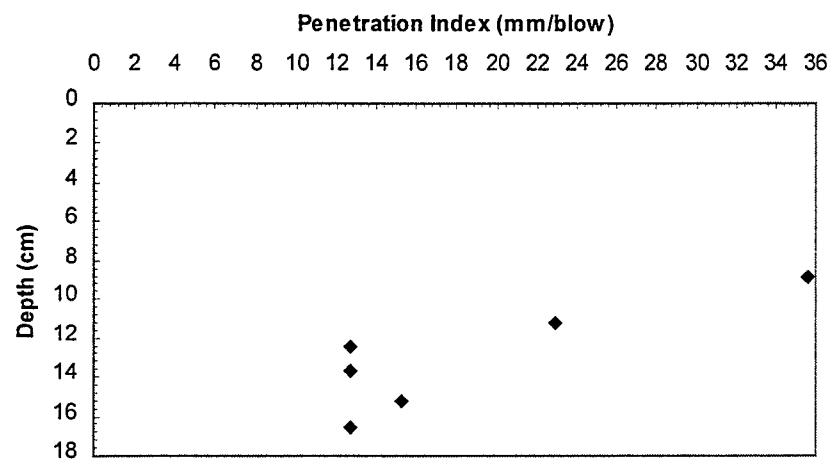


Figure 3.72 The Log of the DCPT (Station: 405+2, Offset: 1.52m RT)

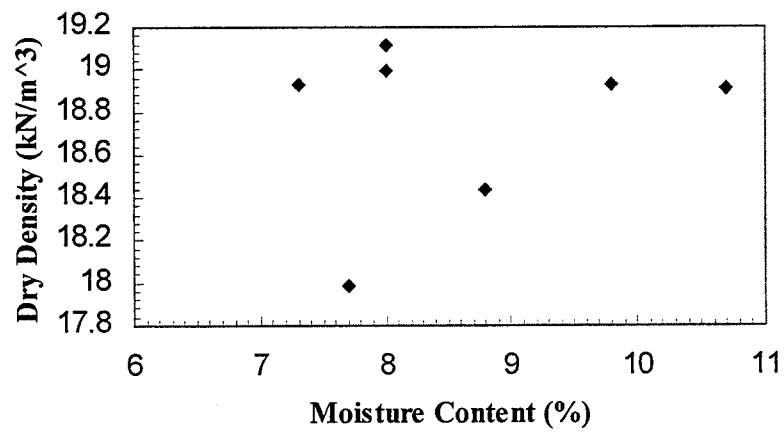


Figure 3.73 The Relationship between Dry Density and Moisture Content with Nuclear Gage Method for US24 By-pass in Logansport, IN

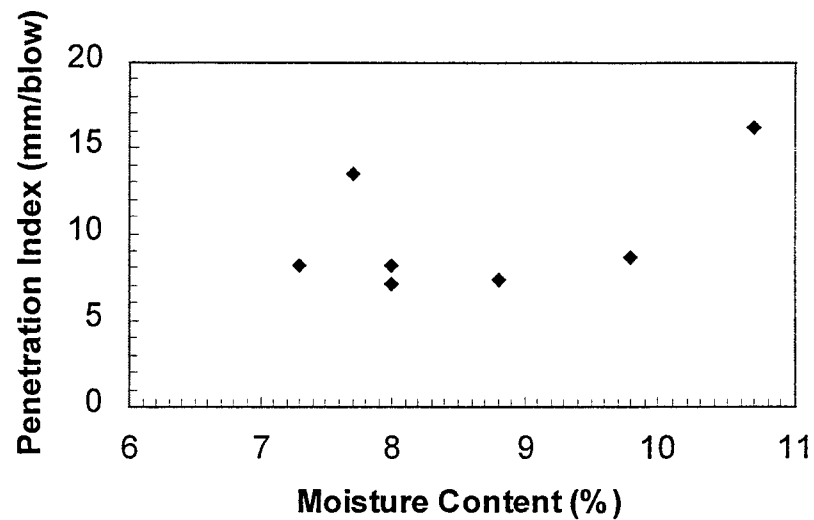


Figure 3.74 The Relationship between Penetration Index and Moisture Content with Nuclear Gage Method for US24 By-pass in Logansport, IN

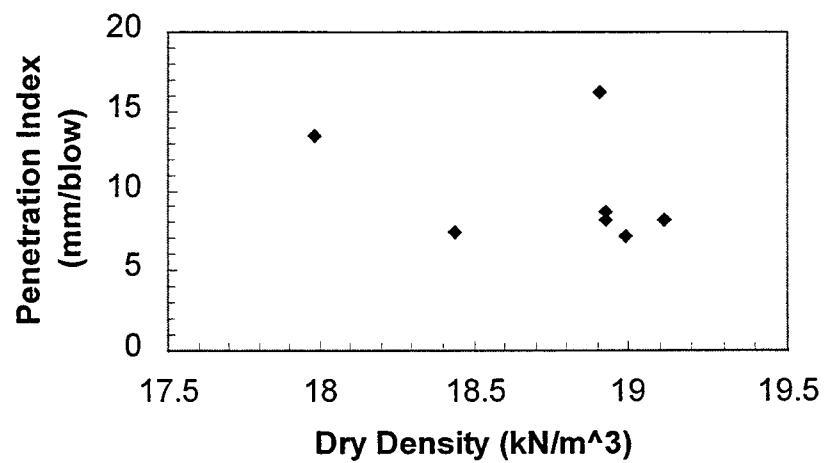


Figure 3.75 The Relationship between Penetration Index and Dry Density with Nuclear Gage for US24 By-pass in Logansport, IN

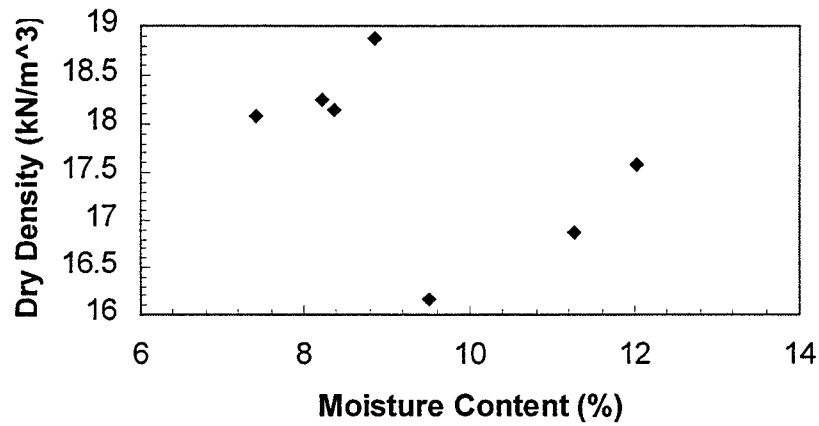


Figure 3.76 The Relationship between Dry Density and Moisture Content with Sand Cone Method for US24 Bypass in Logansport, IN

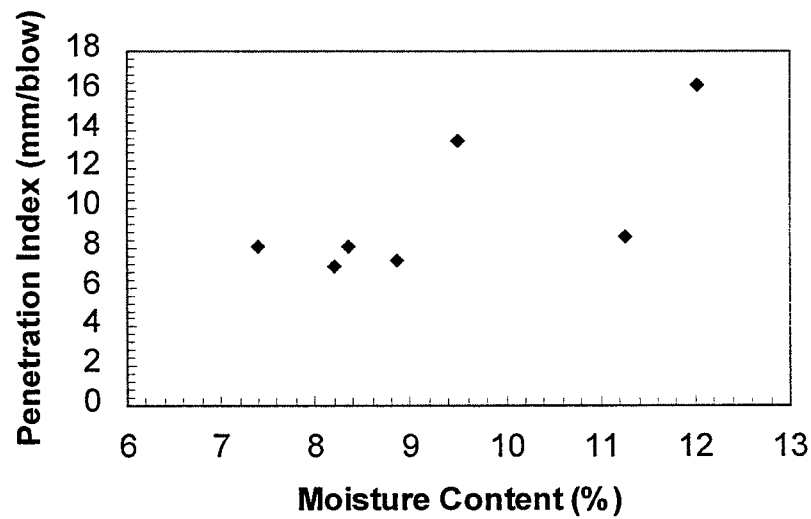


Figure 3.77 The Relationship between Penetration Index and Moisture Content with Sand Cone Method for US24 By-pass in Logansport, IN

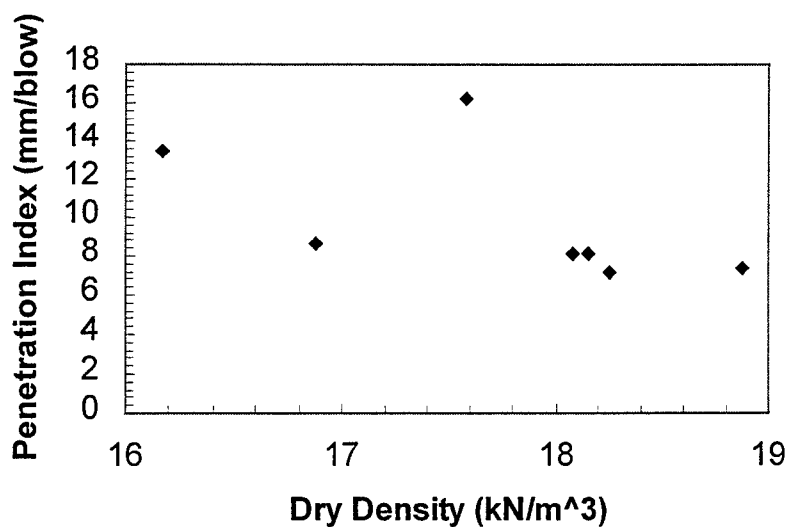


Figure 3.78 The Relationship between Penetration Index and Dry Density with Sand Cone Method for US24 By-pass in Logansport,IN

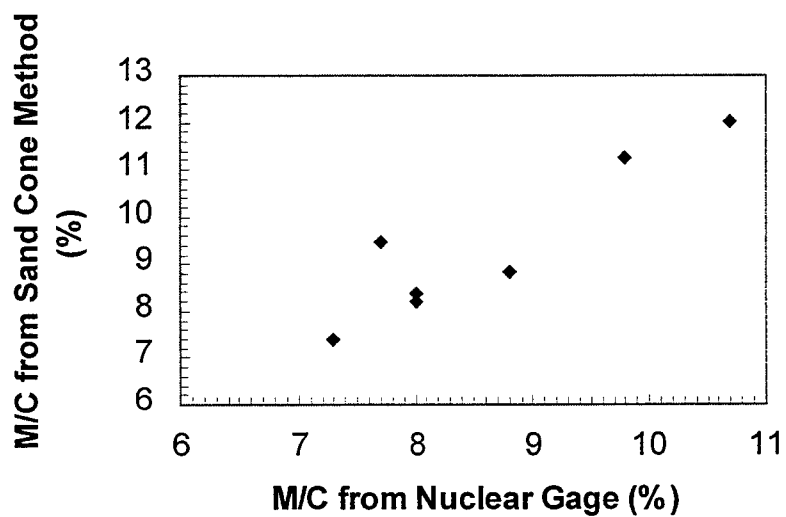


Figure 3.79 Comparison of the Testing Results of Moisture Content from Sand Cone Method and Nuclear Gage for US24 By-pass in Logansport, IN

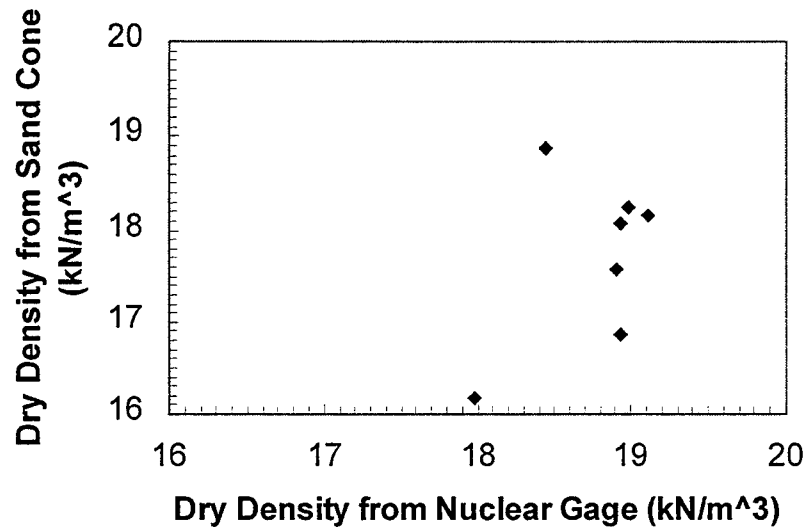


Figure 3.80 Comparison of the Testing Results of Dry Density from Sand Cone Method and Nuclear Gage for US24 By-pass in Logansport, IN

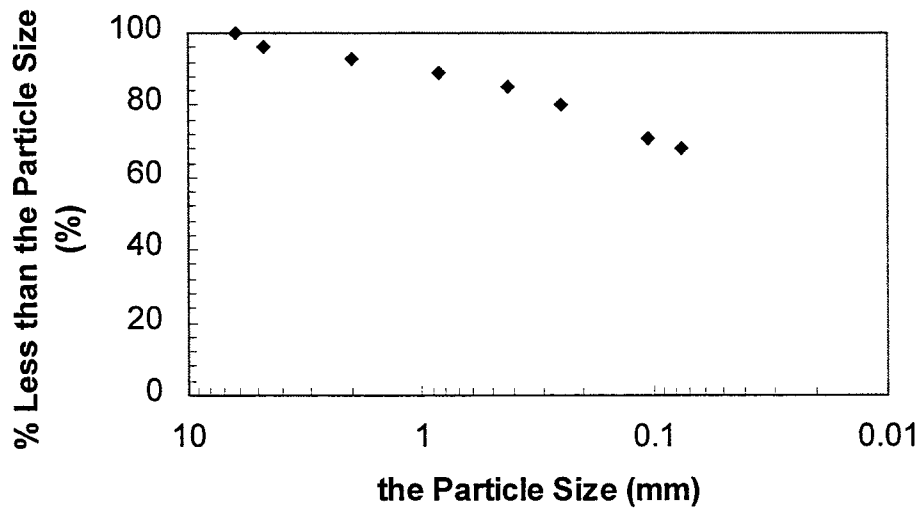


Figure 3.81 The Test Results of Sieve Analysis for US24 By-pass in Logansport, IN

3.2.7 The SR.24 in Logansport

Seven DCPT tests were conducted at the Northeastern corner of SR24 and US35 in Logansport. The compaction equipment utilized was a sheepsfoot roller. The dry density and moisture content were measured with nuclear gage and sand cone method at the same location. The field test results are shown in Tables 3.2.13 and 3.2.14. The logs of the DCPT are shown in Figures 3.82 through 3.88.

The relationship between penetration index, moisture content and dry density from the nuclear gage and sand cone methods are shown in Figures 3.89 to 3.94. The measuring dry density and moisture content are different for the two methods; the comparisons of the two methods are shown in Figures 3.95 and 3.96.

Sieve analysis and Atterberg Limits tests were conducted in the laboratory. The sieve analysis results are shown in Figure 3.97. The w_p is 15.9, the w_L is 25.4 and plasticity index (I_p) is 9.5. The soil is a sandy lean clay (CL).

Analysis:

As in the previous section, the test results from the nuclear gage and sand cone methods are different, as shown in Figure 3.95 and 3.96. For moisture content, the test results of the two methods are quite consistent; but for dry density, the test results present some scatter. The reasons are the same as previously discussed.

Table 3.2.13 Field Test Results for SR24 in Logansport, IN (with nuclear gage)

Location: Northeastern corner of Intersection of US35 and SR24, Weather: Sunny, Date: 7/15/1998

Station	Offset	Dry Density (kN/m ³)	M/C (%)	PI (mm/blow)
---	---	103.2	14.6	33.02
---	---	103	17.5	36.83
---	---	103.8	15.6	32.39
---	---	109.7	9.6	72.90
---	---	104.1	14.9	24.64
---	---	110.7	11.7	32.39
---	---	118.6	5.0	22.12

Table 3.2.14 Field Test Results for SR24 in Logansport, IN (with Sand Cone Method)

Location: Northeastern corner of Intersection of US35 and SR24, Weather: Sunny, Date: 7/15/1998

Station	Offset	Dry Density (kN/m ³)	M/C (%)	PI (mm/blow)
---	---	15.28	16.02	33.02
---	---	15.17	17.28	36.83
---	---	14.53	15.30	32.39
---	---	15.95	9.19	72.90
---	---	16.74	15.02	24.64
---	---	16.69	12.14	32.39
---	---	16.36	5.61	22.12

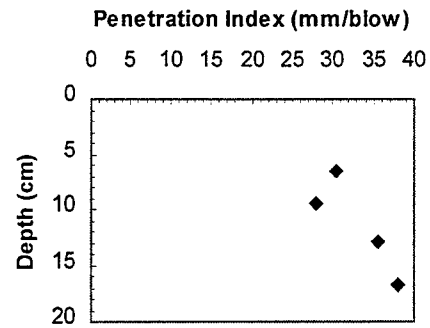


Figure 3.82 the Log 1 of the DCPT for SR24 in Logansport, IN

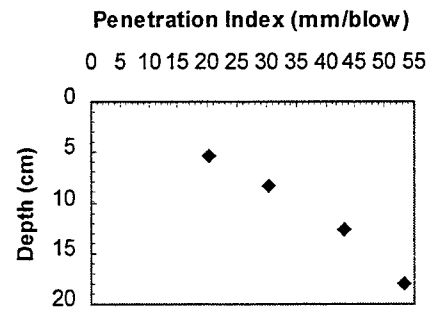


Figure 3.83 the Log 2 of the DCPT for SR24 in Logansport, IN

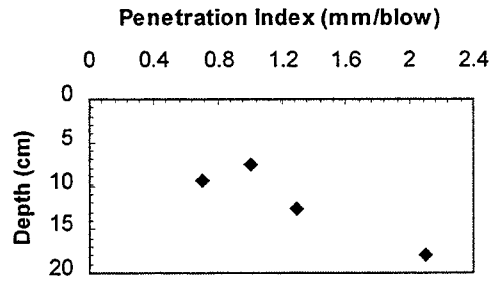


Figure 3.84 the Log 3 of the DCPT for SR24 in Logansport, IN

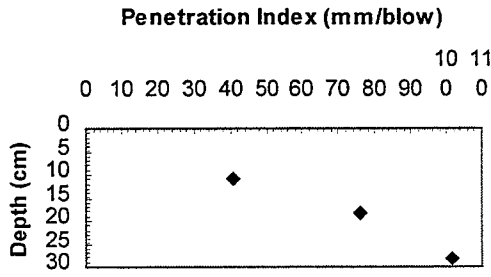


Figure 3.85 the Log 4 of the DCPT for SR24 in Logansport, IN

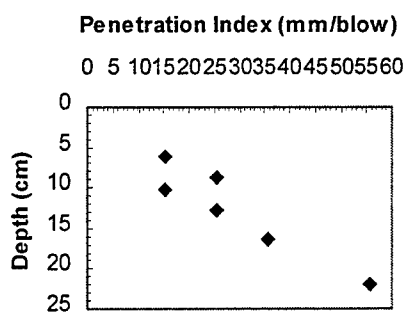


Figure 3.86 the Log 5 of the DCPT for SR24 in Logansport, IN

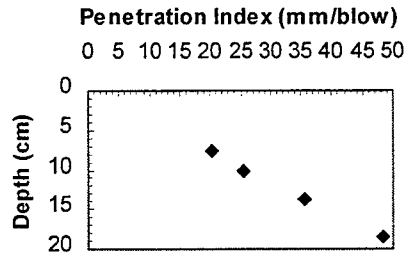


Figure 3.87 the Log 6 of the DCPT for SR24 in Logansport, IN

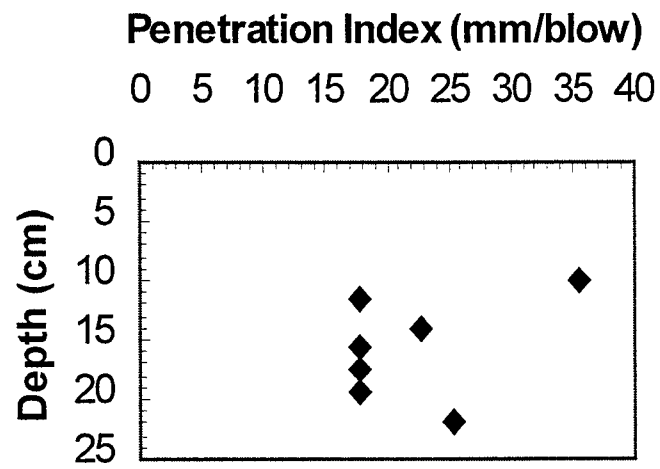


Figure 3.88 the Log 7 of the DCPT for SR24 in Logansport, IN

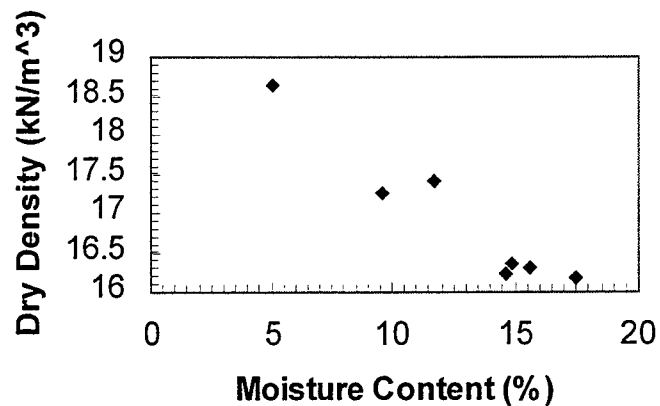


Figure 3.89 The Relationship between Dry Density and Moisture Content with Nuclear Gage Method for SR24 in Logansport, IN

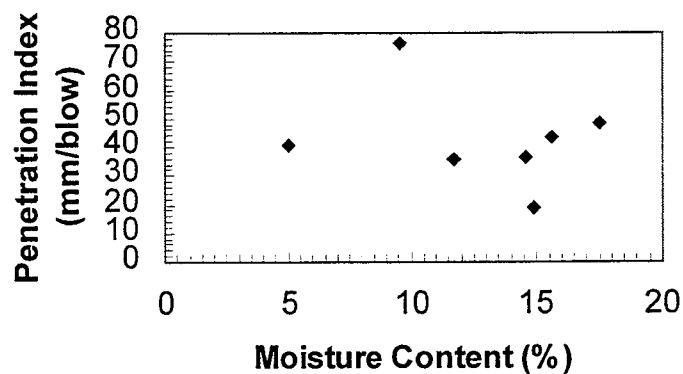


Figure 3.90 The Relationship between Penetration Index and Moisture Content with Nuclear Gage Method for SR24 in Logansport, IN

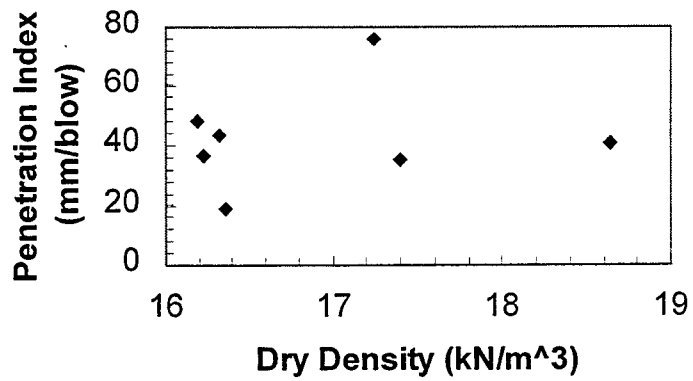


Figure 3.91 The Relationship between Penetration Index and Dry Density with Nuclear Gage for SR24 in Logansport, IN

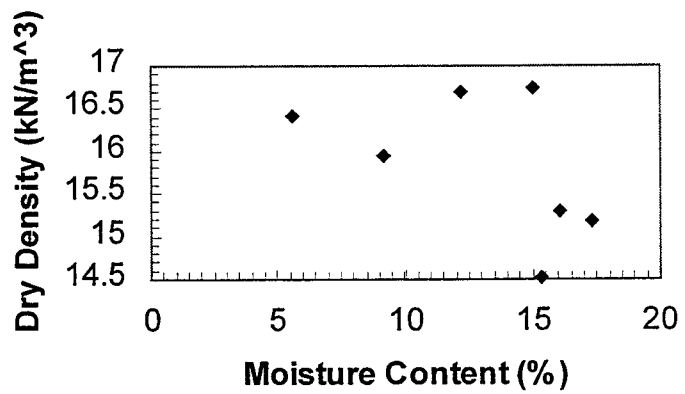


Figure 3.92 The Relationship between Dry Density and Moisture Content with Sand Cone Method for SR24 in Logansport, IN

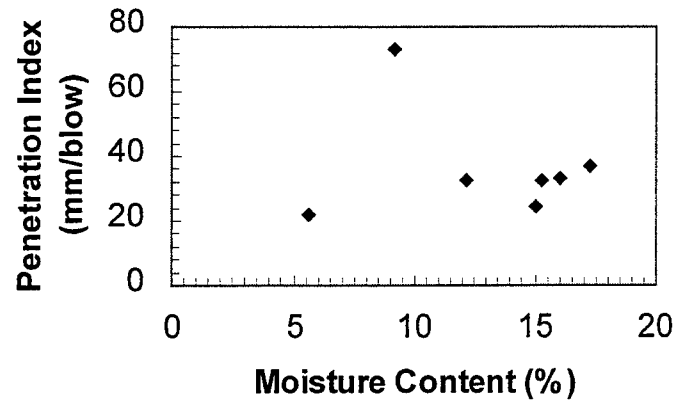


Figure 3.93 The Relationship between Penetration Index and Moisture Content with Sand Cone Method for SR24 in Logansport, IN

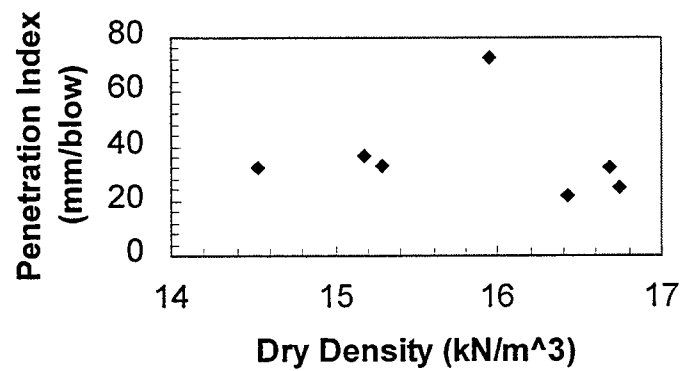


Figure 3.94 The Relationship between Penetration Index and Dry Density with Sand Cone Method for SR24 in Logansport, IN

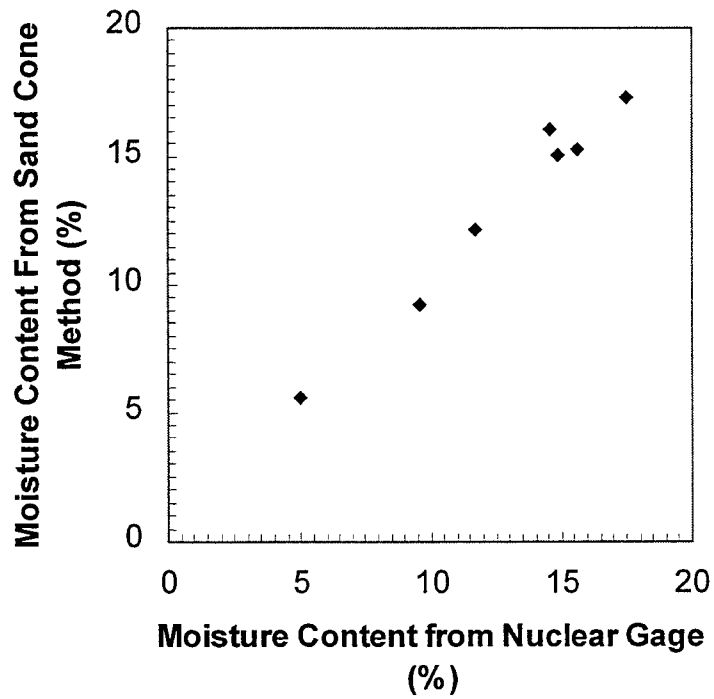


Figure 3.95 Comparison of the Testing Results of Moisture Content from Sand Cone Method and Nuclear Gage for SR24 in Logansport, IN

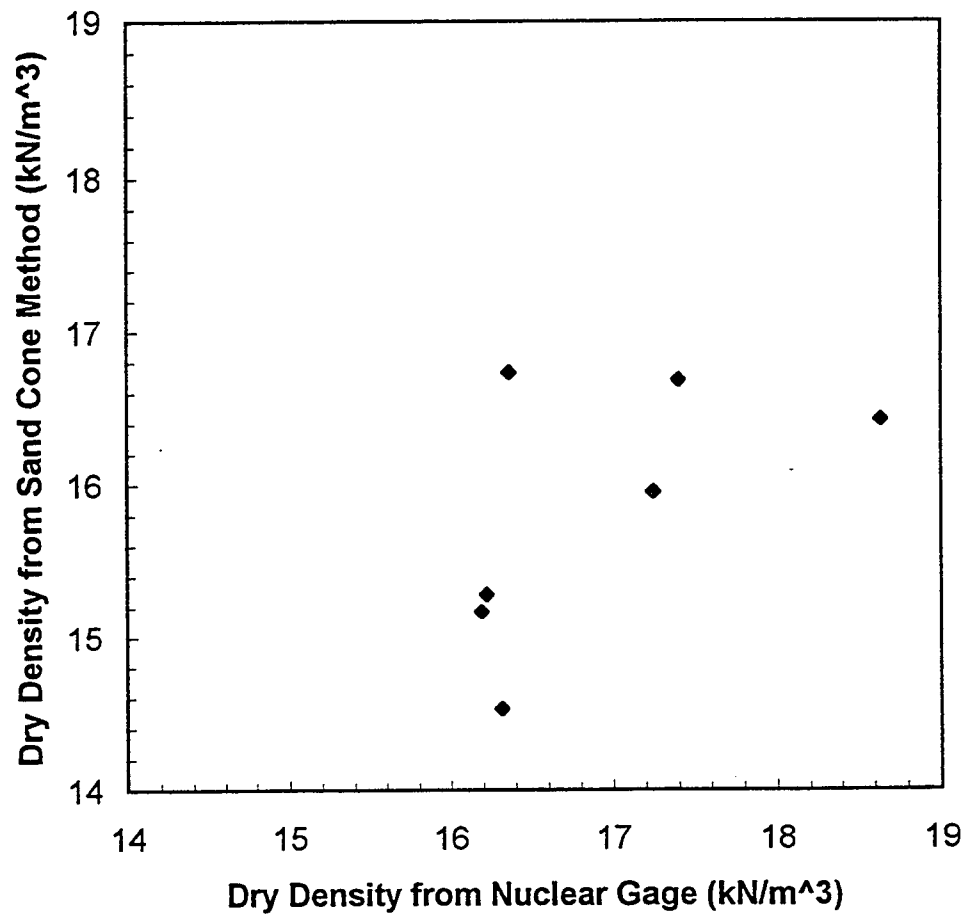


Figure 3.96 Comparison of the Testing Results of Dry Density from Sand Cone Method and Nuclear Gage for SR24 in Logansport, IN

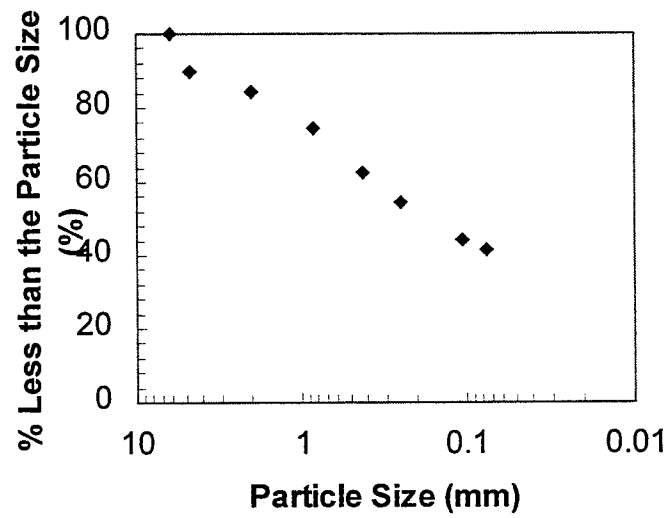


Figure 3.97 The Test Results of Sieve Analysis for SR24 By-pass in Logansport, IN

3.2.8 The US41 in Parke CO.

The DCPT and SPT were conducted on US41 in Parke CO., 3.8 miles north of the intersection of US41 and SR163. Three DCPT and three SPT tests were performed to get the relationship between SPT and DCPT.

The results of the sieve analysis are shown in Figure 3.98. About 28.3% of the soil passes 200# sieve; the soil is a silty sand (SM).

The logs of DCPT are shown in Figures 3.99 through 3.101.

The relationship between DCPT and SPT is shown in Table 3.2.15 and Figure 3.102.

Analysis:

From Figure 3.102, a clear relationship between DCPT and SPT is not established. The reasons may be as follows: (i) DCPT and SPT couldn't be conducted in the exact same location, (ii) there are inaccuracies in both test methods, and (iii) the amount of data is not sufficient.

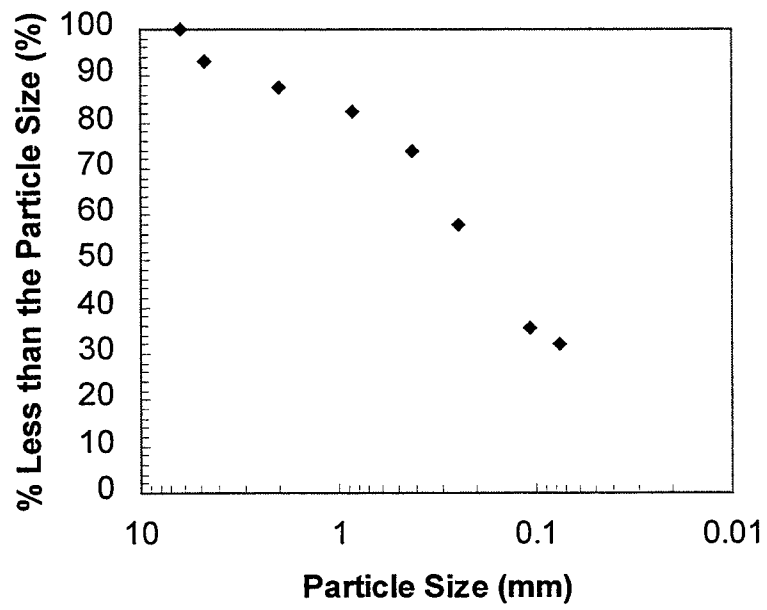


Figure 3.98 The Results of Sieve Analysis for US41 in Parke CO., IN

Table 3.2.15 The Relationship between SPT and DCPT for US41 in Parke CO., IN

PI(mm/Blow)	30.48	22.61	15.49	57.66	35.56	38.86	14.22	19.05	23.62
SPT Blow Count	4	4	4	5	3	3	2	2	3

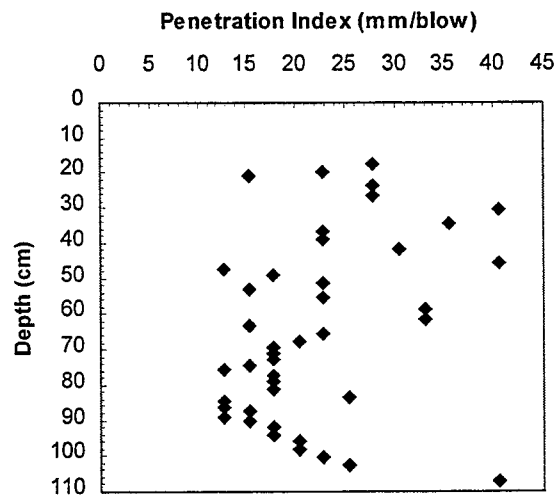


Figure 3.99 the Log 1 of the DCPT for US41 in Parke CO.

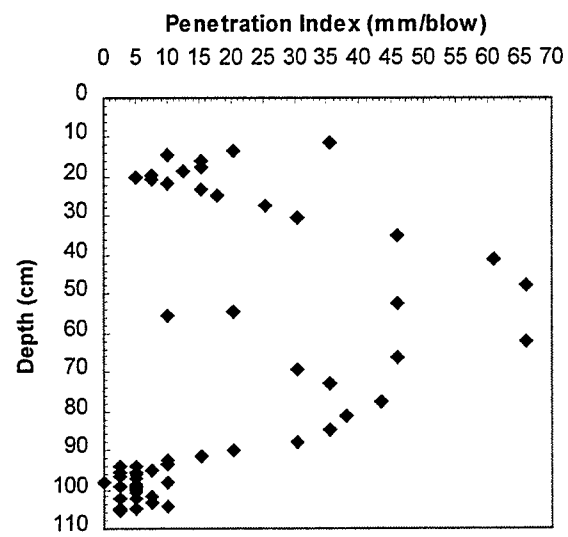


Figure 3.100 the Log 2 of the DCPT for US41 in Parke CO.

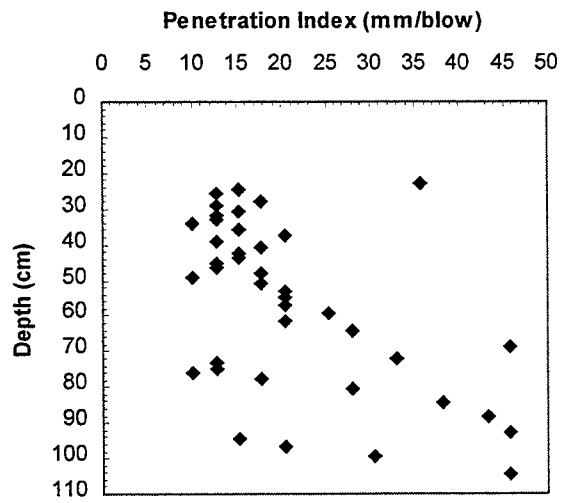


Figure 3.101 the Log 3 of the DCPT for US41 in Parke CO.

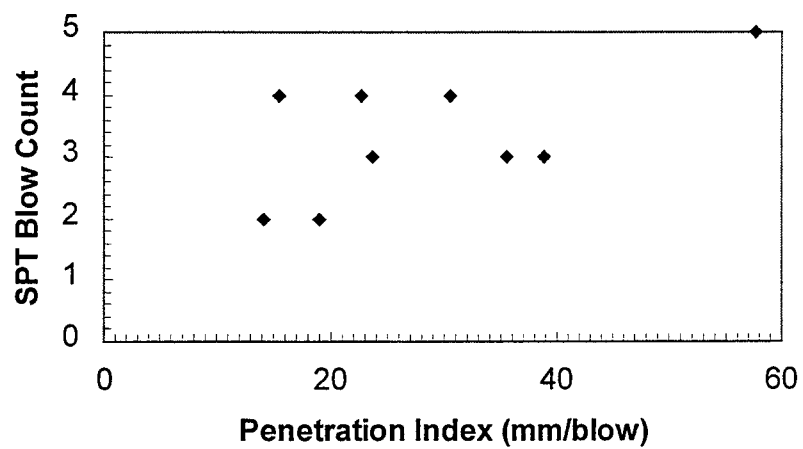


Figure 3.102 The Relationship between DCPT and SPT for US41 in Parke CO, IN

3.3 The Results for Sandy Lean Clay and Sandy Silty Clay

Sections 3.2.3, 3.2.4, 3.2.6 and 3.2.7 all deal with sandy lean clay, although the fraction of the soil passing the 200# sieve and plasticity index values are different. The field data from nuclear gage and sand cone tests for these four soils are summarized in Figures 3.103 through 3.108. From these graphs, the relationship between penetration index, moisture content and dry density can be found. As shown in Figures 3.104 and 3.107, the penetration index first decreases; at a moisture content of about 8%, the penetration index begins to increase. It can also be seen in Figures 3.105 and 3.108 that the penetration index decreases with increasing dry density.

The soil from the Johnson CO. site is a sandy silty clay with w_L equal to 20.25 and plasticity index equal to 6.67. If we combine the field test data and the $S_{u1.0\%}$ contours (Figure 3.34), we can find the relationship between field penetration index and $S_{u1.0\%}$. Then we can relate the field penetration index with M_r through the relationship between $S_{u1.0\%}$ and M_r , given by $M_r = 695.3604S_{u1.0\%} - 5.92966S_{u1.0\%}^2$ (as described in Section 3.2.2). The results are shown in Table 3.3.1.

Table 3.3.1 The Relationships between Field PI, $S_{u1.0\%}$ and M_r for Sandy Silty Clay

PI (mm/blow)	$S_{u1.0\%}$ (kN/m ²)	M_r (kN/m ²)
74.42	26.20	14148.47
93.98	14.48	8825.28
72.9	14.48	8825.28
105.66	13.24	8166.26
100.08	18.48	10824.55
42.67	15.17	9183.52
45.21	13.79	8461.41

The soil from Delaware CO. (2) is a sandy lean clay with w_L equal to 38.92 and plasticity index equal to 21.88. Figure 3.55 shows the relationship between moisture content and dry density from the field test data. The four leftmost points are close to the OMC.

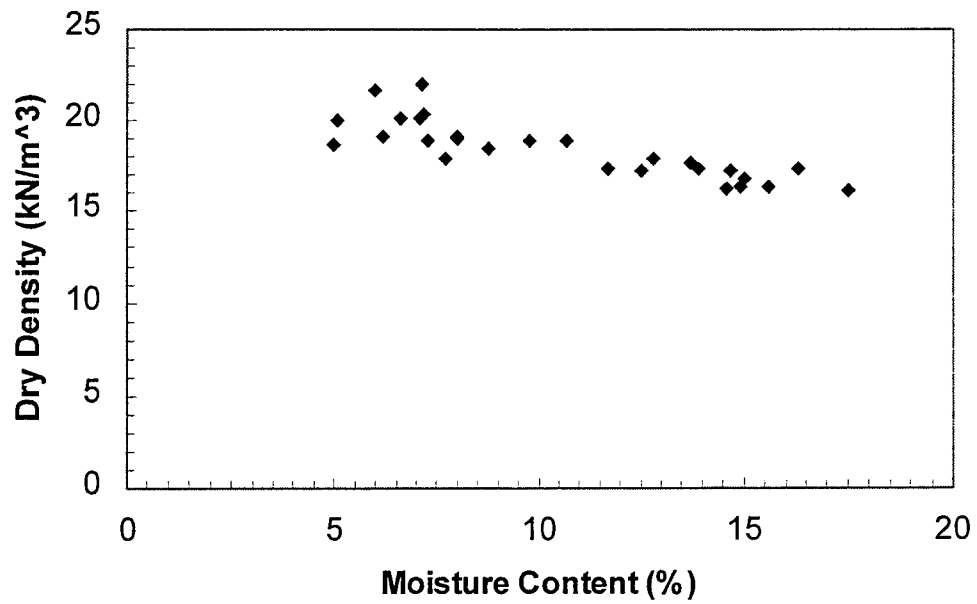


Figure 3.103 The Relationship between Moisture Content and Dry Density for Sandy Lean Clay with Nuclear Gage

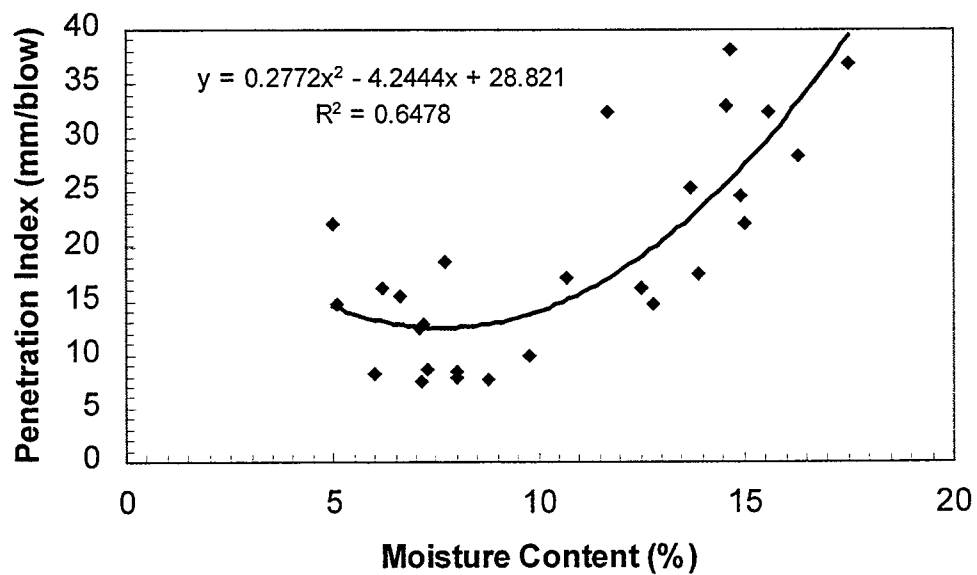


Figure 3.104 The Relationship between Moisture Content and Penetration Index for Sandy Lean Clay with Nuclear Gage

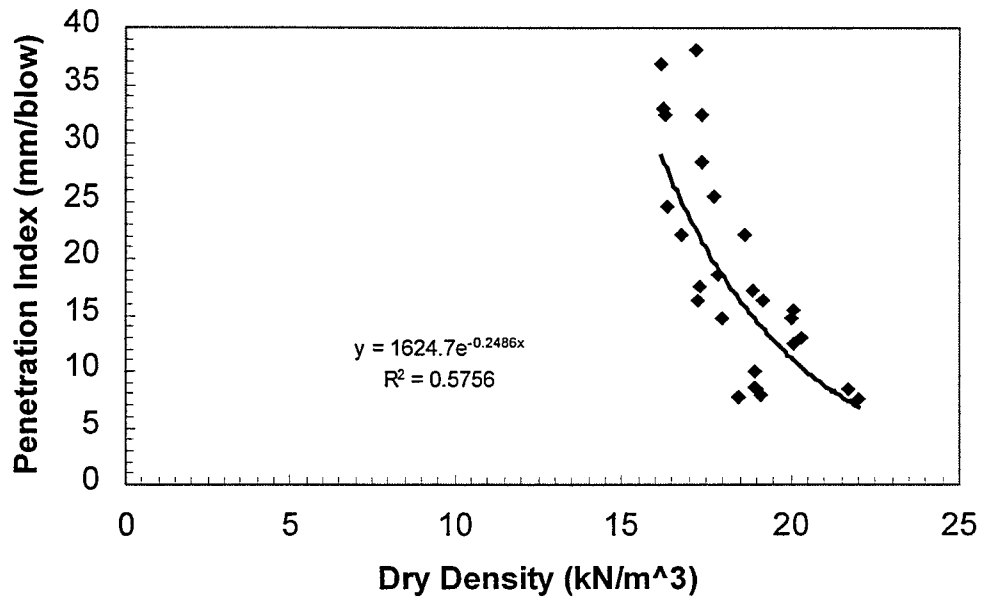


Figure 3.105 The Relationship between Dry Density and Penetration Index for Sandy Lean Clay with Nuclear Gage

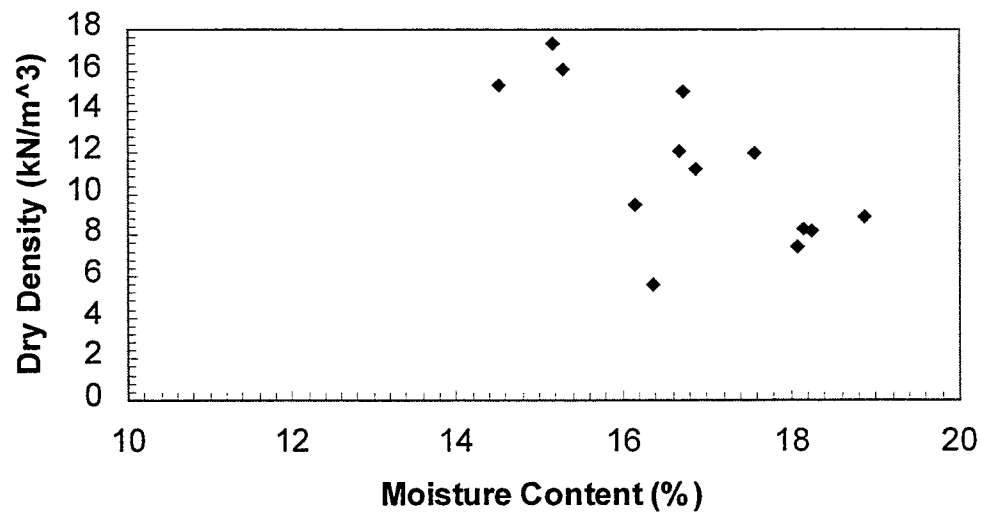


Figure 3.106 The Relationship between Moisture Content and Dry Density for Sandy Lean Clay with Sand Cone Method

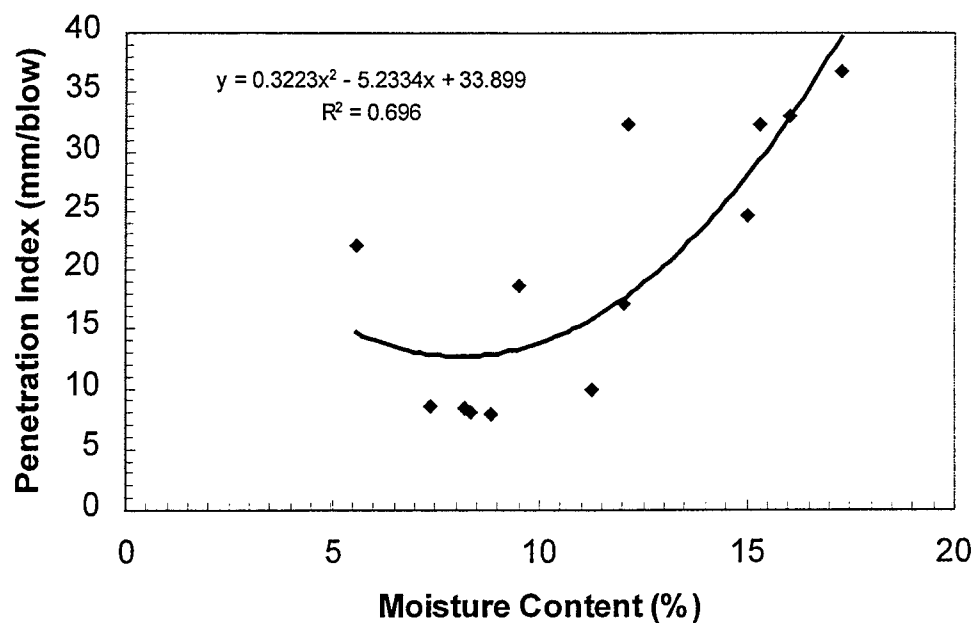


Figure 3.107 The Relationship between Moisture Content and Penetration Index for Sandy Lean Clay with Sand Cone Method

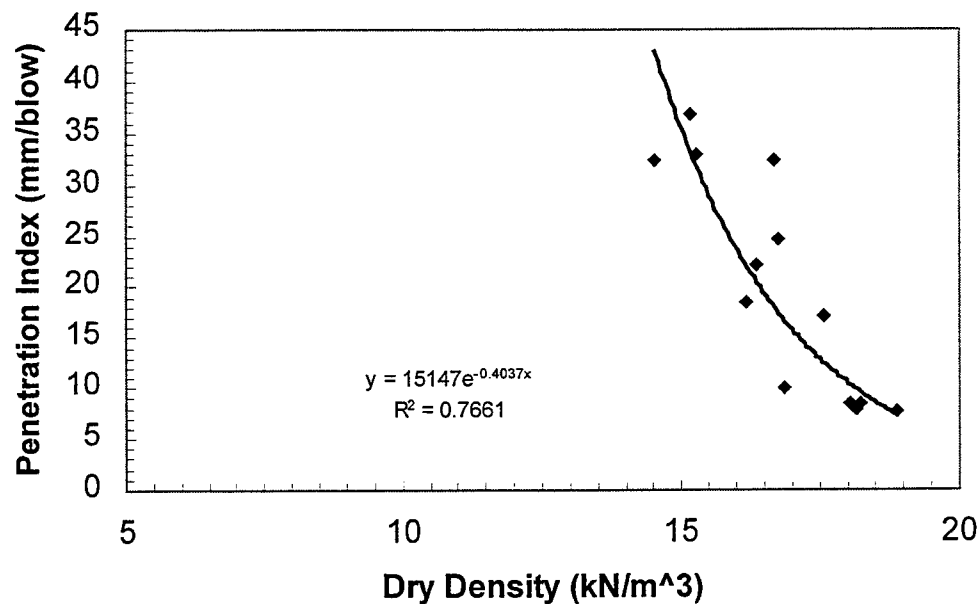


Figure 3.108 The Relationship between Dry Density and Penetration Index for Sandy Lean Clay Sand Cone Method

To create laboratory test specimens having the same fabric as that in the field, samples were compacted according to the instructions in the study of Lee (1997). Unconfined compression tests were then performed for these four points. Using the relationship suggested by Lee (1993), the relationship between field PI, $S_{u1.0\%}$ and M_r is shown in Table 3.3.2.

Table 3.3.2 The Relationship between Field PI, $S_{u1.0\%}$ and M_r for Sandy Lean Clay

PI (mm/blow)	$S_{u1.0\%}$ (kN/m ²)	M_r (kN/m ²)
14.73	28	14821.24
17.53	42	18745.22
25.4	30	15524.12
16.26	47	19583.32

The soils from Johnson CO. and Delaware CO. were sufficiently similar for the results of the tests depicted in Tables 3.3.1 and 3.3.2 to be combined. The results are shown in Figures 3.109 and 3.110. So $S_{u1.0\%}$ and M_r decrease when the penetration index increases.

In order to investigate the magnitude of size effects in laboratory DCPT testing, Figures 3.36 and 3.110 may be compared. From Figure 3.36, we see that the equation for M_r in terms of PI is

$$M_r = -452.3PI + 14932$$

based on the laboratory DCPT testing; from Figure 3.110, we see that the equation for M_r in terms of PI is

$$M_r = -86.878PI + 17273$$

based on the field DCPT testing. Table 3.3.3 illustrates the values of M_r that would result from different values of PI based on these two equations. The ratios of the resulting resilient modulus values may be taken as an indication of the amount of correction that would be needed for M_r -PI correlations developed from laboratory DCPT testing to be applicable in the field. According to Table 3.3.3, a correction in the 30 to 50% range would be sufficient for finding field M_r values of well compacted soils.

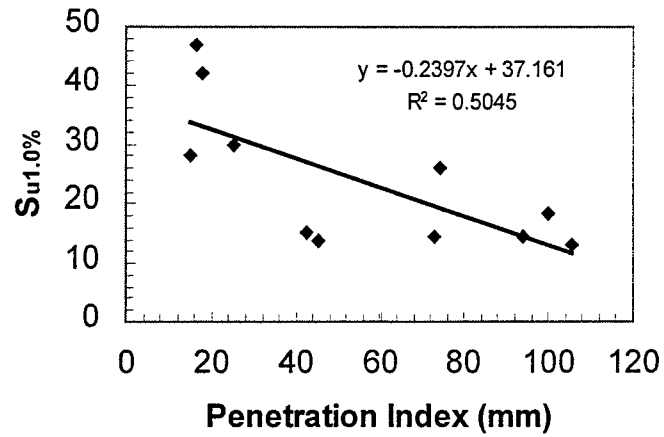


Figure 3.109 The Relationship between Field PI and $S_{u1.0\%}$

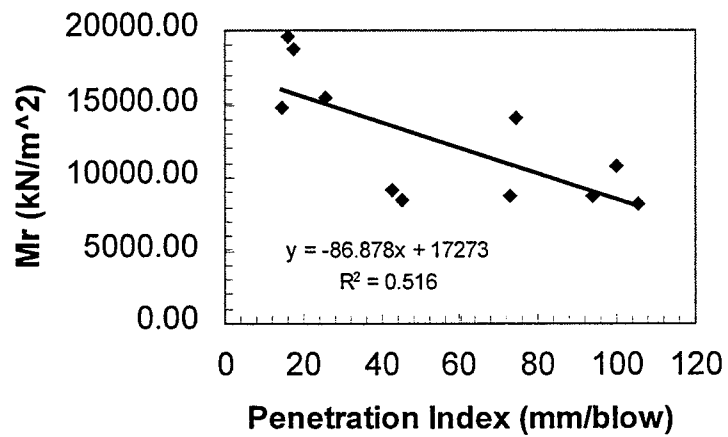


Figure 3.110 The Relationship between Field PI and M_r

Table 3.3.3 The Relationship between M_r from Field and M_r from Laboratory

PI (mm/blow)	$M_{r,field}$ (kN/m ²)	$M_{r,lab}$ (kN/m ²)	$M_{r,field}/M_{r,lab}$
6	16751.73	12218.2	1.37
8	16577.98	11313.6	1.47
10	16404.22	10409.0	1.58
12	16230.46	9504.4	1.71
14	16056.71	8599.8	1.87
16	15882.95	7695.2	2.06
18	15709.2	6790.6	2.31
20	15535.44	5886.0	2.64
22	15361.68	4981.4	3.08
24	15187.93	4076.8	3.73
26	15014.17	3172.2	4.73

3.4 The Relationship between DCPT and SPT

The DCPT and SPT were conducted at the same time and location in Evansville and Parke CO. The soil for Evansville was clayey sand; and the soil for Parke CO. was silty sand. The data from these two sites are combined as follows:

(1) For the depth from 0 to 6 inches, the results are shown in Table 3.4.1 and Figure 3.111.

Table 3.4.1 The Relationship between DCPT and SPT (0 to 6 inches)

PI (mm/blow)	SPT Blow Count
11.40	13
11.75	2
14.15	5

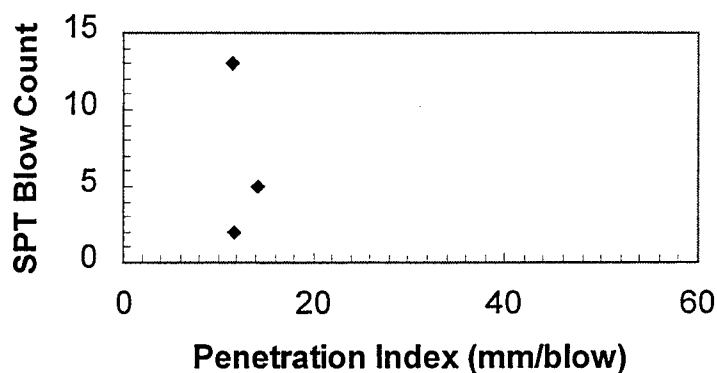


Figure 3.111 The Relationship between the DCPT and SPT (0 to 6 inches)

(2) For the depth from 6 to 12 inches, the results are shown in Table 3.4.2 and Figure 3.112.

Table 3.4.2 The Relationship between DCPT and SPT (6 to 12 inches)

PI (mm/blow)	SPT Blow Count
5.54	15
7.04	2
11.07	6

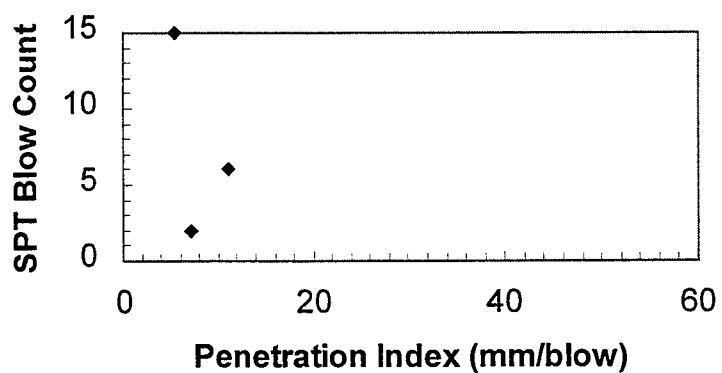


Figure 3.112 The Relationship between the DCPT and SPT (6 to 12 inches)

(3) For the depth from 12 to 18 inches, the results are shown in Table 3.4.3 and Figure 3.113.

Table 3.4.3 The Relationship between DCPT and SPT (12 to 18 inches)

PI (mm/blow)	SPT Blow Count
8.26	13
5.53	4
12.07	8
30.48	4
57.66	5
14.22	2

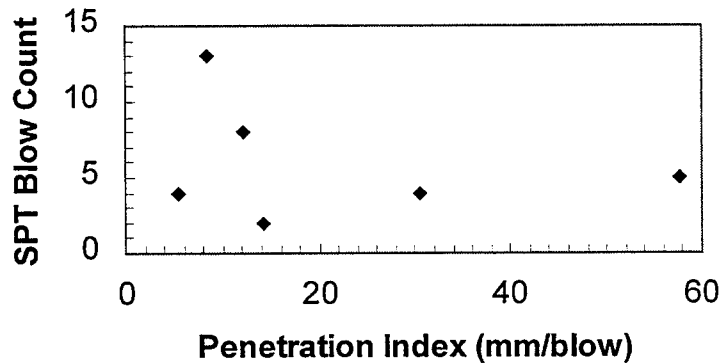


Figure 3.113 The Relationship between the DCPT and SPT (12 to 18 inches)

(4) For the depth from 18 to 24 inches, the results are shown in Table 3.4.4 and Figure 3.114.

Table 3.4.4 The Relationship between DCPT and SPT (18 to 24 inches)

PI (mm/blow)	SPT Blow Count
13.18	8
9.68	16
4.12	2
22.61	4
35.56	3
19.05	2

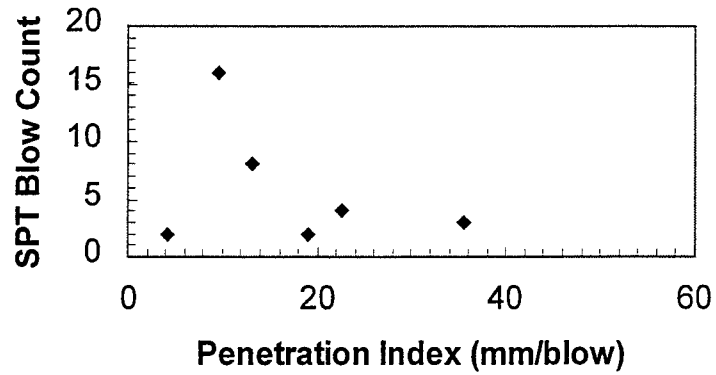


Figure 3.114 The Relationship between the DCPT and SPT (18 to 24 inches)

(5) For the depth from 24 to 30 inches, the results are shown in Table 3.4.5 and Figure 3.115.

Table 3.4.5 The Relationship between DCPT and SPT (24 to 30 inches)

PI (mm/blow)	SPT Blow Count
10.59	8
3.87	12
3.13	6
15.49	4
38.83	3
23.62	3

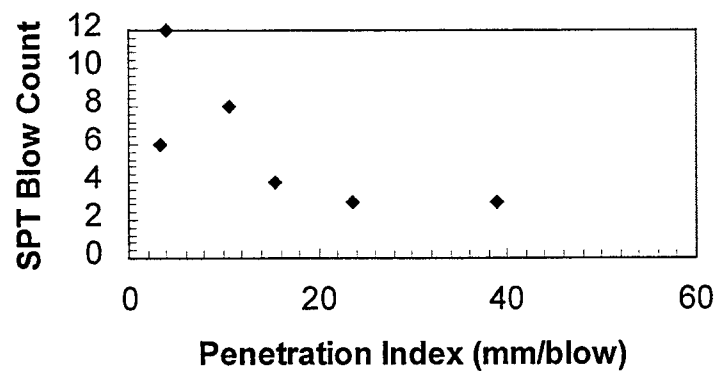


Figure 3.115 The Relationship between the DCPT and SPT (24 to 30 inches)

(6) For the depth from 30 to 36 inches, the results are shown in Table 3.4.6 and Figure 3.116.

Table 3.4.6 The Relationship between DCPT and SPT (30 to 36 inches)

PI (mm/blow)	SPT Blow Count
12.88	9
3.72	9
5.53	8

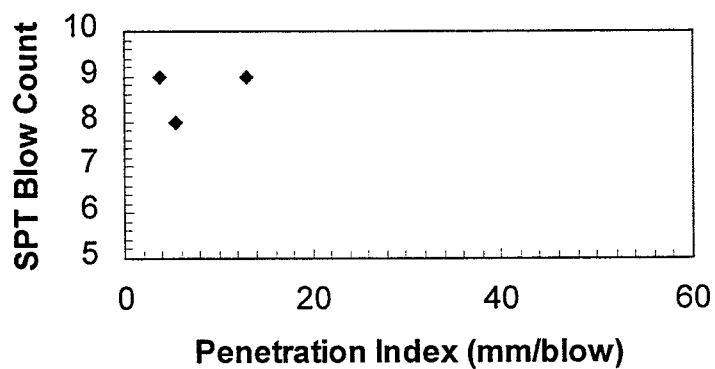


Figure 3.116 The Relationship between the DCPT and SPT (30 to 36 inches)

(7) For the depth from 36 to 42 inches, the results are shown in Table 3.4.7 and Figure 3.117.

Table 3.4.7 The Relationship between DCPT and SPT (36 to 42 inches)

PI (mm/blow)	SPT Blow Count
13.34	12
11.92	2

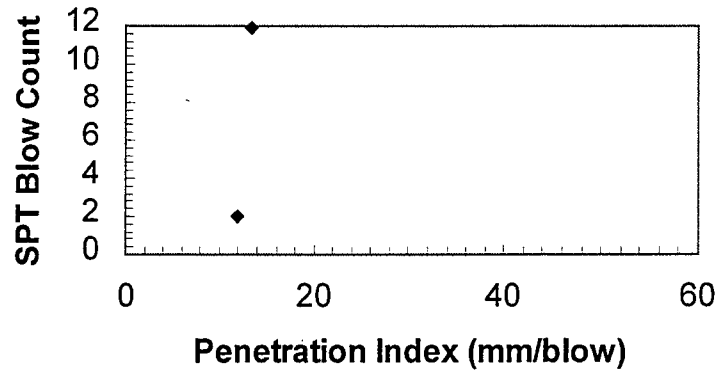


Figure 3.117 The Relationship between the DCPT and SPT (36 to 42 inches)

The general trend is observed that PI increases when SPT blow counts decrease. The slope of the relationship seems to be steeper for higher blow counts and lower PI values. However, no specific, reliable correlation could be found between the two parameters with the amount of information available.

3.5 Summary

(1) Field and laboratory DCPT testing was performed, and the nuclear gage and sand cone methods were used to measure the dry density and moisture content of different soils. The contours reflecting the relationship between laboratory PI, dry density and moisture content were developed for clayey sand and sandy silty clay as shown in Sections 3.2.1 and 3.2.2. The relationships between PI, dry density and moisture content from field testing are shown in Figures 3.103 through 3.108.

(2) In section 3.2.2, for the sandy silty clay, unconfined compression tests were conducted on disturbed samples. Using the correlation by Lee (1993), the relationship between penetration index and resilient modulus was established. The contours of $S_{u1.0\%}$ with respect to dry density and moisture content were also developed. Figures 3.109 and

3.110 reflect the relationship between field PI, $S_{u1.0\%}$ and M_r for sandy lean clay and sandy silty clay.

(3) DCPT and SPT were conducted at the same time and location for two sites, as shown in Section 3.2.5 and 3.2.8; a clear relationship between PI and N_{spt} was not established from these data.

Chapter 4

Conclusions and Future Work

4.1 Conclusions

(1) Field and laboratory tests were conducted on clayey sand, silty sand, sandy silty clay and sandy lean clay soils. The relationships between penetration index, dry density and moisture content obtained from field results present some scatter; however, the trends were clearly that increases in dry density or decreases in moisture content lead to decreases in penetration index. For sandy clay, when all the field data are combined, satisfactory relationships between penetration resistance, dry density and moisture content can be found.

(2) DCPT was also conducted in a 12 inch mold in the laboratory. The soil samples were prepared with different moisture contents and under four different compaction energy levels. The laboratory DCPT testing was performed along these compaction curves. The contours of penetration index with respect to dry density and moisture content were developed based on such testing. However, due to the confining effect of the mold, such relationships should be used carefully.

(3) Unconfined compression tests were also conducted in the laboratory. The relationship between penetration index and the stress at 1% strain in the unconfined compression test is very good. Using the correlation suggested by Lee (1993), penetration index was

related to the resilient modulus. Combining the data for sandy silty clay and sandy lean clay, we also find the relationships between field PI, $S_{u1.0\%}$ and M_r .

(4) DCPT and SPT were conducted at the same time and location for two sites. However, a clear relationship between SPT blow count and PI could not be found for the amount of data available.

4.2 Application to Compaction Control

Compared with some of the other techniques used for compaction control, the DCP is a much more punctual measurement. The penetration index is heavily dependent on what is immediately beneath the cone point. The presence of a gravel or a gravel-size clay clod may give values of I_1 that are too low to be representative of the state of the compacted soil at that location. That this does happen is evidenced by scatter observed in some of the testing presented in this report.

It follows that inspectors should carefully select the location where to do the testing. If a location is selected such that no clods or gravels are present, the measured PI is going to be representative of soil conditions and can be related (as shown earlier) with good success to dry density, water content, and resilient modulus.

It should also be noted that more than one blow is likely to be necessary to drive the cone through the entire thickness of a given lift. So a possible approach for inspection purposes is to carefully select several locations for testing, where no clods or gravels are expected to be present, do the testing, and average the PI over the depth at each location.

4.3 Future work

(1) This study shows that it is possible to, given enough data, obtain satisfactory correlations between penetration index, dry density, water content and resilient modulus. Further testing is needed to develop a complete database.

(2) Once such database is established, it may be possible to develop general or unified correlations between penetration index, dry density, moisture content and plasticity index.

(3) Such correlations will still need to be verified by field performance observations.

LIST OF REFERENCES

Anderson, J. R. and Thompson, M. R.(1995), Characterization of Emulsion Aggregate Mixtures, Transportation Research Record 1492, pp.108-117 .

Ayers, M. E., Thompson, M. R. and Uzarski, D. R. (1989), Rapid Shear Strength Evaluation of In situ Granular Materials, Transportation Research Record 1227, pp. 134-146.

Ayers, M.E. (1990), Rapid Shear Strength of In Situ Granular Materials Utilizing the Dynamic Cone Penetrometer. University of Illinois at Urbana-Champaign, Ph.D. thesis.

Bedford, A. and Drumheller, D. S. (1993), Introduction to elastic wave propagation.

Benson, C. H. and Daniel, D. E. (1990), Influence of Clods on Hydraulic Conductivity of Compacted Clay, J. Geotech. Engrg., ASCE, 116(8), pp.1231-1248.

Bester, M.D. and Hallat, L.(1977), Dynamic Cone Penetrometer (DCP), University of Pretoria, Pretoria.

Bishop, R.F., Hill, R. and Mott, N.F. (1945), Theory of Indentation and Hardness Tests, The Proceedings of the Physical Society, Vol. 57, Part 3, pp.147-159.

Boynton, S.S., and Daniel, D. E.(1985), Hydraulic Conductivity Tests on Compacted Clay, J. Geotech. Engrg., ASCE, 111(4), pp. 465-478.

Broms, B.B. & Flodin, N. (1988), History of soil penetration testing, Penetration Testing 1988, ISOPT-1, De Ruiter (ed.), pp.157-220.

Burnham, T. and Johnson, D.(1993), In Situ Foundation Characterization Using the Dynamic Cone Penetrometer, Minnesota Department of Transportation, report No. Mn/RD-93/05.

Byers, R.K. and Chabai(1977), A.J., Penetration calculations and measurements for a layered soil target, Int. J. Numer. Anal. Methods Gopmech, 1, pp.107-138.

Byers, R.K., Yarrington, P and Chabai, A. J.(1978), Dynamic penetration of soil media by slender projectiles. Int. j. Engrg. Sci 16, pp.835-844.

Chen, W.F., and Saleeb, A.F.(1982), Constitutive Equations for Engineering Materials, Vol.1: Elasticity and Modeling, pp. 516-524.

Chua, K. M. and Lytton, R. L.(1988), Dynamic Analysis Using the Portable Pavement Dynamic Cone Penetrometer, Transportation Research Record 1192, pp.27-38.

Chua, Koon Meng(1988), Penetration Testing 1988, ISOPT-1, De Ruiter (ed.), pp407-414.

Cristescu, N. (1967), Dynamic plasticity, chapter VIII, IX.

Day, S.R., and Daniel, D.E.(1985), Hydraulic Conductivity of Two Prototype Clay Liners, J. Geotech. Engrg., ASCE, 111(8), pp. 957-980.

De Villiers, P. J. (1980), Dynamic Cone Penetrometer Correlation with Unconfined Compressive Strength, University of Pretoria, Pretoria.

Faure, A. G. and Viana Da Mata, J. D (1994), Penetration Resistance Value Along Compaction Curves, *J. of Geotechnical Engineering*, Vol. 120, No. 1, pp.46-59.

Ford, G. R. and Eliason B. E.(1993), Comparison of Compaction Methods on Narrow Surface Drainage Trenches, *Transportation Research Record* 1425, pp18-27.

Forrestal, M. J. et al (1994), An empirical equation for penetration depth of ogival-nose projectile into concrete targets. *International journal of Impact Engineering* 15, 395-405.

Forrestal, M.J. and Luk, V.K.(1988), Dynamic spherical cavity-expansion in a compressible elastic-plastic solid, *Journal of Applied Mechanics*, Vol. 55, pp.275-279.

Forrestal, M.J., Longcope, D.B. and Norwood, F.R., A model to estimate forces on conical penetrators into hard geological targets, *J. Appl. Mech.*, vol. 48, March 1981, pp. 25-29.

Forrestal, M.J., Norwood, F. R. and Longope, D.B.(1981), Penetration into targets described by locked hydrostats and shear strength, *Int. j. Solids Structures* Vol. 17, pp. 915-924.

Goodier, J.N.(1965), On the Mechanics of Indentation and Cratering in Solid Targets of Strain-hardening Metal by Impact of Hard and Soft Spheres. *Proceedings of the 7th Symposium on hypervelocity Impact*, Vol. III, PP. 215-219, AIAA, New York.

Hill, R.(1948), A Theory of Earth Movement near a Deep Underground Explosion. Memo No. 21-48, Armanent Research Establishment, fort Halstead, Kent, U.K. (1948).

Holtz, D. Robert and Kovacs D. William (1981), An Introduction to Geotechnical Engineering, Prentice-Hall, Inc., Chapter 5, "Compaction", pp109-165.

Hopkins, H.G.(1960), Dynamic Expansion of Spherical Cavities in Metal. Chapter III, Progress in Solid Mechanics, Vol. 1, edited by I.N. Sneddon and R.Hill.

Juang, C. H. and Holtz, R.D.(1986), Fabric, Pore Distribution, And Permeability of Sandy Soils, J. Geotech. Engrg., ASCE, 112(9), pp. 855-868.

Kleyn, E. G. (1975), the Use of the Dynamic Cone Penetrometer (DCP), Transvaal Roads Department, Report No. L2/74, Pretoria.

Kleyn, E. G. and Savage, P. F. (1982), The Application of the Pavement DCP to Determine the Bearing Properties and Performance of Road Pavements, International Symposium on Bearing Capacity of Roads and Airfields, Trondheim, Norway, pp238-246.

Kleyn, E. G., Maree, J.H., and Savage, P. F. (1982), The Application of a Portable Pavement Dynamic Cone Penetrometer to Determine In Situ Bearing Properties of Road Pavement Layers and Subgrades in South Africa, European Symposium on Penetration Testing, Amsterdam, Netherlands, pp277-282.

Kleyn, E. G., Van Heerden, M. J. J. and Rossouw, A. J.(1982), An Investigation to Determine the Structural Capacity and Rehabilitation Utilization of a Road Pavement Using the Pavement Dynamic Cone Penetrometer, International Symposium on Bearing Capacity of Roads and Airfields, Trondheim, Norway, 1011-1026.

Kleyn, E.G. and van Heerden, M.J.J. (1983), Using DCP Sounding to Optimize Pavement Rehabilitation, Annual Transportation, Johannesburg.

Lambe, T.W. (1958), the Structure of Compacted Clay, J. Soil Mech. Found. Div., ASCE, 84(2), pp. 1-34.

Lee, Woojin (1993), Evaluation of In-Service Subgrade Resilient Modulus with Consideration of Seasoned Effects, Ph. D. Thesis, Purdue University, West Lafayette.

Lee, Woojing, Bohra, N.C., Altschaeffl, A.G. and White, T.D.(1997), Resilient Modulus of Cohesive Soils, Journal of Geotechnical and Geoenvironmental Engineering, Vol. 123, No. 2, February, 1997, pp131-136.

Little, D. N.(1996), Assessment of In Situ Structural Properties of Lime-Stabilized Clay Subgrades, Transportation Research Record 1546, pp.13-23.

Livneh, M, Ishai, I. and Livneh, N. A.(1994), Effect of Vertical Confinement on Dynamic Cone Penetrometer Strength Values in Pavement and Subgrade Evaluations, Transportation Research Record 1473, pp.1-8.

Livneh, M. (1987), the Use of dynamic Cone Penetrometer in Determining the Strength of Existing Pavements and Subgrade, Proceedings, 9th Southeast Asian Geotechnical Conference, Bangkok, Thailand.

Livneh, M. and Ishai, I. (1985), Evaluation of Flexible Pavements and Subsoils Using the South African Cone Penetrometer, Transportation Research Institute, Publication Number 85-301, Technion.

Livneh, M. and Ishai, I. (1988), the Relationship between In Situ CBR Test and Various Penetration Tests, Penetration Testing 1988, ISOPT-1, De Ruitter (ed.), pp445-452.

Livneh, M.(1989), Validation of Correlations Between a Number of Penetration Tests and In Situ California Bearing Ratio Tests, Transportation Research Record 1219, pp56-67.

Longcope, D.B. and Forrestal, M.J. (1983), Penetration of targets described by a Mohr-Coulomb failure criterion with a tension cutoff, *Journal of Applied Mechanics*, Vol.50, pp327-333.

Lubliner, Jacob (1990), *Plasticity theory*, chapter 7.

Luk, V.K. and Forrestal, M. J. (1987), "Penetration into semi-infinite reinforced-concrete targets with spherical and ogival nose projectiles", *Int. J. Impact Engrg* Vol. 6, No. 4, pp. 291-301.

Luk, V.K. Forrestal, M.J. and Amos, D.E. (1991), Dynamic spherical cavity expansion of strain-hardening materials, *Journal of Applied Mechanics* 58, 1-6.

Scala, A.J. (1956), Simple Methods of Flexible Pavement Design Using Cone Penetrometers, *Proc. 2nd Australian-New Zealand Conf. Soil Mech. and Found. Engrg.*, pp. 73.

Seed, H. B, Chan, C. K.(1959), Structure and Strength Characteristics of Compacted Clays, *Journal of the Soil Mechanics and Foundations Division, Proceedings of the American Society Civil Engineers*, Vol. 85, No. SM 5, October, 1959, pp87-127.

Skempton, A. W. and Bjerrum, L. (1957), *A Contribution to the Settlements Analysis of Foundations on Saturated Clay*, *Geotechnique*, London, England, 7, pp.168-178.

Thipgen, L.(1974), Projectile penetration of elastic-plastic earth media, *J. Geotech. Div., Am. Soc. Civ. Eng.* 100, pp279-293.

Turnbull, W. J. and Foster, C. R. (1957), Compaction of Graded Crushed Stones Base Course, *Proc. 4th Int. Conf. Soil Mech. Found. Engrg.*, 2, pp.181-185.

Xu, Y., Keer, L.M. and Luk, V.K.(1997), Elastic-Cracked model for penetration into unreinforced concrete targets with ogival nose projectiles, *Int. J. Solids Structures*, Vol.34, No.12, pp.1479-1491.

Yankelevski, D. Z. and Adin, M.A.(1980), A simplified analytical method for soil penetration analysis, *International Journal for Numerical and Analytical Method in Geomechanics*, vol 4, 233-254.

Yew, C.H. and Strirbis, P.P.(1978), Penetration of projectile into terrestrial target, *Journal of the engineering mechanics division, ASCE, EM2*, pp403-423.

Yoder, E.J., Shurig, D.G. and Colucci-Rios, B.(1982), Evaluation of Existing Aggregate Roads to Determine Suitability for Resurfacing, *Transportation Research Board, Transportation Research Record 875*, 1-7.

Yong, C. W.(1969), depth prediction for earth penetrating projectiles, *J. Soil Mech. Found. Div., Proc. Am. Soc. Civ. Eng* , 95, 803-817.

